First record of fish microfossils from Ramsåsa, site C, Skåne, southern Sweden

J.M.J. Vergoossen

Vergoossen, J.M.J. First record of fish microfossils from Ramsåsa, site C, Skåne, southern Sweden. *Scripta Geologica,* **126**: 1-78, 2 figs, 15 pls; Leiden, November 2003.
J.M.J. Vergoossen, Paleontologie, Biologisch Centrum Rijksuniversiteit Groningen, Kerklaan 30, NL 9751 NN Haren, The Netherlands (J.M.J.Vergoossen@biol.rug.nl).

Key words – Osteostracan, thelodont, acanthodian fish scales, Whitcliffian, Sweden.
Within the thelodont dominated fauna of Ramsåsa, site C, Skåne, southern Sweden (Ludlow, Whitcliffian), the scales of the *Thelodus parvidens* group outnumber those of the combined *T. sculptilis*-*T. admirabilis* groups, some specimens of which are indistinguishable. Scale forms that might belong to one of several *Thelodus* taxa are designated as forma *baltica* (new form), forma *T. radiosus* Lehman, and forma *T. ramosus* Lehman, whereas forma *T. querceus* Lehman is introduced to cover a particular (heterogeneous?) group of monocuspid scales previously assigned to *T. trilobatus* Hoppe. Among the acanthodians, *Nostolepis striata* scales predominate. The checklist of *N. striata* trunk scales is extended to 62 characters. The smallest nostolepid teeth known so far are illustrated. The histology of *Radioporacanthodes biblicus* is shown in detail and the presence of wide arcade canals connecting the anterior grooves to the first pores of the radial pore rows is demonstrated. Problematical poracanthodid scales (formerly included in '*Poracanthodes porosus*'), chiefly from Estonia, are described as forma *bifurcata* (new form). The ontogeny and functioning of the porosiform pore system in some of these scales are discussed. New, small scales of an unnamed acanthodian taxon (morph 5) are described. The fauna is placed in the Upper Ludlow (Whitcliffian) within the *T. sculptilis* biozone.

Contents

Introduction 1
Material, methods and preservation 2
Glossary 2
Systematic palaeontology 3
Osteostracan fishes 3
Thelodont fishes 5
Acanthodian fishes 20
Correlation 41
Scale quantities 42
Acknowledgements 45
References 45
Appendix 1, 2 48

Introduction

A microvertebrate assemblage from Ramsåsa site C *sensu* Grönwall (1897) (site 3 *sensu* Larsson, 1979, p. 180) in Skåne, southern Sweden (map in Vergoossen, 2002c, text-fig. 1) is described. The fossils derive from an unregistered sample housed in the fish collections of the Swedish Museum of Natural History, Palaeozoology Department,

Stockholm (NRS). The exposure ("along a little rill"; Moberg, 1910, p.140) was in layer 4 *sensu* Grönwall (1897), now interpreted as the highest part of the Öved-Sandstone Formation (Jeppsson & Laufeld, 1986), the younger of the two formations making up the Upper Silurian Öved-Ramsåsa Group and dated as Pridoli by Jeppsson & Laufeld (1986). The stratigraphic position of the Öved-Sandstone Formation is discussed further in the correlation section and Vergoossen (1999b, 2002a-c).

Grönwall (1897, p. 218) and Moberg & Grönwall (1909, p. 9) published a measured section of the exposure, marking the horizons that yielded *Leperditia* and a bivalve, but mentioned no fish remains. The lithology of this section differs from that recorded by Larsson (1979, p. 180) from site 3, which consisted of red limestone and soft red mudstone. Larsson wrote that the exposure (no longer accessible) yielded the tentaculids *Odessites lebiensis* and *Tentaculites loxus*, which are restricted to the *Ligonodina elegans* conodont zone, indicative of the youngest Silurian in Skåne. Larsson did not mention fish remains. For further geographical references concerning Ramsåsa site 3, see Larsson (1979).

Material, methods and preservation

The small "block" available for examination carried a site label with the designation Ramsåsa, locality C, and a collection label with the name of E. Stensiö, 1924. The rock received a serial working number (SW 5) and weighed *c.* 36 g. It was a fine-grained, red brown, sandy, micaceous limestone, with many fossils including rare gastropods, bivalve or brachiopod fragments, rare ?phyllocarid remains and ostracode moulds.

The rock was dissolved in dilute acetic acid (10%), but this bath did not sufficiently 'clean' the scales. For fear of destruction (Vergoossen, 2002c), no attempt was made to remove the adhering particles from the material in a second bath. For further remarks on preservation, see also the systematic descriptions and the section on scale quantities. To facilitate picking, the residues were sieved into fractions with mesh widths 0.106-0.212-0.355-0.425-0.5 mm.

The material described in this paper is housed in the Swedish Museum of Natural History, Palaeozoology Department, Stockholm (prefixed P) and in the National Museum of Natural History, Leiden (prefixed RGM), where material from the author's collection (prefixed V or JV) will be deposited.

Glossary

A1, A2	first canal of the agps (counted from left to right); A2, second canal, *etc.*
agp	anterior groove canal of the pore system
anterior(s)	see agp
arc	arcade canal between the radial canals of the pore system
arca	arcade canal connecting anterior grooves to the first pores of the radial pore series in *Radioporacanthodes biblicus*
AT	total number of acanthodian remains
ATS	total number of acanthodian scales
avc	ascending vascular canal

Bla	basal lamina
Cla	crown lamina
den	dentinal plexus
erratic	Late Silurian, Baltic-derived boulder
fib	Sharpey's fibres
La 1, La 2	crown lamella that was first formed; lamella that was formed next, *etc.*
lac	basal lacuna
lap	lamellar subdivision of primary crown
longitudinal	(in the description of osteostracan armour fragments) direction into which the 'growth lines' of the dentine ridges are oriented, following a course from anterior to posterior
Nla	neck lamina
mar	median pair of short anterior crown riblets or ridges
micla	micro or finer lamination within one large lamina
P1	first large pore over a radial; P2, second large pore, *etc*.
pc	pulp cavity
pore	in the discussion of pore system of the porosiform/punctatiform acanthodians: exoskeletal hole, unless stated otherwise
R1	first radial pore row (counted from left to right); R2, second row, *etc*.
radial(s)	see rpr
rpr	row of radially arranged, interconnected pores of the pore system, looking like a radial canal
(r)vc	(radial) canal of vascular system
supla	superposed lamella
TT	(of the) thelodont total
ventral/ventrad	used in the same sense as visceral/viscerad

Other terminology as in Vergoossen, 2002a-c

Systematic palaeontology

For general remarks see Vergoossen (2002c). All measurements were taken on largest diameters, unless stated otherwise. The microvertebrate assemblage is listed in Appendix 1.

Osteostracan fishes

Figs. 1-7.

Remarks — The osteostracan remains consist of plate and scale fragments. Several morphological forms can be distinguished. In the descriptions, the term external opening has been preferred to external pore, because the presence of a pore system with sieve plates has not been demonstrated beyond doubt in Scanian remains examined by me. Only the most regular openings were measured in the scans. Apart from preservation, one of the measuring problems is the gullies leading up to the pores (to be included or not, and where are boundaries of gullies?) in combination with pore limits or walls (the angle from which they are viewed also effects their size). Even when the perforations look uniform, there will always be a range of sizes. For these

reasons a high number of measurements are needed to approximate factual data.

Variant 1 plates (P9030, Fig. 1) have narrow, parallel, smooth- and flat-topped, longitudinal ridges that do not rise above the surface and are separated by one row of mostly uniform-sized external openings. Larger openings (Fig. 1a) are probably post-mortem artefacts. Aperture diameter (Fig. 1b) is *c.* 0.025 mm. The smallest diameter measured is 0.016 × 0.019 mm, the largest *c.* 0.027 mm. The continuous ridges and rows of external apertures run parallel and straight longitudinally, except where new ridges and openings were inserted; here their course is slightly curved. In some apertures a mosaic of radially arranged smaller openings could be observed (Fig. 1b). Such mosaics, or their relicts, occur in all the osteostracan remains described and resemble sieve plates in the pores of *Oeselaspis* sp. indet. from the Halla Beds on Gotland (Gross, 1968, fig. 11i). Further research is needed to ascertain that the mosaics are not preservational artefacts. A flat, sculpture-free, wide plate margin can be present. Total height of plate *c.* 0.131 mm, height of sculpture-free layer *c.* 0.043 mm (cf. Vergoossen, 2002a, pl. 1, figs. 1-2).

On P9031 (Fig. 2), hemicyclaspid, longitudinal ridges are hard to distinguish; towards the plate margin a few, short oval to longitudinal, smooth lumps occur (on P9030, Fig. 1 a, c, the ridge ornament passes into a more lumpy, rounded and widened type near the plate margin). A sculpture-free margin is lacking. The spongy layer under the surface layer shows the large rectangular canal openings of the vascular plexus (Fig. 2a). In vertical section the surface layer looks like a dense wall compared to the spongy layer; it is pierced only in a few places by round vascular openings. Laminar bone forms the basal layer. At the plate margin, this bone forms a rim that is deeper than, and slopes outward and away from, the main part of the plate. Height of surface layer, 0.1 mm; middle layer, 0.147 mm; the basal layer (without rim), between 0.041 and 0.052 mm; with rim, 0.094 mm (measured in transverse section; Fig. 2a). Size of twelve openings around 0. 02 mm (Fig. 2a), largest 0.022 × 0.022 mm, smallest 0.015 × 0.014 mm.

On a different fragment (Fig. 3; upper layer preserved, without plate margins) the longitudinal ridges are discontinuous, of different length, height and orientation. Anteriad, from right to left on the plate (Fig. 3a, b), the ridges can increase in height (and rise slightly above the surface) and become shorter. The ridges radiate from midanteriorly (Fig. 3c) and are fairly straight in the middle of the plate (Fig. 3a), whereas they tend to curve centrad anterolaterally. Anterior to the radiation point, ridges tend to become indistinguishable (Fig. 3a). Many external apertures open at sharp angles to the surface and are directed posteriad, in the same direction that the ridges grew, as also indicated by the short and oblique gully leading away from each aperture. Where external openings are lacking (Fig. 3c), the ridges can slope upward anteroposteriad, in the direction of growth and of the ultrasculpture (fine, parallel, diagonal lateral striae on the ridges, of the same kind as in P9036; Fig. 7). These striae are interpreted as relating to increment, unless stated otherwise (cf. ornamental ribs, Afanassieva, 1999, p. 121; reflecting the arrangement of the dentinal tubules, Gross, 1968, p. 393; see also variant 2, below). In visceral direction, the ridges can widen out ('like a mountain slope') at their posterior end. Dimensions of ten openings vary between 0.016 × 0.018 and 0.033 × 0.027 mm.

A posteriad orientation of the longitudinally parallel ridges and an oblique, posteriad orientation of external openings is obvious from the worn, rectangular (hemicyclaspid?) scale fragment P9030 (Fig. 4b). The crescent-like openings (pores?) are

situated in shallow grooves between the ridges and are larger than in the fragments described above. Dimensions range between *c.* 0.032 × 0.023 and 0.038 × 0.032 mm (measured on five openings). Chevron-shaped striations occur on the ridges, which must have had a more sharply edged top (Fig. 4a). The ridges are interconnected by wing-like, oblique, lateral extensions at the ridge base. The unornamented anterior zone (overlapped area) is bounded by a basal rim. The deep, faintly laminated base makes up *c.* 45% of total scale height. A scale from Helvetesgraven (Vergoossen, 1999b, pl. 1, fig. 3) has two rows of round openings between the ridges; ultrasculpture was not observed on that specimen.

A worn and curved plate fragment (Fig. 5) has large external openings of irregular size and shape and oriented posteriad, between wide, more or less parallel (partim longitudinally apposed?), flat-topped ridges. The wing-like ridge interconnections have the same orientation as the ultrasculpture of parallel, diagonal striae on the ridge walls. The spongiose layer (Fig. 5a) underlies the external layer.

Variant 2 (Fig. 6) has a short, high, narrow ridge anteroposteriad inclined and rising well above the surface. At its widest part the ridge is about twice as wide as at its narrowest part (*c.* 0.046 mm; Fig. 6b). The ultrasculpture pattern on the ridge is not uniform; on their path to the top, the striae on the ridge walls bend posteriad. The striae ascending from the midanterior ridge top follow an almost straight, posteriad course across two-thirds of their length. The pattern of the fine lines is analogous to fingerprints, which are not growth related. The spacing and height of the papillae that form the dermal ridges in the finger are connected with the mechanical load to which the skin can be subjected. This is regarded as a genetically determined protection device (Leonhardt, 2000). The surface of the plate is concave on one side of the ridge and convex on the other. The external appearance of the openings is best characterised as infundibular; near the surface the holes widen out. This widening is shallow and ring-shaped. Aperture diameter measured before widening out, varies between *c.* 0.009 × 0.01 and *c.* 0.013 × 0.013 mm; diameter of entire external opening varies between *c.* 0.021 × 0.022 and *c.* 0.027 × 0.036 mm (measured in only specimen). This sort of opening is also seen in a fragment from Ramsåsa H (Vergoossen, 2002a, pl. 1, figs. 6-7; ridge has a much flatter top). Dense unlaminated bone forms the basal layer.

Whether all these variations would occur in one taxon is difficult to determine. Ridges separated by one or two rows of openings and crescent-like or posteriorly directed external openings are also seen in Late Silurian - Early Devonian Osteostraci indet. from North Greenland (Blom, 1999, fig. 27) and in Middle Devonian osteostracan tesserae from the Baltic (Otto & Laurin, 1999).

Thelodont fishes

Remarks — The external thelodont squamation (=squamation exclusive of oropharyngeal and branchial scales) consisted of scales with centripetally growing crowns, whose ornament and size were more or less fixed. The base grew centrifugally and was capable of (limited) growth expansion. By analogy with modern sharks, scales were shed during the lifetime of the thelodont, and new ones were inserted to compensate for lost scales and for increase in body size. The squamation was always a combination of old and young scales. If the analogy of modern sharks is extended to the morpho-

genesis of the entire squamation (Reif, 1985), then morphogenesis of thelodont squamation would begin in the later phase of the embryonic development from the dorsal side of the body. With the exception of *Lanarkia* and, possibly, *Loganellia* (Turner, 1992; Märss & Ritchie, 1998), little is known about when or how the body became covered with which scale forms. Concerning the development of the body zonal differentiation of the squamation during fish growth, it is reasonable to assume that, with the insertion of new scales, the diversity in scale morphology increased since the spacing of squamation zones expanded, i.e., in a young fish the zones occupied a smaller area of the body than in an older fish. Even the insertion of new differentiation zones is possible, adding morphologically transitional or new scale forms. Against this background it is hardly surprising that, in the detailed study of large quantities of thelodont scales from one sample (in the present study probably from one bed), forms that are not representative of 'well-known' scleritomes, scale groups or species are collected again and again.

Thelodus parvidens Agassiz *in* Murchison, 1839 *sensu* Märss, 1986b

Figs. 8-23.

Remarks — This designation refers to the species in its widest possible sense, in contrast to *Thelodus parvidens* Agassiz *sensu* Gross, 1967, which represents the most restricted concept of the species and refers to the glabrous scales as originally described and figured by Agassiz.

Incised glabrous (*cephalopectoral*) *scales* (Figs. 8-10) — For terminology and background, see Vergoossen (2002c). (Sole specimens, confined to Ramsåsa C.)

Anterolaterally incised, multicuspid, glabrous scale P9038 (Fig. 8) combines features of oral, cephalopectoral and trunk scales of *T. parvidens* and *T. sculptilis*, and is about thrice as long as wide. Crown downturned anterolaterally, but with five upturned, pointed, posterior cusps. Central crown smooth and flat. Anterolateral notches shallow and oriented centroposteriad. Flattened lobes at the anterior corners of the crown largest, together with an adjoining lateral rimmed lobe (right in Fig. 8a). The smooth crown surface narrows posteriad (Fig. 8a), this narrowing marking the beginning of the cuspidate posterior edge. Midposterior cusp with rightward twist (Fig. 8c). Steep neck, about one-third of total scale height. In dorsal view (Fig. 8c), the crown conceals the neck and most of the base, which is ellipsoid and ventrally flat, and has a mid-anterior constriction that marks off a short, rounded, viscerad curving spur.

P9039 (Fig. 9) is twice as long as wide. The rounded anterior crown rim is more strongly bent ventrad than the posterior rim with median right angle. One crown side shallowly notched, the other straight. Crown widest just before centrad twist of lateroposterior rims. Upper crown flat (Fig. 9b). Crown overhangs neck, which measures *c.* one quarter of total scale height. Posterior neck ribs do not reach highest neck parts. Base ellipsoid and moderately thick (at deepest point about one quarter of total scale height).

The postero-incised crown of P9040 (Fig. 10) has a parabolic shape with five short posterior, rounded triangular dents (median longest), in contrast to *costatus* crowns figured by Gross (1967, pl. 1, figs. 9, 11); compare with Turner (2000, pl. 4, figs. 6-8; Gorstian to early Pridoli). Upper surface flattened behind its highest anteromedian

point (Fig. 10a). Anterolateral crown margin curved. Crown overhanging neck and lateroposteriorly, also base. Riblets of irregular height and thickness in lateroposterior neck (*c.* four per 0.1 mm). Neck steep and anterolaterally marked off from base by rim (Fig. 10a).

Forma Thelodus trilobatus Hoppe, 1931

Figs. 11-23.

Remarks — Vergoossen (2002c) treated the Scanian scales of *T. trilobatus sensu* Gross, 1967, as a separate form group, irrespective of their classification. This treatment is continued herein.

Scales with monocuspid crowns (Figs. 11-18) — Including forma *Thelodus querceus* Lehman, 1937 (Figs. 11-15). Gross broadened Hoppe's concept of *T. trilobatus* and also included scales with crowns whose lateroposterior rims form a single midposterior cusp, and without additional lateroposterior posterior cusps or spinose rims (Gross, 1967, pl. 2, fig. 18; from the 'Beyrichienkalk'). The specimen illustrated by Gross (crown with lanceolate median ridge pair) and two of the monocuspid scales figured by Turner (1973, fig. 4F; 1984, fig. 4.4C; Ludlow Bone Bed) represent forms that I did not collect from Scania. A scale from Helvetesgraven (Vergoossen, 1999b, pl. 1, fig. 8) looks like '*Thelodus querceus*' Lehman, 1937, but might have *Katoporodus*-type histology (see below).

For the relatively infrequent monocuspid crowns *trilobatus* is an unsuitable designation. 'Postpectoral' and 'precaudal' (Märss, 1982, 1986a) do not refer to *T. trilobatus* scales directly or exclusively. They are also unsuitable because they refer to hypothetical placement on the body in any thelodont scale taxon and for their generalised morphological implications, even within one taxon. Monocuspid scales can show costatiform features or a combination of *bicostatus* (cephalopectoral) and *costatus* (oral) features, in that they possess a median pair of sharp, longitudinal parallel ribs (intermediate surface smooth and flat) and oblique side ridges usually shortening lateroposteriad and with intermediate folds (Fig. 12). The side ridges are directed posteriad and can reach the median ridge pair. All monocuspid scales lack an anterolateral neck and, in this respect, they differ from *T. bicostatus*. This group of scales will be described below and separately from the multicuspid *T. trilobatus* scale group and separately from the scleritome *T. parvidens sensu* Märss, 1986b (cf. Vergoosen, 2002a). They will be compared to *Thelodus querceus*.

Gross (1967, p. 26) used the term "eichenbladformig" (=oak-leaf shape or querceus) to characterise *Katoporodus* head scales and pointed out that the absence of a neck distinguished *Katoporodus* from *T. trilobatus* scales. However, Gross (1967, pl. 2) also figured *T. trilobatus* scales that would seem to lack an anterolateral neck. In some of the Scanian 'neckless' scales (Fig. 11b; Vergoossen, 1999b, fig. 8: "*T. parvidens* = *T. querceus*"), a tendency of the crown towards a more oak leaf shape can be observed. Such scales can have *Katoporodus*-type histology in specimens from Helvetesgraven. *Katoporodus tricavus* Gross, 1967, from the 'Beyrichienkalk' might even be synonymous with *Thelodus querceus* Lehman, 1937, from Ramsåsa (F). Gross (1967, p. 27) had not observed *Katoporodus* in the Ramsåsa beds. In my samples from Ramsåsa (C, D, H), common *K. tricavus*

trunk scales are absent. These trunk scales are not rare in the Helvetesgraven fauna (new record, cf. faunal list by Vergoossen, 1999b). There are indications that at least some Scanian *T. querceus*-like scales possessed the typical *T. parvidens/trilobatus* kind of histology. In this paper the name *T. querceus* has been used in its proper generic sense.

P9042 (Fig. 11) has one ridge parallel to and on each side of the median pair. This ridge is situated between the lateral crown rim and the nearest ridge of the median pair (Fig. 11a). There are about four lateral oblique ridges (Fig. 11b). The anteriormost is situated at half the scale's length. The base is anteriorly extended. Base and crown are slightly bent to the left (Fig. 11a). P9043 (Fig. 12) has a short, parallel, anteromedian ridge pair between and parallel to the median pair, which is separated by a shallow fold. Oblique ridges longer than in the previous scale. Which ridge forms the lateral crown rim is unclear. Both scales resemble *T. querceus* from Ramsåsa F in side view (Lehman, 1937, fig. 23C). Other scales resembling *T. querceus* in side view are shown in Figures 13-15. P9044 (Fig. 13) has three converging median instead of parallel ridges. The ridge exactly in the middle begins further anteriorly and is flanked by shallow folds. A pair of convex lateral rims ascends from about half way along the scale's length and meets the median ridges in the posterior crown point. The basal spur (*c.* 25% of total base length) dips downward from the anteromedian basal constriction, but not very steeply. The base of the original *T. querceus* scale (Lehman, 1937, fig. 23) had no spur. In P9045 (Fig. 14b) some oblique ridges are restricted to the upper lateroposterior crown. In P9046 the oblique ridges disappear posteriad (Fig. 15b). The anterior basal 'tongue' is one of the largest forward basal projections among the scales in the sample. In the Baltic region such a base is usually associated with *Thelodus* species (*T. laevis, T. carinatus*) predating the late Whitcliffian Kuressaare Regional Stage of Estonia, rather than with scales of *T. trilobatus* or *T. parvidens*.

In side view, P9047 (Fig. 16) resembles *T. querceus*, but oblique side ridges are absent. Crown ridges and rims show a more or less parallel arrangement (Fig. 16a); a fairly wide, longitudinal median platform or fold, as in P9042 and P9043, is not recognisable. A low basal rim forms the lateral and posterior base. The anterior base has a well-developed, partly fused, double or a subdivided spur with a viscerad inclination of *c.* 45° relative to the plane of the visceral basal surface. In P9048 the parallelism of the four crown ridges towards the posterior is conspicuous, especially in crown view (Fig. 17a). The inter-ridge space widens anteriormost (by contrast, this space is constricted anteriormost in the scale in Fig. 14a). Anterior basal process projected forwards from slight basal constriction (Fig. 17b), in almost the same plane as the visceral side of the base, i.e., it is nearly horizontal (Fig. 17c). The low lateroposterior basal ring contrasts with the thick anterior base. In P9049 (Fig. 18) a certain parallel course of the crown ridges is noticeable (Fig. 18b). Anteriormost the inter-ridge space tends to be constricted. Short oblique side ridges in upper neck. Base with blunt forward extension. Visceral basal surface flat. In this and other scales (Figs. 12b, 17c), the anterolateral upper basal rim ascends anteriad. Angle of ascent best visible in lateral view (Fig. 18a). The feature is always associated with a horizontal course of the entire visceral basal surface, inclusive of spur. The feature also occurs in multicuspid scales (Gross, 1967, pl. 2, fig. 17a). Gross gave no comment. Contrary to the position that the horizontal visceral surface of the base suggests, these scales were probably inserted in the corium at an angle instead of horizontally, with the anterior scale part reaching deeper vertically

than the posterior part, perhaps as a compensation for body curvature. When such scales are illustrated in lateral view a false impression can be created of how the scale was fixed on the body in life in relation to the angle of insertion. Lateral views of scales without ascent of the rim convey a more factual impression of the scale's anchored position. Turner (2000, pl. 5, figs. 1-2) figured a large monocuspid *Thelodus trilobatus* scale from the Late Silurian of the Welsh Borderland with parallel crown ribs. This scale differs from the ones in Figures 17-18 by the lateroposterior extension of the crown over neck and base, and approaches a Scanian *T. trilobatus* variant (Lehman, 1937, fig. 20 IIIA), not observed from site C (cf. also *T. clavaeformis*; Lehman 1937, fig. 24).

Summing up, 'monocuspid *Thelodus trilobatus* scales' show considerable morphological diversity. Their morphological affinities are at least as close to *T. costatus* and *T. bicostatus* as to *T. trilobatus*. *Thelodus querceus*-like scales need not be part of the *T. parvidens* squamation. 'Neckless' forms include *Katoporodus* scales, forms with a lateroposterior neck could be part of a separate *T. costatus - bicostatus - trilobatus* scleritome. Despite the conflicting data, *T. querceus* is considered a useful name for the morphs described above, which are not regarded as an independent taxon.

Polycuspid scales (Figs. 19-23) — In P9052 (Fig. 19) the median crown cusp curves to the right, as does the basal spur. Possibly the orientation (curve) of the spur stands in relation to the orientation (curve) of the posterior crown ridges and the orientation of the entire crown as in P9055 (see below). The visceral surface of the basal ring is nodose. In P9053 (Fig. 20) the base has two diverging anteromedian spurs. The median prong extends forward, the other curves right (in anterior view). Nodose visceral surface of basal ring. In P9055 (Fig. 22) and P9054 (Fig. 21) a longer or shorter longitudinal ridge subdivides the median ridge pair of the crown; these scales have two basal prongs that curve left in anterior view. In P9055 the prongs are separated and the crown is oriented left (Fig. 22a). In P9054 (Fig. 21) the prongs have a suture or a furrow. It is not quite clear whether the crown was polycuspid. Scale P9056 (Fig. 23) has a forward and crenulated anterior basal extension, with shallow longitudinal folds between the crenulations (Fig. 23a). Such features are possibly traces of rhizoid formation restricted to the anterior base. Lateroposterior base ring-like and low; visceral basal surface flat. The median ridges on the crown converge and continue as a single median ridge posteriad.

Remarks on basal spurs — Apart from Silurian *Thelodus trilobatus* (Gross, 1967, pl. 2, fig. 14, from the 'Beyrichienkalk'), two or subdivided median basal spurs have been reported from Devonian turiniids (e.g., *Turinia pagei*: Karatajute-Talimaa, 1978, pl. 37, fig. 7; Turner, 1984, fig. 4.7A; *T. antarctica*, Turner & Young, 1992, fig. 7g; *T. gavinyoungi*, Turner, 1995, figs. 3U-V). Both *Thelodus trilobatus* and the turiniids are of the Thelodontida Karatajute-Talimaa, 1978. Double spurred specimens of *T. trilobatus* from the Scanian Ludlow are only known from the Ramsåsa C sample. Within this material double spurs are very rare (*c.* five scales). Gross (1967, p. 19) thought that a doubled spur was a deformation, but now this condition is considered just another of the wide range of (sometimes bizarre) basal shapes that occur on some scales of some thelodonts. Turner & Van der Brugghen (1993) also remarked on pathology and basal

processes. In some Ramsåsa C scales, the two spurs could represent a transition to a more rhizoid base. Compare this with a scale of *Turinia australiensis* from western New South Wales (Turner, 1997, fig. 4J) and one of *Australolepis seddoni* (Turner, 1986b, fig. 3P). In the turiniids more spurs would seem commoner than in *Thelodus* (*trilobatus*), but the feature might just have been more commonly illustrated. Comparative figures are not available. Perhaps the feature can be used as a marker for a particular stratigraphic level within Öved Sandstone Formation. The notches between some spurs (Figs. 20, 22) might represent openings for the lateral line system.

***Thelodus sculptilis* Gross, 1967**

Figs. 24-32; 33-41?, 42-45.

Remarks — This section describes *T. sculptilis* scales with features that have received little attention.

Cephalopectoral scales (1) — The lateroposterior crown edge of P9067 (Fig. 30) is shallowly notched and lobed. Anteromedian crown with pair of grooves characteristic of the species. Smooth crown surface flat in central part, with ventrad curving margin all around. Microstructures (dentinal features?; no ultrasculpture) occur on the curved surface (not visible in the printed photos). P9068 (only scale) has a chiefly smooth pentagonal crown with one broken edge. Anterior crown strongly curved (Fig. 31b). A pair of shallow anteromedian grooves fading out towards mid crown and a more lateral groove (right crown half; Fig. 31a) divide the anterior crown into 3-4 lobes (Fig. 31b), like a trilobite cephalon. The lobulation affects the course of the anterior crown rim. Crown overhangs neck all around. Lateroposterior, vertical neck ribs. Central base concave (Fig. 31b). Anterior base damaged (Fig. 31a).

Cephalopectoral scales (2) — *Thelodus radiosus* Lehman, 1937 - or, where the following taxa meet, *T. sculptilis* Gross, 1967, *T. admirabilis* Märss, 1982, and *T. parvidens sensu* Gross, 1967. Gross (1967) first described and figured *T. sculptilis* from Ramsåsa Quarry (site F) and thought it was a short-lived taxon confined to Scania. The histology was *T. parvidens* type, crown morphology was diagnostic; rhombic, often broader than long, with deep, sharp furrows (deepening anteriad) and ridges. Posterior crown rim cuspidated (up to seven cusps), often with median peg, or triangular with shorter or longer furrows anteriad. A strong median rib pair could be present. Length 0.4-0.7 mm, width 0.3-0.7 mm.

Märss (1982) diagnosed *T. admirabilis* as medium-sized thelodont scales, with convex or flat crown, anterior edges downturned. The crowns have ridges that tend to be lobulated, represented by steep centrad furrows on the anterior body or longitudinal furrows on posterior body scales. Deep notches separate the medial from the lateral lobes in the distal scale part. When comparing it with other *Thelodus* species, Märss (1982) wrote that the numerous dentine ridges and steep furrows between them, and a pointed peg-like posterior projection, characterise *T. admirabilis.* Most of the crowns of *T. sculptilis* scales are anteriorly bifurcated. The furrows are not steep. It is uncertain whether smooth scales from the Kuressaare and Kaugatuma Stages belong to *Thelodus parvidens* only or also to *T. sculptilis* and *T. admirabilis*.

What exactly Märss (1982) meant by smooth scales was not stated, but is crucial to distinguishing between these species. Smooth scales of *T. parvidens* have no furrows or pegs. The posterior crown rim is triangular and the anterior rim is a smooth line, i.e., without crenulations, notches or furrows. Such a rim was not mentioned in the species diagnoses of *T. sculptilis* or *T. admirabilis*, but is illustrated in two scales (cephalopectoral and postpectoral) of *T. sculptilis* from the Ludlow Tahula Beds (Märss, 1986b, text-fig. 21, fig. 18, pl. 23, fig. 10, where the anterior rim has just a very slight fold). If smooth *T. parvidens* scales are part of both the *T. sculptilis* and *T. admirabilis* squamations, this may imply form grading of the scales of these species to smooth *T. parvidens* scales. By their nature the crowns of such transitional scales should have anterior rims without notches, furrows or crenulations, and triangular posterior rims. Their surface should not be entirely smooth, but bear few furrows and, depending on the spacing between the furrows, ridges. Such forms will be discussed below.

Apart from ornament typical of a specific place on the body (body zonation series) and ornament gradation (morphoseries), the crown ornament of many *Thelodus* scales from Ramsåsa reflects a certain conservatism. It recalls the ornament of older taxa from the region and, in particular, that of the *laevis, schmidti* and *goebeli* forms, even though these differ histologically. For this reason it is hardly surprising that determination of Scanian *Thelodus* scales on the basis of morphological features alone (by lack or negligence of histological features) should have lead to identifications referring these scales to one of the older taxa. Lehman (1937) introduced new taxa for forms that he could not assign to any available species. One of these was *Thelodus radiosus* (*op. cit*., fig. 21), assigned to *T. schmidti*? by Turner (1984). The anterior crown rim and margin are smooth, and beyond this smooth zone the crown surface carries *c.* ten straight and short longitudinal ridges. A scale identified as *T. schmidti* by Lehman (1937, fig. 7) has a smooth anterior crown rim interrupted by one shallow longitudinal furrow and fewer (4-5), somewhat longer, radial ridges. Turner (1984) reassigned this scale to *T. sculptilis*. In the Scanian material these two specimens fit within a morphological series comprising smooth *T. parvidens* forms on one end, and Late Whitcliffian scales with *T. parvidens* histology and referable to other groups (e.g., *T. admirabilis*, *T. traquairi*) on the other end, with the *T. sculptilis* squamation placed in an intermediate position. Such transitional variants will be referred to as forma *T. radiosus* or radiosiform, below.

Forma T. radiosus, or the radiosiform scale type (Figs. 33-41) — On the basis of all available information, the specimen in Figure 26 is readily identified as *T. sculptilis*. It has an uninterrupted anteromedian crown rim of considerable length.

P9070 is a good starting point for the radiosiform series. The smooth anterior crown rim has a short midanterior notch (Fig. 33a). Right anterolateral margin (Fig. 33b) with almost imperceptible notch. The two notches mark off a midanterior zone (Fig. 33b), but the crown is not anteriorly bifurcated, nor are the crowns of other scales described below. Triangular posterior rim. Although this specimen is still wrapped up in a 'jacket' of sediment (Fig. 33c), it is clear from the sharp edges of the neck ribs that the general morphology was only moderately affected by post mortem causes. The original shape is rather well-preserved and this also applies to the other scales treated in this section.

Several specimens have an undivided anterior and a triangular posterior crown rim. P9071 looks like a smooth *T. parvidens* crown (Fig. 34a). In dorsolateral view (Fig. 34b) a pair of shallow median furrows marks off a narrow central region from wider lateral regions. P9072 (Fig. 35) shows one shallow crown furrow, noticeably wider than those in Figure 34b, reaching from the anterior crown edge posteriad. Two shallow and rather wide furrows mark off the median crown part in P9073 (Fig. 36). A tiny, epifaunal gastropod or *Spirorbis*-like fossil was observed on the crown (barely visible in the photos). Some scales have radial ridges. In one (Fig. 37) four blunt ridges are seen, with narrow furrows marking off the right from the left crown half and deepest in mid crown. The two most lateral furrows to the right affect the anterior crown rim minimally. Another scale (Fig. 38) has a furrowed anterior crown rim. Four to five rather sharp, parallel longitudinal ridges with intermediate grooves dissect the median crown, whereas the lateral parts are smooth. A more inclined and laterally compacted scale with converging ridges and perhaps slightly deeper grooves, and without smooth lateral crown areas has been assigned to *Thelodus traquairi* (Fig. 57a). More and coarser ridges and more furrows are seen in P9076 (*T. admirabilis*; Fig. 39), which is as much a *T. admirabilis* as a *T. sculptilis* scale (cf. Märss, 1982, pls. 2-3).

Two specimens have posterior pegs and one furrowed crown half, with the furrows affecting half the anterior crown rim. A posterior peg, slightly turned to the right, occurs in one scale (Fig. 40). The furrows mark off the right from the smooth left crown half. The two most lateral furrows are deepest at the anterior crown margin. The ridges become more lobate anteriad. The right crown half of the other scale (Fig. 41a) is more distinctly furrowed than the smoother left. The furrows only affect the right anterior rim. A central crown zone is marked off. There are three to four sharp ridges (Fig. 41b). The crown has a midposterior notch, the beginning of a peg. The anterior crown of cephalo- or postpectoral scale P9069 (Fig. 32) is downturned; the anterior rim is lobate in the left half; the right crown surface is rather smooth. A posterior peg is absent.

Discussion — Not all the figured radiosiform scales can be assigned to any of the species under discussion (inclusive of *T. traquairi*) without revising the diagnoses of these species. The fauna as a whole does not support the reintroduction of *T. radiosus* as a separate species because the scales cannot be placed within a distinctive independent series. More important than assigning the scale to any taxon is that they are another illustration of how closely the scales of these species are linked morphologically at the time of the deposition of the Ramsåsa C material; from practically smooth to grooved, from shallow to deep furrows, from slight or no anterior notch to anterior bifurcation, from pegless to posterior peg. An increase in furrows, deeper furrows or deeper pegs produce *T. admirabilis* scales. The transition from one (supposed) species to the other, from smooth *parvidens* to (radiosiform) *sculptilis* to *admirabilis* or *traquairi*, is a matter of shape and ornament of the crown becoming more and more complex. Märss (1982, pl. 3) noticed that the ornamentation within *T. admirabilis* becomes more complex in younger beds of the Kingiseppa core. This tendency coincides with the transition between the Tahula and Kudjape Beds of the Kuressaare Stage of the Ludlow (Märss, 1986b, text-fig. 33). Progressively more complex crown ornament can also be observed within the radiosiform scale series in the Ramsåsa C and other Scanian faunas. How should the increase in complexity in the ornament of this form group be explained?

By form grading between scales on different positions of the body in one species, *T. sculptilis*, as suggested by Märss (1986b)? Gross (1967) did not record radiosiform *T. sculptilis* scales. By form grading between the squamations of several species? By factors related to the deposits (or their sequence) from which the scales were won? Whatever the explanation, this finding makes it hard, if not impossible, to keep some scale forms apart at the species level in the Ramsåsa C material.

The morphoseries discussed above are profusely illustrated by Lehman (1937), e.g., Lehman's figs. 4A ('*Thelodus carinatus*'), 5A-7A ('*T. schmidti*'), 10A, 12 I, IX, XIV, XVI, XXI, 13 IV, 14 ('*T. Goebeli*'). Note that Gross (1967) considered the original '*Coelolepis goebeli*' Pander, 1856, a scale form of *Thelodus schmidti* (Pander, 1856) based on similar histology (reclining dentinal tubules) and the absence of round head scales in *C. goebeli*. I prefer the term radiosiform (*parvidens* histology; straight dentinal tubules) to goebeliform because of the shape of the dentinal tubules in the latter. The scale morphologies of the '*schmidti*' histological type, however, show form gradings similar to those with *parvidens* histology described above (cf. Gross, 1967, pl. 1, fig. 29; *T. schmidti* "Schuppe, zu *Thelodus laevis* überleitend", from K1 beds, Wenlock, Saarema, Estonia). Also, see Märss (1986b, text-fig. 18; body zonation scheme for *T. laevis*, from K1, Wenlock, Vesiku Beds).

Polycuspid, postpectoral scales (Figs. 42-45) — The smooth lateral crown wings, the slight longitudinal inclination of the crown, the lateroposterior neck ribs and the absence of an anterior basal process mainly distinguish P9079 (Fig. 42) from scales of *T. trilobatus* (cf. Gross, 1967, pl. 2, fig. 13a-c). The overall similarity to scales of that taxon is as striking as the differences. This also applies to P9080 (Fig. 43), in which the neck is obscured by sediment; each lateral wing bears a longitudinal ridge. Whether the differences are distinctive enough at the species level is another matter. The presence or absence of a basal spur can be growth-related, but was also linked to body position by Märss (1982, 1986a). Regional biostratigraphical evidence (vertical sequence of particular morphs) plays a prominent role in distinguishing between *sculptilis* and *trilobatus* scales, but the present material is unsuited for stratigraphical testing. P9081 (Fig. 44) might grade to P9079; it has an extra ridge on each lateral crown wing and six robust, radiating, smooth posterior blades rather than cusps. It appears to be a characteristic *T. sculptilis* scale, even though it represents a variation from contemporary Estonian forms (cf. Märss, 1986b, p. 45, pl. 23). In scale P9082 (Fig. 45) more pronounced lateral furrows mark off flat and more distinct ridges; median ridge forked; posterior crown rim crenulated. The posterior quarter of the crown shows restricted surface wear (smoothening), which stands in contrast to the fragility of the sheet-like posterior neck ribs that seem unaffected. Polished wear of the external posterior crown is rather common in some *Thelodus* scales (cf. Figs. 35b, 36b) and in the glabrous variants can take on a characteristic lozenge-like pattern, which might result from lifetime factors (e.g., sliding motion, imbrication or a combination of these; or the pattern could indicate that the crown had not completely broken through the corium and was still partly covered by it). Compare with Turner (1991, pp. 100, 102) on imbrication and on (striated) wear patterns.

Pinnal T. sculptilis scale? (Fig. 28) — P9065 (Fig. 28) has a moderately inclined, triangular crown with a narrow, median, triangular, slightly raised platform which

gradually passes into a posterior ridge that ends in the midposterior crown tip. The platform has a median furrow. Two deeper, longitudinal furrows separate the platform from the sharp lateral crown rims, of which one has anteriorly widened out into a smooth and flat lappet. Visceral crown smooth. Anteriorly, a constriction indicates where the crown passes into the neck. Compare this crown with the one in Figure 27. Lateroposterior neck marked off by vertical riblets. Low rhomboid base about as deep as neck. Lateral crown lappet, receding oblique anterior neck (Fig. 28b) and basal depth distinguish this only specimen from a scale from Ramsåsa H (Vergoossen, 2002a, Figs. 9, 48, 54) considered crucial in illustrating a transition from *T. traquairi* 'horn-like' (head?) scales to a subulate scale type from the posterior body. Subulate forms like those from site H are rare in the present sample (five, from the 0.106 fraction).

Thelodus admirabilis Märss, 1982

Figs. 29?, 39.

Remarks — Within the sample, scales of *T. sculptilis* are much more numerous than those of *T. admirabilis*, of which only the more extreme forms can be distinguished. These forms (Fig. 39) resemble those of the older beds of the Kingissepa core best (K3aT, Ludlow, depth 12.40 m; Märss, 1982, pl. 3). Some of the postpectoral specimens described under *T. sculptilis* (e.g., those in Figs. 44-45) might belong here.

Oral or cephalopectoral T. sculptilis or T. admirabilis scale? — Crown of P9066 (Fig. 29) rhomboid, with sharp ridges and deep folds directed posteriad and with a small smooth flat central area. Ridges slightly lobate where they bend centrad at right angles and up from the neck. Midanterior ridge pair is given extra prominence (Fig. 29b) by the folds flanking it; these are wider than the folds between most other ridges. Narrow, flat, midposterior crown ridge with 'ventral' keel (Fig. 29a). Steep neck with *c.* 4-5 vertical riblets per 0.1 mm lateroposteriorly. Latero-anterior neck smooth. Neck/base junction marked by sharp upper basal rim. Rhomboid, low, convex base slightly thickened anteriorly (Fig. 29b).

Thelodus traquairi Gross, 1967

Figs. 46-65, 110.

1937 *T. ramosus* [sp. nov.] Lehman, pp. 31-32; fig. 25. Ramsåsa, loc. F.
1937 *T. Schmidti* Pander; (Lehman, pp. 20-21; fig. 5). Ramsåsa, loc. F.
2002c *Thelodus* cf. *T. traquairi*; (Vergoossen, pp. 111-113; figs. 59-60). Ramsåsa, loc. D.
2002c *Thelodus* sp. indet. (Vergoossen, pp. 115-117; figs. 78-81). Ramsåsa, loc. D.

Remarks — The sample contained enough scales of this species to illustrate several morphoseries. The scale variation confirms or supports previous identifications of forms that could only doubtfully be grouped with *T. traquairi* because their morphology was too different or too rare or too general; the latter is especially true for head scales.

High crowns are exceptional in site C material. Gross (1967, p. 20) characterised the slightly different *T. traquairi* scales from the Ramsåsa beds as follows; strongly inclined crowns (his illustrations show strongly angular forms), 'wing forming' of the ridges weaker, neck and posterior neck ribs better developed, common ridge forking,

thickening of proximal ridge ends and forming of basal humps. These observations are confirmed by my research, which has not given further reason to assign this scale group to any *Lanarkia* species on the basis of close morphological affinity (Vergoossen, 2002a, c). Recently, Märss (1999, p. 1090, 1092) used the term '*traquairi* type' for high cone-shaped scales of what she interpreted as (previously unknown) head scales of *Nikolivia elongata* from the Boothia Peninsula, Arctic Canada (Late Silurian-Early Devonian). The presence of a 'transitional morphoseries' (within a 1.2 m high section) to conventional *N. elongata* scales was used as an argument to support this interpretation. The term '*traquairi* type' in this sense comes down to transferring a series of features distinctive at the species level to the generic level, but the implications for *Thelodus traquairi* as an independent taxon were left undiscussed. In microvertebrate palaeontology, no doubt inspired by biostratigraphical constraints, 'transitional morphoseries' have become widely accepted as a tool to group morphs into taxa (*vide* the present paper), but the reliability of the tool is questionable, especially when histological back-up is lacking, either because the microstructure was destroyed or when it is not diagnostic at the species level. Both are the case in the material from Ramsåsa C, D, H.

Form grading between scales from different body areas can be wholly absent in squamation types in modern sharks (see illustrations in Reif, 1985). The hypothesis that all morphological variation in recent shark scales can be derived from a simple standard scale type by morphological transformation (Reif, 1985) and the hypothesis that each thelodont body was covered by transitional morphoseries of scales are separate concepts that must each be proved in its own research field.

When scale forms (within a limited group of well-known taxa with clearly defined (series of) scale variants, preferably from one stratigraphic level) cannot be placed within an existing scale series and no new species can be created for these forms because they do not show enough variety, 'transitional morphoseries' are of no use at all. My research has partly focussed on such scales in the Scanian material. Reliability of the tool also becomes questionable when scale types were 'forced' into series, e.g., when they were won from different stratigraphical levels. This factor was ruled out as much as possible for the Scanian material by the listing of assemblages per rock. Relatively rare and isolated morphs on a fish body, or morphs from a much-restricted place might hardly show transitions to other squamation types. If scales from a fish with a predominantly uniform integument were placed within a squamation showing 'transitional morphoseries', then the mistake might never be discovered without complete fish. One way to reduce the chance of such errors is to keep an open eye and to offer sensible alternatives, preferably as many as possible.

Head (?) and transitional to head(?) scales — The crowns of the head? scales (cf. Fig. 46) can closely resemble crowns of *Thelodus costatus* (Pander, 1856) *sensu* Gross, 1967. The midposterior dorsal or ventral crown can show considerable morphological variation (depending, for instance, on density or length of the ridges, or their angularity). Compare the scales in Figures 55c and 56c; contrary to the first, the latter has a convex, smooth, midposteroventral crown. On the smoothness of the posterior crown in scales of '*Lanarkia costata*' (= *T. traquairi*), see Gross (1947, p. 109). An angular midposterior 'ventral' ridge is seen in the oral? scale in Figure 60b. Also compare the scale in Figure 48c with that in Figure 51a, in which the midposterior dorsal ridge has become flat

and blunt, and almost 'peg'-like. A peg is also developed in the more post-pectoral?/trunk? scale type in Figure 61b. *Thelodus sculptilis* and *T. admirabilis* crowns can have similar midposterior crown features and 'pegs'. The morphological variability of the peg is not known. All this variety may have got to do with the transition from/towards more conical/ costatiform or other (radiosiform) head scale types in *T. traquairi.*

Within the current interpretation of the scleritome squamations of *T. sculptilis, T. admirabilis* and *T. traquairi* form grading occurs (see also section on *T. radiosus*). In the Estonian sequence (Märss, 1986b) and model for the Microvertebrate Standard, these taxa first appeared nearly simultaneously. The differences in scale morphologies could have developed by increasing ornamental complication from ancestral oral/ cephalo-pectoral regions, when viewed from the perspective of the reconstructions made by Märss (1986b) of the complete squamations of these scale taxa. For a different view on the 'derivation' of different squamations, see Turner (1991, p. 111), who considered *T. trilobatus* (postpectoral in Märss's concept) "a good basic scale type from which to derive the later forms of *Turinia*, *Apalolepis* and the nikoliviids."

Conical, costatiform, oral(?) scales — In apical view (Fig. 46a), P9083 shows a conical crown (*c.* 0.5 mm high) of eight converging sharp ridges, one with ventrad bifurcation some distance below the top. The spacing of the ridges is slightly irregular. The crown widens slightly anteriad. Well-developed neck (Fig. 46b) with *c.* 6-7 lateroposterior vertical ribs per 0.1 mm. Convexity and length of neck ribs increase posteriad (Fig. 46b). Some neck ribs bifurcate. Oval base with upper basal rim. Midposteriorly the continuity of the base below the basal rim is interrupted (Fig. 46b).

Other oral(?) scales — P9084 looks costatiform in anterior view (Fig. 47c), but instead of being conical, the crown is drawn out longitudinally into a blunted midposterior peg. The radial, anterolateral crown ridges have steep, convex anterior bifurcations and alternate with deep grooves up to where they converge in the flat and smooth midposterior crown. Some ridges are gently concave (Fig. 47c). The steep posterior ridges (Fig. 47a) do not bifurcate. The neck and round rhomboid base are low. This might be a *T. sculptilis* scale, but is here presented within a framework of scales (Figs. 47-62) grading into ramosiform scales (see below).

Scale P9085 (Fig. 48), the only specimen of this morphology, is longer than wide and has a horizontal sharp middorsal ridge, which is slightly sigmoid (Fig. 48b-c) and bent to the right in its posterior part. This ridge is the continuation of a converging pair of sharp anteromedian ridges (Fig. 48b) that curve up from a very low neck and bend centrad at *c.* 90°. Two sharp, lateral ridges (one on each side of the median pair) run into the median ridge. Two shorter, intermediate lateral ridges (one on each side) do not reach the median ridge. The first and anteriormost lateral ridge is distinctly denticulate; two dents stand out (Figs. 48a-b). A pair of sharp, posterior ridges converges gable-like (Fig. 48c) at the posterior end of the median ridge. Under the gable, there is either one short midposterior neck rib (Fig. 48a) or an intermediate ridge. Low base sloping ventrad, ventrally flat and with anteromedian constriction (Fig. 48b).

The crown of P9091 (Fig. 54) is further elongated and distinctly asymmetric (with rightward twist; Fig. 54a). It has a deep anterolateral fold (right crown half; Fig. 54a)

that reaches the midposterior crown top and is flanked by a pair of subparallel, sharp ridges, one anteriorly trifurcating, the other bifurcating. All ridges ascend steeply from the neck *ab centro,* but soon curve centrad at almost 90°. The lateral ridges end in the median ridge pair and can bifurcate some distance below the junction (Fig. 54b). The posteriormost lateral ridges and the median pair form the midposterior crown top. One or two posterior ridges do not reach the top (Fig. 54b); they stand out and end rather abruptly (Fig 54b-c), as if broken off. Neck higher posteriad than anteriad, with vertical convex ribs. Base and neck make up less than half total scale height. The scale fits both within *sculptilis* and *traquairi* morphoseries.

Transitional to head? scales: forma Thelodus ramosus Lehman, 1937, or ramosiform scales — Scales with a single, unpaired, longitudinal middorsal ridge are more common than the previous form (sole specimen). Vergoossen (2002c, figs. 58-59) discussed two such specimens and affined *T. sculptilis* scales from Ramsåsa D. The morphology of the new finds (Figs. 49-53) compares well with that of '*Thelodus ramosus*' Lehman (1937, fig. 25), re-assigned to *T. traquairi*? by Turner (1984). These variants will be referred to as forma *T. ramosus* or ramosiform, a morph within the Baltic *T. traquairi* scale group. Shared crown features comprise: (1) sharp, oblique, lateral or radial ridges (with intermediate folds) often ending in a longitudinal, sharp, middorsal ridge; (2) the ridges can split up anteriad; and (3) the posterior crown point is often formed by the convergence of the middorsal ridge with a couple of lateral and radial ridges. These features are usually combined with a moderately high neck (all around) which possesses densely packed, convex vertical riblets lateroposteriorly. The crown can vary from rhomboidal and gently sloping posteriad (Fig. 52a) to elongate and nearly horizontal (Fig. 51b). The ventral crown surface between the posteriormost lateral ridges can be wide and smooth (Fig. 53a), and also slightly convex and inclined, which helps to distinguish ramosiform *T. traquairi* from *T. sculptilis* scales. Lateral, intermediate crown ridges and short, upper posterior crown ridges (Fig. 55c) also occur. Intermediate ridges are also not uncommon in conical crowns. The posterior crown point may be smoothed dorsally (Fig. 51b; this specimen also has a smoothed, i.e. wider and coarser, dorsal ridge). In rhomboid ramosiform scales (Fig. 55), the laterad and posteriad shift of the middorsal branching points of the lateral ridges makes the middorsal ridge less conspicuous; such a shift leads to the crown type of P9094 (Fig. 57); compare with the elongate ramosiform scales in Figures 49a, 51b. In P9093 (Fig. 56) a middorsal ridge and associated branching are absent; instead there is a single midposterior converging point, the distal crown point. These features are related to the more general modification from an elongate scale shape to a wider shape with rhomboid crown, and concomitant shortening of ridges. A combination of these changes, without concomitant ridge shortening, leads to P9098 (Fig. 61; see below). That a P9094 crown (Fig. 57) could lead to a radiosiform rhombic crown with parallel ridges is considered less likely, because the latter (Fig. 38) has a distinct anterior crown rim, a feature not known in conventional *T. traquairi* scales.

Postpectoral or trunk scales? (1) Thelodus traquairi and forma baltica, new form: scales with a prominent anteromedian base — P9098 (Fig. 61) fits within a series of progressively flat-

ter and smoother forms with shortening ridges and distinct spurs (Vergoossen, 2002a, figs. 24, 25, *T. traquairi*; Vergoossen, 2002c, figs. 78-81, *Thelodus* sp. indet.). This series might indicate a transition to cephalo/postpectoral/trunk scale types. P9098 is broader than long. The crown has a semicircular outline anterolaterally (Fig. 61a) and is straight posteroventrally (Fig. 61b). The anterolateral crown consists of alternating deep furrows and midposteriorly converging thin ridges. The ridges ascend *ab centro* from the neck and bend centrad at an angle of about 90°, and at *c.* one third of their total length. From that bend to the crown top, their slope is relatively low. The top has a blunted, triangular, peg-like projection (Fig. 61b) formed by the converging posteriormost lateral ridges. Ventral/posterior crown steep, smooth and spread-wing-like (Fig. 61b). Neck low all around, with faint traces of ribs (Fig. 61b). The fairly deep base follows the outline of the crown and has a midanterior constriction that marks off a nodose, forward bulge (Fig. 61a), an indication of beginning spur or rhizoid formation.

The crown of P9099 is damaged and the midposterior converging point of the ridges has broken off. A short anteromedian ridge (Fig. 62a) possibly coalesces with the ridge to its right; the neck is a bit higher than the neck of the previous scale and the posterior neck ribbing is better expressed. The lateral view (Fig. 62b) shows the contrast between the massive anterior lump of the base and the lower posterior basal part.

P9100 (Fig. 63) has an anteromedian basal constriction, and a short, vertical and thick spur-like process. The crown is almost horizontal (Fig. 63b). The ridges stand out wing-like; they are shorter and their number is reduced when compared to the scale in Figure 61a. Both P9100 and the next, P9101 (Fig. 64), grade to a smoother crown with midventral keel; their crown projects markedly farther over neck and base posteriorly than the crown in Figure 61. A posterior crown peg is lacking.

In P9101 (Fig. 64, only specimen) an anterior neck is hardly distinguishable, as in P9102 (Fig. 65), which is a more elongate specimen with asymmetrical crown. This crown does not project over the base posteriorly (Fig. 65b); the anterior basal constriction (Fig. 65a-b) is better expressed than in the previous base. This scale brings us back to cephalopectoral scales of *Thelodus sculptilis*, which complicates any decision about identity.

Forms represented by such specimens as P9100 (Fig. 63) and P9101 (Fig. 64) would seem to derive from *Thelodus traquairi*, being also smoother and/or spurred variants of some of the scales figured from the "Upper Ludlow" of "Ramsåsa" by Gross (1967, pl. 4, figs. 16-18). Such scales as shown in Figures 63-64 are extremely rare in roughly contemporary material from the Estonian Tahula Beds at my disposal (Fig. 110; histology of *T. parvidens* type *sensu* Gross, 1967). Similar forms, associated with conventional *T. traquairi* scales, are not rare in an undescribed fauna (sample V-Ri/9g/1), from Ringerike, '9g', Oslo basin, Norway (for further remarks on this fauna in relation to the Ramsåsa faunas, see section on forma *bifurcata*, and also Vergoossen, 2002a). However, these forms were also noticed in contemporary *T. sculptilis* faunas from erratics from Groningen, northern Netherlands, without conventional *T. traquairi* scales. Regardless of species, the *Thelodus* form group represented by the scales in Figures 63-64 and those in Vergoossen (2002c, figs. 78-81), are here designated forma *baltica*, new form. If forma *baltica* scales should derive from a new species, this taxon must be closely related to a known species, since other scales of the new species which might fit into the morphoseries with forma *baltica* are not specifically distinctive enough to be detected in any material examined.

Postpectoral or trunk scales? (2) — A posteriad migration of the convergence of the ridges along the longitudinal axis or midline of the crown is illustrated in the series of scales comprising the specimens in Figures 60 (head/oral scale?), 58 and 59 (trunk scales?). The posteriad migration of the converging point of the anteromedian ridge pair (Figs. 60b, 56a, 59a) is particularly well illustrated. The laterally compressed crown (Fig. 58) transforms into a broader, more rhomboid crown (Fig. 59), the number of ridges is reduced (Figs. 58, 59) and a more or less horizontal (Fig. 60) crown becomes an inclined crown (Figs. 58, 59). These changes do not wholly agree with a change from oral (Fig. 60) to postpectoral or precaudal scales (Figs. 58, 59) in terms of the body zonation concept of Märss (1986b).

Although the crown of P9097 (Fig. 60) has no middorsal ridge, its features are comparable to crowns that have such a ridge (ramosiform scales and the one in Fig. 54c). The anterolateral ridges are lobate where they curve centrad. The lateroposterior neck ribs are robust. Scales P9096 (Fig. 59a) and P9095 (Fig. 58a) have fewer ridges (five). In anterior view, the crowns compare with that in Figure 62a. In P9096 the ventral crown surface is steep and smooth (Fig. 59b). Where the lateroposterior crown rims meet, at the midposterior top, they form an angular, gable-like structure (Fig. 59b). Anterior to the lateroposterior rim (Fig. 59b) the smooth crown border widens distad. One of the median ridges widens anteriad (Fig. 59a). The base is low. In P9095 (Fig. 58) the narrower crown has a median ridge pair flanked by down-stepped side ridges (Fig. 58b). There is a distinct anteromedian basal lobe (Fig. 58b). Many of the features recorded in this section are also seen in the body zonation scheme for *Thelodus sculptilis* scales from the Ludlow Ramsåsa beds by Märss (1986b, text-fig. 22), but the general morphology of the latter is different.

Thelodus sp. cf. *T. traquairi*

Figs. 66-69.

Description — In anterior view, the general outline of the crown of P9103 (Fig. 66) is reminiscent of P8842 from Ramsåsa H (Vergoossen, 2002a, fig. 27; *T. traquairi*), in posterior view of a *Thelodus* cf. *traquairi* scale from Ramsåsa D (Vergoossen, 2002c, fig. 61b). The rhomboid crown has a raised median pair of ridges, slightly constricted anteriorly and on a converging course posteriad (Fig. 66a). These median ridges stand some distance back from the anterior basal rim. They ascend rather steeply from the upper base (neck absent anterolaterally), but soon bend posteriad and continue straight in that direction with little slope. The fold between the ridge pair is shallow. About half way along the length of the scale the lateral crown rims ascend *ab centro*, to bend back centrad at *c.* 90° (rounded angles) at halfway or less of their length. Lateral rims and median ridges meet midposteriorly (Fig. 66b). The surface between the median ridges and lateral rims is shallowly concave (Fig. 66c). The lateral crown parts have a wing-like ('spread' wings) appearance. Actually, in their lower half the lateral rims consist of two converging rims, with a shallow intermediate fold (Fig. 66b). Vertical ribs mark off the posterior neck from the smooth and steep posterior/ventral crown surface. Rhomboid base swollen, deeper anteriorly than posteriorly.

Spurred and other (postpectoral?) scales — In anterior view P9105 (Fig. 68) resembles the previous scale and, in side view, even more P8842 from Ramsåsa H (Vergoossen,

2002a, fig. 26). The median platform is more raised, closer to the anterior basal rim and narrower; further narrowing could lead to the morphology of P8842. The median ridge pair is more constricted anteriorly. Spurred base and orientation of spur are shared with P8842, but the base is thicker (and the scale older) and has an anteromedian constriction.

P9104 may or may not belong here. The side view (Fig. 67b) shows similarity to that of P9103 (Fig. 66b). The main differences are in the anterior part of the median ridges with intermediate fold and in the presence of an anterior crown rim, which has receded on either side of the median ridge pair (Fig. 67a). These features are not unusual in *T. traquairi* and *T. sculptilis* scales (cf. Märss, 1986b, pls 22, 23). The median ridges are practically parallel along the greater part of their posteriad course and this contributes to a certain bicostatiform appearance.

Paralogania ludlowiensis (Gross, 1967)

Six small scales of *P. ludlowiensis* were collected. One is a transitional, sensory pore canal scale as figured by Miller & Märss (1999). The others are trunk scales. Loganellid histology could not be demonstrated in any Ramsåsa C thelodont scales.

Acanthodian fishes

Nostolepis striata Pander, 1856 *sensu* Gross 1947, 1971

Figs. 70-77.

Remarks — The analysis of *N. striata* trunk and topospecific scales (Vergoossen 2002b, c) is continued, with the aim of constructing a checklist of characters (see Appendix 2) and with the same restrictions.

Description of trunk scales — Slightly asymmetric scale P9108 (Fig. 70) is twice as long as wide and resembles '*elegans*' forms. The triangular, narrow, elongate crown is moderately inclined and has two parallel, longitudinal anteromedian riblets that bend up and posteriad from close to the basal edge. The crown rims ascend from slightly posterior to the riblets. The right crown rim (Fig. 70a) is more strongly curved in its lower part than the left, curving outwards lateroposteriad. Posterior to the curve the rims continue straight and meet at the sharp posterior point. The crown surface is constricted anteriorly (particularly on the right), and concave in the middle (behind the anterior riblets), and in front of the short, longitudinal midposterior ridge. The lateral crown ledge begins at the level of the broad axis of the base, is slightly curved in its anterior part, and joins the crown rim well below the top, near the point where the posterior crown overhang begins. Overhang *c.* one-third of total crown length. The crown has a sharp midposterior, ventral keel (Fig. 70b). Anteriorly the crown is almost as wide as the base, laterally there is a narrow neck zone. The lateroposterior neck is smooth and moderately high. Rhomboid base longer than wide, with slight median swelling. Neck-base junction forms sharp edge.

Slightly asymmetric scale P9109 (Fig. 71) (anterior surface facing left in anterior view) is twice as long as wide. Triangular, narrow, elongate crown moderately inclined

and with two fairly long midanterior riblets parallel to the crown rims (Fig. 71a). The riblets ascend from close to the basal edge and are not so strongly arched as those in the preceding scale. The left crown rim (Fig. 71a) ascends from the basal edge and at the same level as the left anteromedian riblet. The right crown rim begins further posteriorly and further away from the basal edge. In lateral view (Fig. 71b) the right crown rim is arched in its lower part. The rims run straight posteriad across a little more than half their length, from where they curve centrad towards the posterior tip. The curve of the right rim towards the centre is stronger than that of the left, which is actually slightly sigmoid. Crown medially concave and only very little constricted near the anteriormost part of the left rim. In the upper crown there is a ridge (Fig. 71b) which seems an extension of the right anteromedian riblet, with a piece in the middle missing. This ridge runs into the right crown rim just below the tip. The lateral crown ledges begin at the lateral axis of the base and run posteriad in a straight line (left ledge) or almost so (right ledge). The ledges join the crown rims near the point where these curve centrad (Fig. 71a). The posterior crown overhang is about one third. Low neck. The rhomboid base has sharp basal edges, is longer than wide and almost flat.

Symmetric scale P9111 (Fig. 72) is slightly wider than long, has a rhomboid, moderately inclined crown with rounded anterior margin on a rhomboid base with moderate central swelling. Seven short, anterior, longitudinally parallel crown riblets of different lengths rise from the neck and bend posteriad at right angles. Between the riblets the crown passes gradually into the neck. The crown rims begin posterior to the riblets and are convex in their anterior part, the left rim (Fig. 72b) more so than the right, and constrict the anterior crown surface. In their posterior part the crown rims are straight and converge in the posterior point. Crown smooth and flat posterior to the riblets, and smaller than base; only the crown tip overhangs the neck. Lateral crown rims absent. A broad neck, posterolaterally steeper than anterolaterally, surrounds the crown. The neck-base junction is sharply bounded. Symmetric scale P9113 (Fig. 74) is slightly longer than wide, has a triangular to rhomboid, moderately inclined crown placed medially on a rhomboid base with moderate central swelling. An anteromedian rib set of two short, longitudinal, parallel riblets arches up from the neck. The set is slightly projected forward (Fig. 74a). The riblets are slightly higher than the intermediate space (Fig. 74b, compare Fig. 71a). The crown rims are convex. They begin a little posterior to the rib set, constricting the lower crown surface, and meet in a posterior tip that overhangs the neck, but not the base. The angle at which the crown rims meet posteriorly varies considerably (compare specimens in Figs. 70a, 72a); the angle is related to maximum anterior crown and scale widths. The lateral crown rims (or ledges?) begin at the level of the rounded lateral basal corners and follow a diagonal course in the lateroposterior neck. It is not clear where they end or fade out. The crown is surrounded by a low, slightly sloping neck. The posterior neck was probably concave, as in the preceding specimen. The upper basal edge is blunted. Base larger than crown.

Slightly asymmetric scale P9114 (Fig. 75) is as wide as long, and has a triangular, moderately inclined crown on a rounded base with moderate central swelling. The outer two of the four short, forward-projected, longitudinal anterior riblets that ascend from near the anterior basal edge have a more radial orientation than the median ones (Fig. 75a); some riblets are positioned further posteriorly than others (Fig. 75b). The crown rims practically begin at the level where the anterior riblets fade

out (Fig. 75b) and constrict the lower crown only slightly. In anterior view (Fig. 75a) the right rim begins near the right basal corner, the left rim is further away from the left basal corner and follows a sigmoid course. The right rim is straighter in anterior view. The right rim has a slight twist centrad at one third of its anteroposterior course (Fig. 75b). The posterior crown tip is probably incomplete. The main crown surface is flat. The rather wide right lateral ledge runs from basal level, and from half way the basal length, diagonally posteriad (Fig. 75b). Anteriorly and laterally a narrow upper basal zone (variable in size) surrounds the crown. Only the tip of the crown protruded over the base.

Three scales deserve attention, but are unsuited for detailed description because of their indifferent preservation. Scale P9112 (Fig. 73) is noteworthy for its wide, right lateral ledge, which may have been denticulate. Compare Figure 73 with the *Nostolepis* scales from erratics from Groningen in Text-figs. 1 (RGM 323076, from RGM sample 296186) and 2 (RGM 323077, from V79), both not older than *Nostolepis gracilis* zone (early to middle Pridoli).

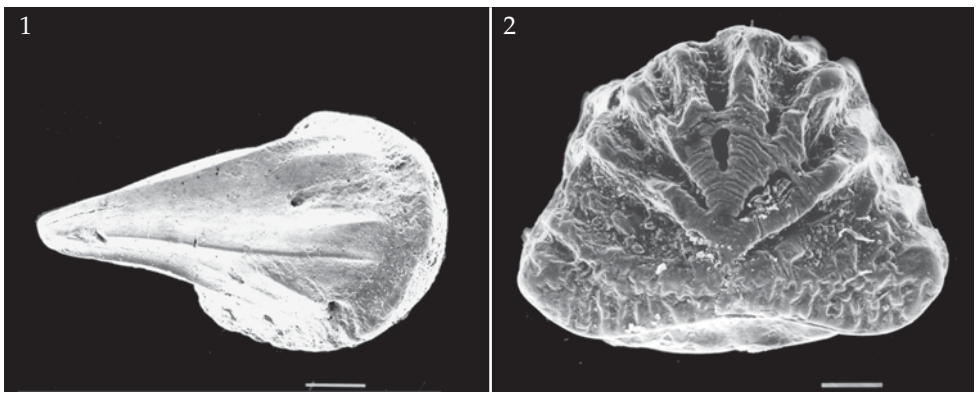

Fig. 1-2. Denticulate lateral ledges (1) RGM 323076. (2) RGM 323077.

In slightly asymmetric scale P9115 (Fig. 76) the anterior part of the rhomboid low crown nearly covers the whole anterior base. In anterior view the left crown rim begins at the basal corner and the right rim very close to it. The two anteromedian, forward lobes begin very close to the anterior basal edge (with damaged median part). The right lobe has a short longitudinal ridge on top (oriented laterad, Fig. 76b), the other lobe has a rounded top. Between the lobes is an anteriorly narrowing trough, which has a round to parabolic opening, largely covered by sediment (median opening in lower crown half). The crown rims lie somewhat higher than the sunken central crown surface (alternatively the upper surface of the mid crown region was removed). For the greater part the rims run straight posteriorwards to meet in the eroded tip. The left rim is longer than the right. In lateral view (Fig. 76b), the right rim curves up from anterolateral. P9116 (Fig. 77) represents a form variant described from Ramsåsa D (Vergoossen, 2002c, fig. 91a), but differs in details of the anterior crown (e.g., orientation of the anterior lobes) and of the base (e.g., straight anterior basal rim, and flat base in the present, only specimen).

Trunk scale feature checklist — Most scales in the sample could not be used for analysis because adhering sediment obscured important features or because of poor preservation. The feature list (revised and improved from Vergoossen, 2002c) is given in Appendix 2. Elaboration of previously listed features (new list numbers 10-11, old list number 11); mixed, e.g., twist of the right rim towards crown centre in upper crown part , all in anterior view (Fig. 71a)

Additional features (new list numbers): 8, ventral crown surface: midposterior keel; 9, starting position of crown rims: same latitudinal level, one rim beginning further posteriad; 12, in lateral view, one or both crown rims arched or not; 13, if arched, which rim and where: in its lowermost part, halfway or elsewhere (specify); 14, the angle at which the crown rims meet; 28, anterior riblets are arched or ascend from the neck at right angles; 30, starting position anterior crown riblets: same latitudinal level or not; if not which is/are positioned further posteriorly than others; 31, length of anterior riblets: of same or different lengths, laterad shorter or otherwise (specify); 37, median opening in lower crown half; 38, midposterior crown ridge; 58, neck-base junction with sharp edge, or blunted; 62, dimensions of base: longer than wide or wider than long.

General and taxon-related remarks on some listed features

Shape of crown (3): elongate crowns — Scales of Silurian to Lochkovian *Nostolepis striata* and allied taxa with such narrow and elongate crowns as the ones described from Ramsåsa C have hardly been figured, apart from those species that have elongate crowns for a regular feature, e.g., *N. arctica* Vieth, 1980. Where they have been figured, a considerable part of the posterior crown is usually missing. Such damaged scales will not, as a rule, be considered here.

'*Diplacanthoides sinuosus*?' Lehman, 1937 (fig. 62 therein) from Övedskloster is the best example illustrated by that author. This scale is twice as long as wide, but the crown does not protrude posteriorly; '*D. dilobatus*' Lehman, 1937 (fig. 29 therein), from Ramsåsa, with posterior protrusion of incomplete crown, was originally probably also twice as long as wide. *Canadalepis linguiformis* from the Lochkovian Member A of Red Canyon River Formation, Ellesmere Island, Canada, can have extremely narrow and elongate crowns (Vieth, 1980, pl. 7, figs. 10-12; the crown in fig. 12 is six times longer than wide), all contained within the base. The composite crown of *Nostolepis applicata* from the same Member A can consist of plates that are twice as long as wide (Vieth, 1980, pl. 4, figs. 8, 12a, 15). The first of the latter specimens is suggestive of *N. striata* tesserae (Gross, 1971, pls 2, 3). The shape of the shorter crown plates on some *N. applicata* scales (Vieth, 1980, pl. 4, fig. 13) resembles the blades on P9124 (Fig. 86b), a tooth? element described below.

Crown rims, starting position (9): one rim beginning further posterior — This feature is closely linked with the asymmetry of the *Nostolepis striata* scales, but is decidedly less frequently figured than scales where the crown rims begin at the same latitudinal level, even though many Late Silurian Baltic samples that I have examined contain numerous asymmetric specimens. The feature is also seen in '*Diplacanthoides retroincisuratus*' (Lehman, 1937, fig. 68a) from the 'Downtonian' of Saarema, in *Nostolepis* sp. A (Märss, 1997, pl. 6, fig. 5), Central Urals, Lochkovian (=*N. striata*, which occurs in the same sample, or a form common to more *Nostolepis* taxa) and in *Canadalepis lin-*

guiformis? (Märss, 1997, pl. 2, fig. 7), Kaliningrad district, Lochkovian (in fauna with *N. striata*). Valiukevicius (1998, pl. 1, figs. 4, 7) figured a *N. striata* and a *N. minima* scales on which one crown rim begins at the midanterior basal corner and the other further laterally. The feature is also present in *Nostolepis applicata* (Vieth, 1980, pl. 4, fig. 7; almost certainly *N. striata*).

Crown rims, anteroposterior path in anterior view (10): mixed — In asymmetric scales, the two crown rims will follow a different path in posterior direction, e.g., one rim can be concave, the other convex, as for instance in '*Diplacanthoides multiincisuratus*' from Saarema (Lehman, 1937, fig. 73A). One rim can also change course, as in sigmoid rims (also present in *Canadalepis linguiformis*, cf. Vieth, 1980, pl. 7, fig. 10a). In some anteriorly constricted crowns of both symmetric and asymmetric scales, one or two rims begin with a (convex) curve laterad, but continue posteriorwards in a straight line as seen, e.g., in '*D. trilobatus*' from Ramsåsa (Lehman, 1937, fig. 31 IA) and *N. striata* from the 'Beyrichienkalk' (Gross, 1947, pl. 26, figs. 7a-8a). A scale of *Nostolepis arctica* from the Lochkovian Member A of Red Canyon River Formation, Ellesmere Island, Canada (Vieth, 1980, pl. 5, fig. 8) has one convex and one much straighter rim, and both rims follow a more leftward course in the posterior crown tip. Sometimes the change in course is rather abrupt, as in a scale of *N. applicata* (Vieth, 1980, pl. 4, fig. 6).

Anterior riblets: length (31) — When the crown is placed close to the anterior basal edge, the anterior riblets in many Silurian *Nostolepis striata* crowns often do not reach the lateral axis of the scale (e.g., Gross 1947, fig. 6a). This also applies to '*Diplacanthoides*' scales *sensu* Lehman (1937), e.g., '*D. sinuosus*' (*op. cit.*, fig. 69A). Longer anterior riblets are noted in '*D. laterolobatus*' from Saarema (*op. cit.*, fig. 67A). Gross (1947, pl. 26, fig. 12a; 1971, pl. 6, figs. 1-2) figured scales of *N. striata* from the 'Beyrichienkalk' with anterior riblets that extend as far as or into the posterior crown half. These are not typical trunk scales in the sense that they show (series of) lateral denticulations and one specimen has a rather flat base. A *N. striata* scale with denticulated lateral rims was figured by Wang (1993, pl. 13, fig. 3) from the upper Gedinnian part of the Nogueras Formation, Celtiberia, Spain. It seems to have anterior ribs extending to the lateroposterior crown margin, but the exact morphology of the crown is not clear enough for proper evaluation. Perhaps the longest riblets, in combination with other features, are commonly associated with topospecific *Nostolepis* (*striata*) scale forms (e.g., tesserae), as would also seem to be born out by most of the following examples. *Nostolepis* sp. A (Märss, 1997, pl. 6, fig. 13; Central Urals, Lochkovian) has one(?) anteromedian rib(?) reaching into the posterior crown half; it looks like a transitional trunk scale. Lateral riblets and anterior crown surface are reminiscent of *N. arctica*, which may or may not occur in the same sample (this is unclear from the text). Scales of *Canadalepis linguiformis* can have far posterior-reaching riblets (Vieth, 1980, pl. 7, fig. 17) that almost reach the posterior crown rim. The anteromedian rib in *C. linguiformis*? (Märss, 1997, pl. 2, fig. 8, Kaliningrad district; Lochkovian) reaches almost as far as the midposterior crown rim. Anterior riblets of more than half the crown length are found on some scales of *Nostolepis applicata* (Vieth, 1980, pl. 4, fig. 7). A far-extending anteromedian rib, if it is one, can be observed in a *Nostolepis* aff. *multicostatus* specimen, from the Lochkovian of Lithuania

(Valiukevicius, 1998, pl. 4, fig. 3) and in another scale of the same taxon (*op. cit.*, pl. 4, fig. 5), where the anteromedian riblet is shorter but still long.

Long anterior riblets are also present in younger nostolepids such as *Nostolepis gaujensis* (Valiukevicius, 1998, pl. 8, fig. 8a, a trunk scale from the Frasnian Sventoji Regional stage, Lithuania), which has specimens with anterior riblets reaching into the posterior crown half, and in taxa other than nostolepids, e.g., *Cheiracanthoides planus* (*op. cit.*, pl. 3, fig. 9 Lochkovian, Lithuania). In *Nostolepis gracilis* Gross, 1947, a contemporary of *N. striata* from the Pridoli onwards, long crown ribs (extending from the anterior crown rim) are a regular feature.

Median opening in lower crown half (37) — This opening slightly differs from the one observed in a trunk scale (transitional to tessera?) of the *Nostolepis arctica* group from the Lochkovian of Dog Ditch Dingle (sample V921118), Welsh borderland, UK (Vergoossen, 1999c). Histological data are not available. Openings in the (median) crown have been recorded from Silurian scales of *N. gracilis* and other genera, e.g., Acanthodian (*Gomphonchus*?) sp. 1 (Vergoossen, 2000, pl. 2, fig. 22). In *N. striata* and allied taxa openings for vascular canals are known from the crown-base transition in tesserae.

Midposterior ridge (37) — This feature of *Nostolepis* scales has not been recorded hitherto.

Nostolepid platelets and tesserae

Figs. 78-83.

Remarks — The *Nostolepis striata* type of histology was observed in anise oil in one broken coronate? tessera. The best-preserved variations have been figured and are described below.

Topospecific platelet (Fig. 78) — P9117 has a pentagonal, slightly convex base with a low, posteriorly inclined, triangular, smooth denticle which is placed medially, and is surrounded by a slightly sloping, wide and smooth upper basal surface. There is a mid-posterior constriction (obtuse angle) where the low, steep posterior neck and the base meet. The anterior surface of the denticle is without anterior riblets and is a bit concave, possibly also from erosion. The platelet is *c.* 0.33 mm long and 0.28 mm wide. The place on the fish body of this plate type is unknown. Shoulder girdle elements such as pinnal and lorical palates usually have tubercular ornament. Smooth crowns without anterior riblets are known from such topospecific scale forms as *Nostolepis applicata* (Vieth, 1980, pl. 4, figs. 13-14), *Canadalepis linguiformis* (*op. cit.*, pl. 7, fig. 1) and from *Paranostolepis glabra* (*op. cit.*, pl. 6), all Lochkovian and from Arctic Canada. The present plate cannot be assigned to any of these.

Multitubercular, coronate plates (Figs. 79-81) — Rounded hexagonal plate P9118 (Fig. 79), *c.* 0.35 × 0.42 mm, has three ridged tubercles in line in the centre. The sculpture free zone of the plate is wide and slightly sloping. The tubercle on the left is linked to the other two at only one contact point; the other two share more contact points. The shapes of the tubercles differ; the one on the left is star-like (Fig. 79a). A curved, sharp

edge forms the top of the largest tubercle on the right (Fig. 79b). The base is concave on the ventral side. Plate P9119 (Fig. 80), *c.* 0.33 × 0.5 mm, lacks such prominent ridges on the tops of the tubercles (cf. Vergoossen, 2002a, fig. 93; 2002c, fig. 104). Part of the base has broken off. The more or less rounded quadrangular plate P9120 (Fig. 81) has three ridged tubercles arranged round the plate centre. The tubercles occupy most of the plate and lie close to each other, but the contact points (mainly in the central plate part) are obscured. A sloping narrow sculpture free zone leads to the plate edges. The tops of the tubercles are worn down. Two must have been pointed and these have *c.* five radial main ridges. The other tubercle is more irregular. The ventral plate side was concave. Size is *c.* 0.46 × 0.53 mm. The tubercular ornament looks like that on a coronate plate from Ohesaare (Gross, 1971, pl. 3, fig. 27), but the thickened central ridge that links the tubercles is lacking in the Scanian specimen. C. Burrow (pers. comm.) considers the ridges to look nodose, as on acanthothoracid placoderms, e.g., *Romundina*. Compare with the 'crenate' ridges in P8870 (Vergoossen, 2002a), a monotubercular plate from Ramsåsa H.

Stellate tesserae (Figs. 82, 83) — P9121 (Fig. 82) has four ridged tubercles on a concave basal plate with broken edges. The tubercles are linked in the plate centre, each by one main ridge. The main ridges of each tubercle converge at the top, which, instead of being pointed, can be developed as a straight or rounded edge. The main ridges can bifurcate. The basal platform around the tubercles slopes to the basal edge. At the foot of the tubercles, between or below the ridges, openings for vascular canals are present. Plate size is *c.* 0.4 × 0.4 mm.

P9122 (Fig. 83) has five short, ridged radial arms rather than tubercles, but the tubercular structure has not yet completely disappeared as a result of fusion. The plate centre where the arms meet is also tubercular (Fig. 83b). The arms decrease in height towards the low plate centre. One arm (Fig. 83a, bottom left; Fig. 83b, bottom right) is laterally more separated from the rest and made up of two smaller, laterally fused arms. The narrow separation areas are complemented by slight notching of the basal edge (Fig. 83b), suggesting that this tessera is a composite of fused, loose platelets. One opening (for a vascular canal?) is seen at the interface of arm and upper basal surface (Fig. 83b). A narrow, smooth upper basal zone surrounds the sculpture. The shape of the base is pentagonal, ventrally it is slightly convex; size *c.* 0.59 × 0.54 mm.

Nostolepid tooth plates ?

Figs. 84-87.

Remarks — The concave oval plate P9123 (Fig. 84), with an irregular, damaged edge, bears a series of six triangular to trapezoid, smooth blades increasing in size posteriad. These blades are inclined lateroposteriad and have sharp edges. Longitudinally the blades are arranged in a curved line; the orientation of their longitudinal axis shifts to the right from anterior to posterior. The most anterior blade stands separated from the rest and has a concave anterior surface; in the posterior blades this surface is slightly convex (Fig. 84b) and these blades are separated in their upper region only. One blade (third from anterior; Fig. 84b) has a sharp-edged lateral surface. One ridged

lateral cusp or tubercle with blunted top is present, at the level of blades three and four. Plate length *c.* 0.4 mm, width *c.* 0.28 mm. Figure 85 shows a rather similar, slightly larger plate (RGM 323060; *c.* 0.45 mm long) from the late Pridoli (fauna with *P. kummerowi*) from an erratic from Groningen (V 85). The blades are more acutely triangular; the most anterior blade is fused to the one behind and the upper basal surface with the row of blades is arched. Openings for vascular canals occur at foot of the row of blades. Gross (1971, pl. 1, fig. 21) figured a *Nostolepis striata* stellate tessera from the 'Beyrichienkalk', which has in one of its 'arms' blade-like structures reminiscent of the blades in P9123 and RGM 323060. A structure showing some resemblance to the one described above has two smooth blades with concave anterior surfaces on a steep base (Fig. 86). The anterior basal edge is round, the lateroposterior edge is more angular. Viscerally the base is concave. The blades are separated; the posterior blade is the bigger and has a posterior inclination in lateral view, whereas the anterior is inclined forwards (Fig. 86a). The edges of the blades are sharp, with the edge of the anterior blade probably broken off; originally it might have had the same outline in anterior view as the large, rounded trapezoid blade. The small blade is situated anteromedially of the large blade. From the foot of the blades the upper basal surface slopes laterad. Plate length *c.* 0.28 mm, width *c.* 0.25 mm and height *c.* 0.22 mm. A round plate with only one blade, RGM 323061 (Fig. 87), from a Pridolian erratic from Groningen, is *c.* 0.08 mm long, 0.19 mm wide and 0.17 mm high. Although the histology of these elements is not known, they are nostolepid in appearance and may include the smallest tooth platelets so far recorded.

Gomphonchus volborthi (Rohon, 1893)

Figs. 104, 111,112.

Synonyms — Probably most scales of acanthodian morph 1, cf. *G. volborthi*, Ramsåsa D (Vergoossen, 2002c, pp. 125, 126, figs. 112-116); partim, scales of acanthodian variant 1, Ramsåsa H (Vergoossen, 2002a, pp. 57, 58, figs. 70-73).

Gomphonchus volborthi, in combination with closely associated acanthodian morph 2, belongs to the most frequently collected acanthodian scales after *N. striata*. Most morphological features recorded from Ramsåsa D scales (Vergoossen, 2002c) are also observed in those from Ramsåsa C.

Rohon (1893, p. 32) stated a size range for *Thelolepis volborthi* from 0.1-0.5 mm. The largest scale length (measured in all Laurussian material available) was *c.* 0. 82 mm; largest width *c.* 0.97 mm; largest depth 0.5 mm. Size of illustrated specimen 0.25 × 0.29 × 0.1 mm. The Laurussian material includes the Ludlow Bone Bed, UK, and *Thelodus sculptilis* assemblages from Estonia, erratics and '9g' beds Ringerike, Norway.

Histology (Figs. 111, 112) — Since the Scanian scales hardly yielded diagnostic histological features, a few scales were examined from the '9g' beds, Ringerike, Norway (sample V-Ri/9g/1; Figs. 111, 112, RGM 323074, slide with two scales; for comment, see Vergoossen, 2003, p. 26), plus ten specimens from an erratic from Groningen (V 6), both with *Thelodus sculptilis* faunas. Basically, the scales from erratics have a *Gomphonchus* type of histology (*sensu* Gross 1947, 1971) with thin ascending vascular neck canals whose tops are interconnected like arched vaults (cf. Gross, 1971, text-fig. 22c; *G. sande-*

lensis). The avcs in the Norwegian specimens are thicker, possibly affected by post mortem factors. In the upper anterior crown the dentinal tubules radiate centrad from between the crown ornament. These tubules are shorter than those in *G. sandelensis*; the tubules in the posterior crown are longest. The base has osteocyte lacunae, but in some scales lacunae were hard to find. The fibres of the connecting tissue are dense. One specimen (Fig. 111a) illustrates superposed laminae in neck and crown, basal increase and almost horizontal Sharpey's fibres directed centrad. The boundaries between the neck laminae mark 'annual' or 'seasonal' long periodicity growth cycles. Distad the avcs seem to be connected by arched networks. A close-up (Fig. 111b) shows finer lamination within evidently large basal 'annuli.' These thinner laminae mark shorter periods of growth ('interannuli'), indicating that basal growth is continuous and gradual rather than a process restricted to outbursts of rapid increase. Very thin superposed lamellae in neck and crown are seen a transversal section (Fig. 112) which also shows radial and ascending canals, dentinal tubules reaching baseward, and horizontal orientation of basal lacunae.

Distribution — Within Laurussia, the oldest record of *G. volborthi* is from the '*Gomphonchus sandelensis*' fauna, Leintwardinian, Hemse Beds, Gotland, Sweden (Fredholm, 1988a, b; but cf. Fredholm, 1988b, p. 243). The taxon is chiefly known from *Thelodus sculptilis* zone faunas (late Ludlow-early Pridoli) of variable composition (Hoppe, 1931; Lehman, 1937; Gross, 1947; Vergoossen, 1999c, 2000). The present record of such a fauna from Norway (Ringerike, '9g' beds) also fits within this time span. The recent records from Sweden (Scania; Klinta, Ramsåsa C, D, H; Öved Sandstone Formation; Vergoossen, 2002a-c, herein) might date from the late Ludlow (late Whitcliffian), within the *T. sculptilis* zone.

***Poracanthodes*? *lehmani* Vergoossen, 1999 b**

Figs. 88-94, 113-115.

Preservational remarks — In scales with worn crowns (e.g., P9128, Fig. 90), strong magnifications are needed to reveal three dimensional remnants of the posterior denticulation of the crown lamellae (Figs. 89b, 90b), which was often eroded away (see also histology section).

Diagnosis — *Poracanthodes*(?) species with lateroposteriorly separated and apposed, denticulate crown lamellae.

Morphological features — (Revised after Vergoossen, 1999b) Crown: 1 rhomboid; 2a anterior rims meet anteromedially at a right angle 2b rounded anterior rim, 2a,b with or without midanterior protrusion; 3 up to 23 or more short, radial smooth or spinose, ridges or riblets along anterior rim; 4 each ridge forms an obtuse angle with each new growth lamella, except anteromedially, where *c.* three ridges lie within the oldest crown part; 5 anteromedian ridges longest; 6 up to 21 lamellae, separated (apposed) from the lateral corners onwards in posterior direction; 7 apposed lamellae oblique, sometimes steep; 8 superposed growth in front of separated lamellae; 9 lamellae with dentate posterior edge and smooth anterior to the dentation; 10 up to ten radial canals

open out very high posteriorly, immediately below the youngest crown lamella; 11 posterior overhang from negligible to more than 50% of scale length.

Neck: 12 steep and high all around; 13 slight, midneck constriction; 14 anteriorly smooth and sloping to sharp boundary with base; 15 posteriorly with alternating openings and columns.

Base: 16 rhomboid; 17a swollen 17b flattened and low; 18a swelling placed centrally or 18b slightly projected in front of crown; 19a lateral corners rounded or 19b with sharp angle.

Size: 20 from 0.17 × 0.17 mm to 0.6 × 0.6 mm, scales are roughly as long as wide.

New morphological observations (Figs. 88-94) — The crown of *P.? lehmani* can have a rounded, midanterior protrusion (Fig. 90a); compare also the holotype (Vergoossen, 1999b, fig. 22). The protrusion might be a topospecific modification. The holotype probably shows more topospecific and other modifications (e.g., spinose, radial, anterior crown riblets; see below). Uncommonly, bifurcation of the radial anterior crown ridges or riblets might occur (Fig. 90a). The ridges are not always strictly radial (oriented centrad) or straight, but can bend laterad (Fig. 90a). They can be smooth and sharp. The spinose appearance of the ridges could be typical of the place on the body where the scales grew or an ontogenetic feature (cf. Vergoossen, 1999a, p. 240 on variant 2 scales of *P. punctatus*, and figs. 36-37) or perhaps be environmentally conditioned. Some ridges look as if they were lateral extensions of the dentate lamellae. In many of these features they differ from the radial anterior crown riblets in, e.g., trunk scales of *Gomphonchus sandelensis* or *Gomphonchoporus hoppei*, where each riblet is a single, straight, unornamented structure. Such ribs, however, also occur.

The presence of a very narrow smooth crown zone in front (or behind) the ridges, as in the holotype (Vergoossen, 1999b), seems atypical. The crown can have up to 21 lamellae. Young lamellae, which are usually well separated along their lateroposterior edge, can also be in touch by their midposterior tips (Fig. 90a); the posteriormost tip of each of several, successive lamellae grew onto the next, younger lamella, thus forming a minimal upper surface interconnection. The separation between the lamellae can also be closed off in different ways; the oblique lamellae turned over in their upper part and continued posteriad in a horizontal course (Fig. 94a) or the lamellae kept growing posteriorwards in their lower part where new lamellae became apposed. Apposition is illustrated in Figure 94b. The lamellae can have a buttressed appearance at the turn-over point (Fig. 94a). Some scales may have had regularly spaced vascular openings in the anterolateral neck (midneck position). The anterior neck can be vertical in its upper half and more gently sloping in its lower half (Figs. 91b, 92). The base can be slightly projected in front of the crown (Figs. 91b, 92) or can be very low, also in specimens with many growth zones in the crown (low base observed in scales from Helvetesgraven, not in scales from Ramsåsa C). Juvenile(?) scales (Vergoossen, 1999b, figs. 26-27) were not observed.

In three scales (Figs. 88-90) parts of crown lamellae are overcrusted by thin tissue sheets with concentric marginal laminations, or marginal laminations surrounding a space with U-shaped vascular openings (Fig. 88c), or by laminated sheets (epifauna?).

Histology (Figs. 113-115) — Summary of histological features listed and revised from Vergoossen (1999b). Pore canal system: 21 two to ten radial canals, which can widen out in posterior direction; 22 the oldest two radial canals begin posterior to the primary growth zones and the number of canals increases during growth; 23 radial canals connected by arcade canals; 24 arcade canals can be interconnected.

Vascular system: 25 radial vascular neck canals; 26 thin dentinal canals ascend from the anterior neck and bend in horizontal direction in each new crown layer; 27 the dentinal canals ascending from the posterior neck bend horizontally in the lower crown parts, where their tubules end between the radial canals of the pore canal system in straight lines; 28 dentine canals and tubules form a plexus in the posterior crown.

Base: 29 osteocyte spaces; 30 Sharpey's fibres.

The ischnacanthid layout of the vascular system is preserved fragmentarily in the scales examined. Only the coarse outlines of the pore canal system could be observed in specimens from Helvetesgraven. The presence of *P.? lehmani* could not be established with certainty from the histology of the examined Ramsåsa C scales. These scales had been selected by morphological criteria under a binocular microscope (150 x). Arcade canals were not observed and the histological images showed differences in histology indeterminable to species level. As it turned out only SEM images could provide evidence for the presence of *P.? lehmani* by revealing patches with the posterior denticulation of the crown lamellae intact.

Many histological details and their expression in the scale morphology remain poorly known. The study of better preserved material should bring more clarity. A few radial canals of the vascular system are seen near the anterior crown margin (Fig. 114). Fungal hyphae are present in photographed specimens.

Morphologically, a small number of tiny scales (see section on scale quantities) cannot be assigned to *P.? lehmani*. The punctatiform histology of these *Poracanthodes* sp. cf. *P. punctatus* Brotzen, 1934, scales is evident. Worn and small specimens of both taxa can be mixed up.

***Radioporacanthodes biblicus* (Lehman, 1937)**

Figs. 116-122.

Remarks — Only two small specimens could be identified. Scale histology was discussed by Vergoossen (2002a). The most important histological features are illustrated herein. See also Märss (1986b, pl. 31, fig. 8, '*Poracanthodes porosus*').

Histological features — (Synopsis, modified from Vergoossen, 2002a.). Crown: 1 between four and seven rhombic crown lamellae; 2 within these large lamellae very fine growth lines occur and indicate a shorter growth periodicity; 3 superposition of thin layers. The thickest layers occur in the anterior crown part; in a posterior direction the layers become increasingly thinner.

Vascular system — 4 large vascular canals are laid down at the neck-base interval; 5 from these wide ascending canals arise; 6 in the lateroposterior neck each avc is connected to the neighbouring avc by short, wide arches. The morphological observation that the avcs and arches are often so wide that they are easily observed in the anterior

and posterior neck at low magnification was not supported by the histology of the specimens examined in anise oil, which have thin avcs; 7 dentinal tubules arise from the arches and bend horizontally in upper crown; 8 where they are developed as, but shorter than, in *Gomphonchus sandelensis*; 9 dentinal tubules densely packed.

Pore system — 10 starts close to the anterior crown edge, but it can also be separated from this edge by a smooth space extending across three to four of the boundary lines between the crown lamellae; 11 four or six radial pore rows not connected by arcade canals; 12 the oldest and longest rprs are the central pair; 13 younger rprs lie a bit further posteriorly (4^{th}-5^{th} growth zone); 14 system grew exclusively by addition of new pores (per growth lamella) to existing rprs when maximum number of rprs had been reached; 15 up to fourteen short, narrow, radial or parallel grooves (often pierced by small-sized pore openings) run from the anterior crown edge, and are connected to the first and larger pore of the nearest rpr; 16 bi-directional.

New histological observations — In general, the nature of the radial 'canals' (of the pore system) in *R. biblicus* is unclear; they might be relics of the pore formation process rather than independent structures as are the radial canals in the punctatiforms. Continuing pore formation left series of radially arranged rows of pores interconnected by funnel-shaped tunnels or tubes. Each tunnel represents a growth track to a new pore. The pores can follow a zigzag course within one radial row. This slightly affects the course of the row so that it deviates from a straight line. The first pore of a radial row can be connected by arcade canals to the anterior grooves. These arcades connect either one or two anterior grooves to the radials. Radials that were newly inserted at the posterior crown edge were probably not connected to anteriors. The system of pores is dorsally closed off by superposed lamellae, only the youngest and posteriorly marginal pores were not immediately closed off and also opened out below the dorsal cover. Since the radial pore rows are not interconnected, and the pores were dorsally covered, the pore system must have received a major functional impulse/activation from its posterior end, at its youngest layout. The radial pore series does not seem to have been entirely closed off longitudinally; each pore narrowed anteriad. At the anterior end of the crown, the pore system became a *cul-de-sac* at an early phase of its development. Here the system probably no longer functioned and what remained were 'blind arms,' where the contact with the anterior grooves was lost during the growth of the scale. A more detailed treatment of some these features is given below. All specimens examined and described are from RGM 323057 (Vergoossen, 2002a), Varbla 502 core, depth 19.10 m, Estonia (Märss, 1986b, fig. 30).

Crown (view, Fig. 116) with four radials and six anterior canals. The connection between anteriors and radials is as follows: R1 ascends from A1; R2 from A3; R3 ascends from A4 and passes over A5; R4 ascends from A6. At the cross over points round pores are seen (R3 has two over A5). The pores cut into adjacent crown lamellae, thus producing chevrons in the median crown part. All connections are in the distal half of the anterior grooves.

Crown (view, Fig. 117): R2 is arcade-like connected to A2 & A3; R3 is arcade-like connected to A4 & A5. The connections are situated in the distal half of the agp; the exact architecture of the connection is hard to unravel. The thin covering of radials by lamellae is best seen posteriorly.

Crown (views, Fig. 118a-c). In Figure 118a, A1 overlies R1. Both are connected by a pore, P1 of A1R1. The connection is at the proximal rather than the distal end of A1 (although the anteriormost end of A1 might be concealed). A1 cuts into the boundary line of the adjacent crown lamella. R2 and A3 are connected by a pore in the distal half of A3 (P1 of A3R2). R2 passes over A2, to which it has an arcade-like connection. A4 is in its posterior half connected by a pore to R3 (P1 of A4R3). A4 has made an incision into the crown. The posterior half of A5 is also connected to R3. The A4 and A5 connections to R3 are arcade-like. A5 is also involved in the incision made by R3P2. It is not clear whether the distal part of A6 is linked to R3P2. The incisions are deep and at the interface of two growth layers, but only in the median crown area were chevrons cut out (cf. Vergoossen 2002a); the scales may have been too small to have developed extra rows of chevrons. Since the lamellae are wide, the distance from one pore to another via the shortest route through the lamella is considerable. The tunnels produced during the pore hole formation process and interconnecting the successive pores in a row evoke the image of a radial canal, particularly the longer. Agps and rprs are covered by superposed lamellae. Figure 118b; deeper crown (view), with very fine growth lines within the larger (posterior) crown zones, indicating regular brief growth cycles within the presumed 'annual' zoning. These fine lines are also seen in the posteriormost part of the floor of R4 (Fig. 118c). The basal attachment tissue (with Sharpey's fibres) is well visible. Figure 118c detail, at the same crown level as in Figure 118b; R4 is not connected to an anterior canal (neither is R4 of the scale in Fig. 120b).

Figure 119a shows a crown and base, with bi-directional (//\\) arrangement of Sharpey's fibres. A detail of R3 (Fig. 119b) illustrates the concave floor. Along the left wall very fine, superposed, longitudinal growth layering can be seen. The right wall and floor reveal that during the development of R3 a centrad shift occurred in its course.

Figure 120a is focused on the crown. R1 is connected through P1 to the distal end of the more deeply situated and short A1, whose proximal end has a thick dorsal cover of superposed layers. P1 was also covered, but the cover is thinner. A1 and R1 still seem to be in open contact. R2 is arcade-like connected to the distal ends of A2 and A3. At the junction of these three there is a pore (P1 of A2 & A3R2), which has cut into/affected the right, adjacent median crown surface. P2R2 still seems to be in open contact with P1R2 although both pores are overlain by lamellae. The proximal ends of A2 and A3 are partly obscured by a thick superposed cover. P2R1 opens out freely under the surface cover at the posterior crown periphery. It is not entirely clear whether this is also the case with P2R2, which is situated further from the posterior edge. Notice the change in course of R2 immediately behind P2. The crown view at a somewhat higher level (Fig. 120b) shows that P1R1 cuts posterocentrad into the adjacent (on the central side) crown surface. R3 was connected to A4 by one half of an arcade, the other arcade half leads to A5. The initial stage of R4, at the crown periphery, has a concave floor showing incremental lining and is dorsally covered by a very thin crown sheet. R4 is not connected to anterior canals, and must have been inserted and formed together with the outer crown edge. Indeed, the incremental lines of the floor continue into the adjacent crown surface. There is no pore here, as in Figure 118c, and the question presents itself how pore formation proceeded from this point. Another, even more intriguing question is whether the state of R4 (apparently without pore)

reflects an already fully operative/functional part of the pore system or an initial stage in the process of becoming fully operative? Such questions touch on the heart of what the system represents. It seems essentially a peripheral system in *R. biblicus*. Vague traces indicate that there might have been one or two additional agps in the central crown part at an earlier growth phase. The posterior, transverse, basal view (Fig. 120c) shows rvcs directed towards the scale centre. The neck and basal view of another specimen (Fig. 121) shows neck laminae, ascending vascular canals in the neck, radial vascular canals and basal lacunae. The crown view of yet another scale (Fig. 122) focuses on the dense dentinal plexus of the midposterior crown.

Distribution — The taxon has now been recovered from a deeper level (depth 9.5-10 m) of the Tahula 709 drill core. This level contains the oldest *T. sculptilis* zone fauna of the core.

Forma *bifurcata*, a problematical (eroded?) poracanthodid scale variant
Figs. 95-102.

1937 *Poracanthodes porosus*, Lehman, pp 50,51; pl. 3, fig. 46 (morphology (1)).
1971 *P. porosus/Gomphonchus hoppei*, Gross, p. 66; pl. 9, fig. 12 (morphology (2)).
1986b *P. porosus*, Märss, pp 56, 57, 89; pl. 30, figs. 1-2 (morphology (3)).
1999c '*concentricus*' form, Vergoossen, p. 51.

Preamble — Morphologically, the scales of forma *bifurcata* may well include *Poracanthodes? lehmani* scales in several states of poor preservation. They are all from the lowermost *T. sculptilis* zone of the Tahula 709 drill core (-7.8-10 m), Estonia, except P9133 (Fig. 95), which is from Ramsåsa C. The histology of morphologically similar scales from a fauna (low in *T. sculptilis* zone) of the Varbla 502 drill core (-19.10 m), Estonia (Figs. 123-128) reveals a porosiform microstructure without the interconnected arcade canals that have been recorded for the *P.? lehmani* scales from Helvetesgraven (see above; Figs. 113-115). It is hard to imagine that the arcade canals in all the scales from Varbla should have been eroded without leaving a trace, the more so because much of the other microvertebrate material from the Varbla fauna shows well-preserved histological features. At present no solution can be offered for this paleontological, partim biostratigraphical, dilemma. I have opted to treat this group of scales in detail, although *bifurcata* specimens are as yet of limited significance within the Scanian faunas. This new name rightly or wrongly suggests a certain coherence, but is also and especially meant to facilitate and invite comparison with other poracanthodid taxa. In particular, it invites contrast with *Radioporacanthodes porosus* (Brotzen) *sensu stricto*, the type species of the porosiforms (Vergoossen 1997, 1999a), which was not identified from the faunas under discussion (Helvetesgraven, Ramsåsa C,D,H, Varbla 502: -19.10m, Tahula 709; -7.8-10m).

The palaeontology of the earliest, Whitcliffian (Late Silurian) poracanthodids from the Baltic region is even more complex than first thought when a revision of the genus *Poracanthodes* was proposed (Vergoossen, 1997). This complexity was ignored when '*Poracanthodes porosus*' (a long ranging taxon comprising scales of *R. biblicus, R. porosus sensu stricto*, forma *bifurcata*, worn scales of *P.? lehmani* and others) was given the

biostratigraphical status of deeper shelf zonal fossil and equivalent of *T. sculptilis*, zonal fossil for the shallow shelf (Märss, 1997, 2000).

Etymology — The name refers to the bifurcate branching of the crown surface that can accompany the insertion of a new radial between two existing radials.

Diagnosis — Crown of flank scales has large rounded pores arranged per lamellae and in two to twelve radial rows of distinctly unequal length. Insertion of new, distinctly shorter radials can be accompanied by bifurcate branching of crown surface between two existing radials. Longest pair of lateral radials diverges from mid anterior crown at an angle of 90°. Crown lamellae covered by very thin superposed upper crown layers.

Material — One hundred and twenty four scales. P9131 (Fig. 95), Ramsåsa C, Skåne, southern Sweden. RGM 323062-323067 (Figs. 96-101), RGM 323073 (Text-fig. 4), RGM 323071, slide with 25 specimens, Tahula 709 drill core, - 7.8 m; RGM 323068, RGM 323070, slide with 7 specimens, Tahula 709, - 8.4 m; RGM 323069, slide with 7 specimens, Tahula 709, - 9.5-10 m; RGM 323072, slide with 50 specimens, Varbla 502 drill hole, depth 19.10 m, Saarema, Estonia. Twenty six specimens from erratics (including *Sphaerocodium/Girvanella* limestones) with faunas typical of *Thelodus sculptilis* zone, Groningen, northern Netherlands.

Age. *Thelodus sculptilis* zone, late Ludlow to early Pridoli.

Scale length	Width	Height	Base length	Width	Height
0.21	0.27	0.2			0.06
		0.21	0.27	0.36	0.06
		0.23	0.26	0.35	0.1*
		0.23	0.3	0.4	0.08*
0.35	0.48	0.3	0.3	0.4	0.1
0.43	0.43	0.4	0.43	0.43	0.2
0.46	0.6	0.3			0.15
0.65	0.71	0.6	0.6	0.63	0.35
0.61	0.78	0.6	0.6	0.75	0.2*
0.7		0.6	0.6	0.7	0.25
0.6		0.7	0.5	1.1	0.3*
		0.75	0.1	0.4	0.35
0.95*	1.15*	0.61	0.7	1.1	0.3

* = dimension incomplete

Scale morphology — (Features shared with *P.? lehmani* are numbered between square brackets; for same features, same number and lettering were used; unnumbered features are not shared, because they have not been recorded for *P.? lehmani*.) Size ranges of scales in mm, measured chiefly on smallest and largest specimens of all available material. In rows with blank boxes only the largest length or width is given.

Most scales are wider than long, few are as long as wide [20]. As a rule the posterior crown overhang varies from negligible to little [11], but it is unclear in how far this was influenced by the preservation of the thin crown cover. The height of some scales can be disproportionate in relation to length and width (table above, penultimate

specimen). Within the available dimensional and morphological ranges distinction between typical trunk scales and topospecific variants cannot be made, but some topospecificity will be reflected by extreme values.

The crown is rhomboid [1] or fan-shaped, flat and horizontal. The anterior crown rim is straight [2a] or rounded [2b]. The anterior crown margin has up to *c.* 22 short, smooth and rounded radial riblets [3]. Their length usually decreases laterad [5]. In rhomboid scales the anterolateral crown rims are usually straight, but sometimes one (or both) of the rims is slightly concave, resulting in a slight constriction of the anteromedian crown (Figs. 97a, 99a), which gives this part more prominence (cf. 2ab in *P.? lehmani*). The crown surface consists of smooth, concentric crown lamellae slanting posteriorwards, sometimes very steeply [7] (Fig. 98a, anterior lamellae). Lamellae often look flat and horizontal, but these were worn down (Fig. 96c). The upper part of each lamella is separated shallowly from the preceding [6], but in its lower region each lamella is in contact with the preceding. Up to 18 lamellae were counted [6]. The posteriormost part of each lamella is rounded rather than pointed. The first lamella can be in touch with the median pair of radial anterior riblets (Fig. 99a). As a rule, the riblets lie at obtuse angles to the lamellae [4]. The lamellae make a dip where the pores lie, thus producing conspicuous radial segmentation of the crown surface (Fig. 102). The successive lamellar segments increase in size posteriad. The upper rim of the segments is either semicircularly curved or straight. The regularity of the segmentation makes it unlikely that this crown type merely represents a presevational artefact.

The segmentation can make the posterior crown rim crenulate. Sometimes segmentation and crenulation are best visible in posterolateral view. When segmentation and the crenulation of the posterior crown rim become inconspicuous, resemblance with *Poracanthodes? lehmani* is great (cf. Figs. 91a, 93a with 99 a, c). The lamellae are pierced by round to oval pores, arranged in radial rows.

The pores are situated in the lower half of the lamella. In some examples, when a new radial row is inserted, a small passageway leads to the first pore of that row (Fig. 99b, radials 3, 4, 5). Some radial pore rows seem to be discontinuous across a distance of several lamellae (Fig. 99b, radials 2, 5), but such discontinuity was not observed in histological images. The number of radials [10] varies between two and twelve (in the largest specimen measured, from erratic V6). High numbers correlate with a straight anterior crown rim. These features could reflect maturity and topospecificity. The radials are situated low in the crown and their course is straight or a bit curved centrad. They do not run entirely horizontally, but slope into deeper crown levels from their starting point (Fig. 96a). This feature is also not visible in the histological images, but might be linked with the insertion of new radial pore rows. The longest and oldest radial(s) [22] can be traced back to the second growth lamella (Fig. 101a). Since the oldest lamellae are situated midanteriorly in the crown, the oldest radials often run diagonally across the crown towards the middle of the opposite, latero-posterior crown rim (in rhomboid crowns, Fig. 98a). The two oldest radials lie *c.* 90° to each other. The newer radials are often found in the central and most lateral parts of the posterior crown half. Often the posteriormost lamellae are only preserved fragmentarily. Canal floor and roof are rounded. The radials open out at the posterior crown edge, below the youngest lamella [10]. In other poracanthodids, e.g., in *Poracanthodes punctatus*, the openings of the radials are lower in the neck. The posterior openings of the

radials that were measured vary from 0.016-0.032 mm in horizontal section (at widest point), with most common values between 0.02-0.025 mm. Some postmortem influence must be allowed for. Only the posteriormost crown region can slightly overhang neck and base [11]. Compared with what is known from other poracanthodid scales this overhang is negligible.

The high neck is concave all round, with the constriction in the upper neck part [13]. Anteriorly the neck is smooth [14]. The posterior neck shows shallow recessions at regular intervals, but conspicuous neck pillars or openings for the entry of vascular canals were not observed [cf. 15].

The rhomboid [16] base is moderately convex [17a], with swelling anteromedially [18]. The lateral corners of the base can be sharply drawn out laterally (Fig. 97a).

The histology of the scales from the Varbla fauna (Figs. 123-128) — The vascular system and the structure of the base look essentially ischnacanthid (e.g. scales in Figs. 124b, 126d, f-g). The very thin surface cover of the crown was often not, or not fully, preserved and this may lead to misinterpretation of the original state of the pore system, which must have been entirely closed off dorsally by superposition, with the exception of the peripheral pores, as in *R. biblicus.* The beginnings of the system can be studied in Figures 123 and 124. Figure 123a is a crown view of a young specimen with *c.* six lamellae, four rprs. The lamellar boundary lines continue and dip over the radials. P1-4 in R1 are shown. R1P1 is smaller than R1P2, which is smaller than R1P4. R1P1 was laid out in the second lamella very close to the lateral boundary line of La1. A funnel-like tube, widening posteriad, runs from P1 to P2, which is laid out adjacent to boundary line La2. This pattern is similar to that in *R. biblicus*, the radials resulting from the ongoing pore formation process. They are not independent structures. Interconnections between the radials are absent. Unlike *R. biblicus*, however, forma *bifurcata* has no anterior grooves connected by arcades to the radials and no chevron-like incisions of the pores into the adjacent crown surface. R2 and R3 were probably inserted in La5. Figure 123b is a deeper view, focussing on the open distal ends of the rprs under the dorsal cover (lamellar superposition). Notice the increasing thickness (decreasing transparency) of the cover anteriad. The distal end of R4 is dorsally open; the thin superposed cover was destroyed. Radial vascular canals are seen near the anterior crown margin. Figure 123c shows details of the open distal ends of newly inserted R2 and R3 (funnel-shaped), both covered by a thin lamella sheet or thin lamellae sheets(?).

Crown view (Fig. 124a) of scale with six radials; R2 shows a chain of posteriorly widening and anteriorly narrowing little funnels, R6 meanders. The tree-like branching of the crown as a result of the insertion of radials is characteristic. Vague lamellae can be seen in the anterior crown and vague dentinal tubules midposteriorly. Deeper crown view (Fig. 124b) with long dentinal canals (rvcs) in the posterior scale; basal lacunae in growth zone arrangement.

Crown view (Fig. 125) with bifurcate branching of the crown caused by the insertion of new radials; six rprs, and at least 11 lamellae. R2 originates from halfway along the left lateroposterior edge of La2, directly behind the 'embryonic' or primary crown area (=between the central pair of anterior crown riblets). This region is further subdivided by *c.* three short parallel, latitudinal lamellae. Rvcs also in primary area.

Crown view (Fig. 126a) with *c.* four radials. *Circa* seven lamellae were formed, but their total number is hard to determine because of the complicated pattern of boundary lines, especially in the posterior crown. The lamellae 'dip' at the junction with the radials. The resemblance between the oldest crown area (= bounded by La2; Fig. 126b) and the crown morphology of acanthodian morph 2 scales (see below) is striking. Figure 126c shows a detail of R4, with peripheral pore, plus fine incremental (short periodicity) lining in the superposed cover of R4 and within its floor. Figure 126d shows vague dentinal tubules of the superposed layers, reaching across several lamellae. In Figure 126, boundary lining within 'La1' (primary region) may indicate that the pore system was not laid out until *c.* 4 lamellae had formed (cf. Fig. 125). The anterior part of the midanterior groove crosses a couple of these oldest boundary lines. A cross sectional view (Fig. 126f), mainly through anterior crown and neck, shows vascular system (radial vascular canals, ascending canals in neck, dentinal tubules in neck and crown) and superposed neck lamellae connected with basal laminae. A posterior cross sectional view (Fig. 126g) shows neck and basal lamination, opening for rvc's in neck, dentinal plexus, plus fine superpositional layering and the arrangement of the lacunae parallel to the basal growth zones.

A lateroposterior view (Fig. 127a) illustrates superposition of crown/neck lamellae to the right, very high neck and low base, lacunae in basal pyramid; in R2 the crescent -like partition of an older growth lamella (ola) can be seen anterior to the peripheral or distal opening. The partition does not reach the total height of R2. The distal opening of R2 is, to the left, partly blocked by a younger growth lamella (yla, Fig. 127b).

Figure 128 is a crown view of a specimen with six radials (new R4 hardly noticeable); dipping lamellae over radials; disappearance of boundary lines between lamellae, and the total destruction of lamella partitions in R6 (much as in Fig. 96b); dorsally covered pores visible in R2.

Forma *bifurcata* had a system of marginal(ly functioning) openings or pores per 'annual' crown lamella. In crown view these pores are arranged in radial rows. The system had no radial pore canals; the 'canals' are probably preservational artefacts.

Ontogeny and function of the pore system — The beginning of the canal system was closely linked with the formation of the first two surface 'pores', one on each posterolateral rim of the first or second large crown lamella, and roughly in the middle of each rim. This phase was probably preceded by a pore free crown of *c.* three lamellae within the primary crown region.

The 'pore' system was laid out simultaneously with the lamellar addition at the periphery of the crown, as suggested by the presence of fine incremental lines. Both pore formation and lamellar growth were gradual, continuous processes, not abrupt annual outbursts of growth activity in which one complete 'annual' lamella was formed. The boundary line between each 'annual' lamella is distinctly thicker than the regular, thin pattern of lines within these boundaries and parallel to them. The pore formation activity could have been slightly reduced after a pore had been formed, as the 'chains' or series of anteriad narrowing small funnels might indicate. All the pores per lamella were formed simultaneously. New pore series may have been inserted when a critical width between extant pores of a lamella was reached, as the distance between these pores is roughly the same. Soon after they were formed, or perhaps

even during their formation, the pore openings were closed off dorsally, an indication that pores received major, external, functional impulses from the caudal direction ('behind'), and under the dorsal cover. It is not clear whether the pores in a longitudinal row were still in contact, as might have been the case in *R. biblicus*. Perhaps they contained sensory receptors (short-lived soft tissue?) (e.g., cillae that were regenerated each 'yearly' growth cycle?).

Comparison — Scales of *bifurcata* differ morphologically from those of the type species, *R. porosus* (Brotzen, 1934; redefined by Vergoossen, 1999a) and other late Ludlow to Lochkovian Baltic porosiform poracanthodids by the following features. [1] The longest radials make a right angle anteriorly. In general, the radials never follow a subparallel, longitudinal course in *bifurcata,* as they do, e.g., in *R. biblicus*. [2] The crown surface is cut up by (bi)furcations. This repeated branching results from insertion of new radial series and produces a typical pattern of (alternating) short and long radials. [3] The crown is wider than long, fan-shaped and has radial rows of concentrically apposed segments, which increase in size posteriad. [4] The total number of radials is 2-12, vs 6 in *R. porosus*, 4 or 6 in *R. biblicus* (Lehman, 1937) and 4 in '*Poracanthodes*' *subporosus*, Valiukevicius, 1998. [5] Chevron-like incisions, made by the pores in the crown, are absent. [6] An anteromedian sulcus in the crown is absent.

The *bifurcata* scales differ from those of *Zemlyacanthus menneri* (Valiukevicius, 1992) also by the following features. [7] They possess a superposed crown cover, which closes off external openings, except in the posterior periphery. [8] Osteocyte spaces are present in the base. [9] Arcade canals between the radial pore series are absent.

Forma *bifurcata* differs from *Zemlyacanthus menneri*, *R. biblicus* and '*P*'. *subporsus* [10] by the presence of anterior crown riblets/ridges.

Other differences: [11] In *Gomphonchoporus* the pore system is laid out in the posterior crown half only. [12] *R. biblicus* has anterior pore grooves connected by arcades to the radial pore series. [13] In *bifurcata*, the radials open out at the posterior crown edge, directly below the youngest lamella, as in *R. biblicus*. Other poracanthodids, e.g., the punctatiform *Poracanthodes punctatus*, have radial canals that open lower in the neck.

The description of *bifurcata* scales was partly modelled on the morphological features shared with *P.? lehmani* scales. In addition, *bifurcata* is distinguished from *P.? lehmani* by [14] the 'unornamented' posterior edges of the crown segments or lamellae. A few scales are also considerably larger than *P.? lehmani* scales, but the size differences might reflect greater maturity or different position on the body. Another morphological distinction concerns the thin and fragile surface cover of the crown [7, above]. In the best scales from Estonia and erratics these covers are so transparent that the typical bifurcations at a lower crown level shine through in transmitted light. Such covers have not been observed *P.? lehmani* scales.

Conclusion — Although it cannot be ruled out that Estonian scales of forma *bifurcata* harbour eroded *P.? lehmani* scales (a species unknown from erratics), simply too many morphological, histological, preservational and distributional differences have been observed to assume that all these differences should (or could) be attributed to preservational factors alone, and to assume at the same time that all *bifurcata* scales are synonymous with *P.? lehmani* scales.

Geographic and stratigraphic distribution in the Baltic area — Upper Ludlow, Tahula Beds, K3A Regional Stage - lowermost *T. sculptilis* zone, near border with Uduvere Beds, K2U, Estonia (Märss, 1986b) (common). Late Ludlow (- early Pridoli?), *T. sculptilis* zone, Ramsåsa, site C, Skåne, southern Sweden (extremely rare). Pridoli?, 'Ramsåsa quarry' (locality F/locality 8), Skåne, southern Sweden. Erratics of the northern Netherlands, in faunas typical of the *T. sculptilis* zone (not rare).

Spines

Fig. 103a-c.

Remarks — Both smooth and noded spine fragments were collected. The largest, probably ischnacanthid, is about twice as wide as high (mpe = measured at its proximal end; Fig. 103c) and about 1 mm long (Fig. 103a, leading edge). It has three smooth ridges. The arched median ridge is widest (0.27 mm, mpe) and pierced by at least four longitudinal canals over a mostly closed pulp cavity (Fig. 103c). The median ridge is flanked by one smooth narrower ridge (width ratio of ridges *c.* 3:6:2, mpe). These side ridges are flattened laterally (Fig. 103b-c), one is also flattened dorsally (Fig. 103b, right ridge). The ventral part of the side ridges was rounded. There is a groove along the trailing edge.

Indeterminable acanthodian scales

Remarks — Morphs 2-4 (see Vergoossen 2002c) are also present in the Ramsåsa C sample. New morphs will be described in consecutive numbers, starting up from 4.

Morph 2, cf. *forma bifurcata*

Fig. 105.

2002c cf. Morph 2, Vergoossen, p. 126; figs. 116-117.

Remarks — Some scales show affinity to the oldest scale parts of *bifurcata* specimens (cf. Fig. 126b). The differences are chiefly in size (morph 2 is much bigger- the present scale and the oldest parts in Fig. 126a differ in size by *c.* 500%), in the absence of a fully developed pair of lateral lamellar pores, and in the ornamentation of the anterior crown margin. P9137 (Fig. 105) has a smooth, horizontal, rhombic crown with a rounded anterior rim and blunted, wavy, anterior ornament, originally probably with short radial ridges. Lateroposteriorly the youngest growth zone of the crown is lowered and marked off by a groove along the preceding growth zone. The crown tip (broken off) overhangs neck and base. The sloping neck shows alternating openings and columns. The base is close to pentagonal, mostly larger than the crown and swollen centrally. Neck and base make up almost total scale height (each by *c.* 50%). Size; *c.* 0.43 mm long, 0.54 wide, 0.16 deep. Largest measured specimen; 0.85 × 0.87 × 0.55 mm (from '9g' beds, Ringerike, sample V-Ri/9g/1).

Morph 2 was observed in late Ludlow-early Pridoli (*Thelodus sculptilis* zone) faunas of variable composition, but always in association with *G. volborthi*, from the Ludlow Bone Bed at Ludlow, UK; from Ringerike, '9g' beds, Norway; from erratics, northern

Netherlands. The Swedish finds (Ramsåsa C, D; Öved Sandstone Formation) may date from the late Ludlow (lower span of *T. sculptilis* zone or slightly older).

Morph 5

Figs. 106-109.

Remarks — Morph 5 scales are rare, small (mostly < 0.25 mm), and fragile (due to thin crowns). Their microstructure is not preserved. The damaged and eroded scale P9138 (Fig. 106) has a horizontal, anteriorly rounded, rhomboid and centrally slightly concave crown with *c.* six, more or less straight and parallel anterior ribs that fade out just before half the crown's length. The central rib is joined halfway by the rib to its right (in anterior view). The ribs are separated by shallow folds that narrow to a V or U shape near the anterior crown rim, giving the rim a scalloped instead of a straight outline (cf. P9141; Fig. 109). The crown is smooth posterior to the ribs, with a pointed tip. Lateroposteriorly the crown overhangs neck and base by 30% of the crown's length. There is no overhang anterolaterally. The neck, medially constricted in all scales, makes up most of the scale's height. Base rhomboid, very low and slightly projected forward of crown. P9139 (Fig. 107) has four or five anterior ribs, the central pair reaching across half the crown. The fold between the central ribs is wider. The surface posterior to the ribs is flat. The lateroposterior crown overhang is larger than in P9138. The smooth anterior neck is concave. The posterior neck has few openings (midneck or lower) and widens out baseward in a rather steep, but straight, slope. The base is not projected forward. In P9140 the four anterior ribs are more curved in side view (Fig. 108a). As in the preceding scale, the U-shaped narrowing of the folds between the ribs is less marked, perhaps due to the wider spacing of the ribs. The posterior neck has at least five median openings alternating with pillars. Scale P9141 (Fig. 109) has an almost pentagonal crown and only three weakly expressed (eroded?) anterior ribs (median ribs and fold most marked); the smooth anterolateral crown margin is gently convex on one side. There is an opening (for vascular canal?) low in the midanterior neck (Fig. 109b). Posterior neck with few alternating openings and pillars. Base flat.

Comparison — Morph 5 scales were not observed in the other Scanian samples examined (Helvetesgraven, Klinta, Ramsåsa H, D). Nevertheless, the scales are reminiscent of acanthodian sp. 1 scales from Ramsåsa H, and particularly P8874 (Vergoossen, 2002a, figs. 105, 106), which mainly differs by its shorter anterior ridges, the gentle baseward bend of the anterior crown margin, considerably less posterior crown overhang and a moderately swollen base. P8873 (*op. cit.* figs. 102-104) is also morphologically close, differing mainly in having more (eight) and shorter ridges, by the absence of an anterior crown rim, and by its swollen base. In a crown from Klinta (K5; Vergoossen, 2002b, fig. 40) three ridges reach into the posterior crown half and the posterolateral crown overhang is considerably less. An unfigured scale from the present sample identified as *Gomphonchus sandelensis* has a concave posterior upper crown surface and an anteromedian depression (both perhaps as a result of erosion?). For depressions in *G. sandelensis* crowns, see also Gross (1971, pl. 9, fig. 17). As a rule, the anterior riblets in *G. sandelensis* (if present) are short, radially arranged and more numerous (Gross, 1947, pl. 24, fig. 13a); somewhat longer and less than six also occur

(Gross, 1971, pl. 9, figs. 15-16). However, folds narrowing to a V-shape towards the anterior edge producing a scalloped anterior margin were not recorded by Gross. Such margins would seem to be present in Lochkovian *Gomphonchus* scales figured from Bohemia (Märss, 1997, pl. 7, figs. 3-10), which differ from morph 5 scales among others by the YYY shape of the anterior crown (*op. cit.*, pl. 7, fig. 5) and their bulging base. A scalloped/VVV shape might be present in a Pridolian scale from the Miastko 1 core (Poland) identified as *G. sandelensis* by Märss (1997, pl. 4, fig. 13). YYY and VVV-shaped anterior crown rims occur in some *Gomphonchoporus hoppei* scales (Vergoossen, 1999a, figs. 41, 51, 52, 55, 57), but in these the folds between the ribs widen anteriad. This widening is also seen in the Polish and some of the Bohemian scales. The anterior crown rim in *Nostolepis gracilis* is a straight or rounded line, the crown ribs commonly extend as far as the posterior crown and are often more numerous. Scales with typical *N. gracilis* morphology have not been observed in any Scanian samples. Illustrations of *Cheiracanthoides planus* crowns (Valiukevicius, 1998, pl. 3, figs. 9-15) are reminiscent of the present crowns, but the number of ribs is lower. Size, neck and base morphology also differ, e.g., no alternating openings and pillars were recorded from *C. planus*. For all the reasons advanced, the morph 5 scales cannot be assigned to any of the taxa mentioned above.

Correlation

The following taxa from the Ramsåsa C fauna are relevant to dating and correlating the sample; the zonal fossil *Thelodus sculptilis* (common), the slightly younger *T. admirabilis* (in so far as recognisable - less common) and *Paralogania ludlowiensis* (very rare). This is the first record of the co-occurrence of these taxa in one fauna, which is, on the whole, characteristic of a *T. sculptilis* zone fauna (late Ludlow- early Pridoli). The vertical and horizontal distribution of these taxa within the East Baltic Microvertebrate Standard sequence, on Gotland and in Scania, and the implications for the dating of the Scanian faunas were discussed by Vergoossen (1999b, 2002c). A few additional aspects of their occurrence in the present fauna must be considered.

The scales of *Thelodus admirabilis* best resemble those of the older beds of the Kingissepa core (K3aT, Ludlow, depth 12.40 m; Märss, 1982, pl. 3). Associated fish fauna in the core include *Gomphonchus sandelensis*, *Nostolepis striata*, *Thelodus sculptilis* - all roughly as common as *T. admirabilis*; *Thelodus parvidens*, *T. traquairi* and '*Poracanthodes porosus*' - are markedly less common (Märss, 1986b, fig. 33). All these taxa also occur in the Ramsåsa C fauna, but quantitatively there are noteworthy differences (see next section).

Contrary to the only other Scanian record, from the Helvetesgraven fauna (Vergoossen, 1999b), *T. admirabilis* is not associated with *Andreolepis hedei*, an older zonal fossil; as in the Helvetesgraven fauna, *T. admirabilis* is associated with *Poracanthodes punctatus*-like scales, pointing forward in time to a younger zonal taxon (see also section on acanthodian scale quantities below).

Within Scania, *P. ludlowiensis* was recorded from Ramsåsa D (SW24), where it is associated with *Thelodus carinatus* (Vergoossen, 2002c). The latter, older element is missing in the present fauna.

Regarding *T. sculptilis*, a series of ramosiform scales was discussed (see above) that showed a gradual transition from a nearly smooth crown to a progressively more

complex crown ornament within the same fauna. It is conceivable that this increase in ornamental complexity was coeval with, or preceded, that in *T. admirabilis* crowns from progressively younger beds of the Kingiseppa core, at the transition between the Tahula and Kuressaare Stages of the Ludlow (Märss, 1986b, fig. 63), since the *T. admirabilis* scale form can be partially morphologically interpreted as progressively more complex *T. sculptilis* scales.

The only Scanian fauna recently studied with *T. sculptilis* as its predominant element is that from Ramsåsa H, also with the porosiform *R. biblicus* and the punctatiform *P.? lehmani* besides *P. punctatus*-like acanthodian scales (Vergoossen, 2002a). The Ramsåsa C and H faunas are less conservative in aspect than the fauna from Ramsåsa D (SW 24), and do not feature both old and new zonal fossil, as the faunas from Helvetesgraven. For the most up-to-date correlation charts, see Vergoossen (2003, chapter 6).

The only previous records of *bifurcata* scales from well-documented sections are from the Upper Ludlow Tahula Beds (K3aT), very low in the *Thelodus sculptilis* zone, close to the boundary with K_2U Regional Stage, Estonia ('*Poracanthodes porosus*' of Märss, 1986b, pl. 30, figs. 1a -2a, from cores Tahula 709, depth 7.7m and Sakla, depth 13.4m). Within the Scanian late Ludlow, the scales of the earliest poracanthodid taxa have been collected in low numbers and identification to species level causes problems resulting from preservation, in combination with small size. These factors could have affected their distributional data, which are not yet properly understood. Reinvestigation of the material from the standard sequence may establish how far the new or revised poracanthodid taxa could be successive.

Scale quantities

Precise figures of specimens per taxon have, as a rule, been avoided, because considerable uncertainties attend the morphological identification of scales in the sample, especially in the finest fractions. Taxonomic determinations are also influenced by preservation, form grading, or a combination of these factors with others. The morphological details needed for identification of scales in the fractions 0.106 (or finer)-0.212 mm often require SEM images, which makes their identification impractical and financially unattractive. When a taxon's material only, or largely, derives from these sample fractions (as in the case of several acanthodian taxa) the uncertainties about identity lead to additional quantitative misrepresentations. The impact of this depends upon the number of the unidentified scales of such a taxon.

Form similarity has long been recognised in thelodont head scales and plays an important role in the identification of the scales within the Scanian faunas examined (see, for example, Vergoossen, 2002c). In the Ramsåsa C assemblage increasing complexity of the scale crown was discussed as another factor making it hard to distinguish between scales of the *Thelodus sculptilis/admirabilis* scale groups (see above). The conservative crown morphology was also mentioned (see above). A clear-cut identification of scale forms can further be hampered by the absence of a record of long-standing taxonomic treatment or by a controversial hypothetical one. *T. radiosus* is an example of the first, and its integration in a scleritome *T. sculptilis*, is an example of the second; the form has vanished within this scheme.

In the case of the acanthodians, identification problems at the species level are par-

ticularly related to preservation and the levelling of morphological distinctions, such as between scales of the poracanthodid taxon *Poracanthodes? lehmani* and of forma *bifurcata*. *Poracanthodes? lehmani* was discovered 'by accident' during SEM photography; one scale, the holotype, happened to be included in a selection of '*Poracanthodes porosus*' material from the Tahula 709 drill core.

Identification at the generic level was considered unreliable for most smooth-crowned acanthodian scales with *Gomphonchus sandelensis*-like appearance because they suffered badly from wear. Since the number of *G. sandelensis* and *G. sandelensis*-like scales is low, this has not greatly influenced the totals. In general, histology is of no great help in the study of the Ramsåsa C material. At the species level histological features are either shared, such as for the predominant *Thelodus* scale groups, or diagnostic details are lacking, as for acanthodian scales.

For all these reasons and others (see below), more general quantitative observations have been made, based on the present sample and supported by observations on other Ramsåsa samples examined or the literature. When precise figures for a taxon are given, ambiguous assignations were excluded as much as possible. All figures and percentages are meant to draw attention to tendencies, not facts.

Scale quantities per sample — A selection of 2100 scales was examined. The figures have been biased due to fewer larger scales (from fraction 0.355 mm upwards) could be picked because adhering sediment hampered their determination. Small scales were cleaner. The fraction residue that remained unexamined was larger for the 0.106 fraction than for the other fractions.

Scale quantities of agnathous fishes per sample — Osteostracan remains comprise *c.* 2% of the entire fauna. The number of thelodont scales is double that of the acanthodians (*c.* 65% - *c.* 32%). Apart from the factors mentioned in the section on correlation, there is a general correlation between water depth and the relative abundance of thelodonts vs acanthodians. The scales of the scleritome *T. parvidens* and of the *T. sculptilis/T. admirabilis* scale groups (all *sensu* Märss, 1986b) predominate, together making up *c.* 58% of the total number of examined scales, with *c.* 31% scales of the scleritome *T. parvidens* and *c.* 27% of the *T. sculptilis/T. admirabilis* scale groups. In this sense, the Ramsåsa C fauna is a *T. parvidens* rather than a *T. sculptilis/T. admirabilis* fauna (compare the ratios of *Paralogania ludlowiensis* and *T. parvidens* scales from Ludlow Bone Bed faunas; Turner, 2000). Conventional *T. traquairi* scales (*sensu* Gross, 1967) make up *c.* 2% of the thelodont total (TT). This percentage doubles when unconventional forms (Vergoossen, 2002a, c; and herein, e.g., forma *baltica*) are included. Scales of the genera *Loganellia* and *Paralogania* together comprise *c.* 1% TT. The scales of the scleritome *T. parvidens* comprise *c.* 39% glabrous scales of *T. parvidens sensu stricto* (*sensu* Gross, 1967), *c.* 43% polycuspid *T. trilobatus* scales and *c.* 14% head scales (= ridged conical forms and incised forms; but see below). Among the polycuspid *T. trilobatus* scales the posterior crown part is so much damaged in about a third of the scales that it is more proper to state that they were probably polycuspid. One monocuspid *T. trilobatus* scale was collected to *c.* ten polycuspid forms, in total 37 monocuspid scales. The rarest *Thelodus* scales are *pugniformis* and *bicostatus* (one per *c.* 350 *Thelodus* scales for *pugniformis*, one per *c.* 150 for *bicostatus*), but they were collected from all fractions except 0.106.

Scale quantities of agnathous fishes per fraction — Osteostracan remains were collected in all fractions down to the 0.106 mm; the largest 0.5≤ mm yielded twice as many remains (30) than all the smaller fractions together. Most *Thelodus bicostatus* scales were found in the 0.5≤ mm fraction; six out of the total of nine, perhaps indicating that it is mainly a medium-sized scale type (cf. Lehman 1937, p. 94; Gross, 1967, p. 18). This may also apply to the glabrous scales of *T. parvidens sensu stricto* (cf. Lehman, 1937, p. 94; Gross, 1967, p. 10), of which more than half the number of scales (153 out of 266 in total, *c.* 58%) were collected in 0.5≤ mm fraction, with only 5 (*c.* 2%) in 0.106 and 27 (*c.* 10%) in 0.212 mm fractions. Monocuspid *T. trilobatus* scales, morphologically a fairly diverse group, were collected from all fractions, but the majority (*c.* 75% = 28 scales) were found in the 0.106 mm fraction, whereas polycuspid scales are evenly distributed throughout the fractions. *Thelodus costatus* scales, here defined as only comprising ridged, conical head scales (see also Vergoossen, 2002c) were not collected; glabrous incised forms were included as '*T. parvidens* head scales.' In this category (see above), *c.* 10% of the scales might also be assigned to *T. sculptilis*. The number of *T. sculptilis* scales is highest (about one third) in the 0.212 mm fraction and lowest (*c.* 10%) in the 0.106 mm fraction. About 10% of the scales counted as *T. sculptilis* consist of head scales that are difficult to assign with certainty. These were practically all collected in the largest fraction (0.5≤ mm fraction). No *T. admirabilis* scales were collected from (or recognised in) the 0.106 and 0.212 mm fractions. The first recognisable scales occurred in the 0.355 mm fraction and this agrees well with measurements of Märss (1982). Conventional *T. traquairi* scales first show up in the 0.355 mm fraction; when unconventional forms are included all size ranges are represented.

Acanthodian scale quantities — *Nostolepis striata* trunk scales make up about 38% of all the acanthodian scales and were collected in about equal numbers from all fractions except 0.5≤ mm, which contained slightly fewer. Trunk scales of the *elegans* form group make up less than 2% acanthodian total (AT) or acanthodian scale total (ATS), were mostly collected in the 0.5≤ mm fraction and absent from the 0.106-0.212 mm fractions.

Head plates, probably nostolepid, make up *c.* 6% ATS. One nostolepid head plate was collected to *c.* six *Nostolepis striata* trunk scales. If the *elegans* scales are added to the *N. striata* trunk scales the ratio is less than one in seven. The number of stellate, coronate and indeterminable head plates each comprise roughly one third of the total plate number. The plates occur in all fractions.

Five, probably nostolepid, squamae umbellatae were collected, all from the largest fraction. Four squamae proniae were collected, *c.* 0.5% AT, and when set off against the number of *Nostolepis striata* trunk scales the percentage is 1.5%. The smallest specimen was found in the 0.355 mm fraction. Structures identified as nostolepid tooth plate remains make up *c.* 1% when compared to the nostolepid trunk scale total. The smallest was picked from the 0.212 mm fraction. When all topospecific nostolepid scales and plates are included in the count, the latter two percentages drop only slightly.

The number of scales that look like *Gomphonchus sandelensis* is largest in the 0.106 mm fraction, which contains more than 75% of these scales. The small scales include many worn specimens that are hard to identify under the binocular microscope and

can include scales from other taxa, especially poracanthodid scales. In total these '*G. sandelensis*' scales make up *c.* 10% AT.

The distinction between the form variants of *Gomphonchus volborthi* and acanthodian morph 2 was hard to make in much material, and the two taxa were combined for this section. More than 50% of the scales were collected from 0.106 and 0.212 mm fractions. The scales were present in all fractions. Their total number comprises *c.* 20% AT.

Poracanthodid scales are present in each fraction and comprise *c.* 20% AT. The scales of *Radioporacanthodes biblicus* (2, plus 2 possible specimens) and of forma *bifurcata* are rarest (together, at best, 1.5% AT). A large part of the poracanthodid scales might belong to *Poracanthodes? lehmani*; the small size of many of these scales is an extra obstacle to their identification. About 20 specimens (3% AT), all from the 0.106 mm fraction, were referred to the punctatiform *Poracanthodes* cf. *P. punctatus*.

Scales of acanthodian morph 5 comprise less than 2% AT and nearly all (11 out of 13 specimens) were collected from the 0.106 mm fraction. Ischnacanthid tooth whorl fragments comprise less than 1% AT.

Acknowledgements

Ulf Borgen is kindly thanked for loan of NRS material. Bert Boekschoten (Rijksuniversiteit Groningen, RUG), Carole Burrow (University of Queensland) and Susan Turner (Queensland Museum) read the manuscript, and made valuable suggestions to improve it. As ever, Jan Zagers (Electronic Microscopy, Biology Centre, RUG) made the micrographs, but this time in the medical SEM lab, for which I also express thanks to Ietse Stokroos. Wiebe Haaima, Jim Robot (Graphic Service Centre, RUG) and Rudmer Nijman (professional photographer) did a lot of invaluable work preparing the scan images for publication. Martin Staal and Ger Telkamp (Laboratory for Plant Physiology, RUG Biology Centre) made available digital camera and microscopic facilities to take the histological photos. The reviews of this paper by the referees are acknowledged as memorable.

References

Agassiz, J. L. R. *In* Murchison, R. I. 1839. *The Silurian System (1st Edition).* London: 1-768.

Afanassieva, O. B. 1999. The exoskeleton of *Ungelaspis* and *Ateleaspis* (Osteostraci, Agnatha) from the Lower Devonian of Severnaya Zemlya, Russia. *Acta Geologica Polonica*, **49**: 119-123.

Blom, H. 1999. Vertebrate remains from Upper Silurian – Lower Devonian beds of Hall Land, North Greenland. *Geology of Greenland Survey Bulletin*, **182**: 1-80.

Brotzen, F. 1934. Erster Nachweis von Unterdevon in Ostseegebiet durch Konglomeratgeschiebe mit Fischresten. II. Teil (Paläontologie). *Zeitschrift für Geschiebeforschung*, **10**: 1-65.

Fredholm, D. 1988a. Vertebrates in the Ludlovian Hemse Beds of Gotland, Sweden. *Geologiska Föreningens i Stockholm Förhandlingar*, **110**: 157-179.

Fredholm, D. 1988b. Vertebrate biostratigraphy of the Ludlovian Hemse Beds of Gotland, Sweden. *Geologiska Föreningens i Stockholm Förhandlingar*, **110**: 237-253.

Grönwall, K. A. 1897. Öfversikt af Skånes yngre öfversiluriska bildningar. *Geologiska Föreningens i Stockholm Förhandlingar*, **19**: 188-244.

Gross, W. 1947. Die Agnathen und Acanthodier des obersilurische Beyrichienkalks. *Palaeontographica, A*, **96**: 91-158.

Gross, W. 1967. Über Thelodontier-Schuppen. *Palaeontographica, A,* **127**: 1-67.

Gross, W. 1968. Die Agnathen-fauna der silurischen Halla-schichten Gotlands. *Geologiska Föreningens i Stockholm Förhandlingar*, **90**: 369-400.

Gross, W. 1971. Downtonische und dittonische Acanthodier-Reste des Ostseegebietes. *Palaeontographica, A*, **136**: 1-82.

Hoppe, K.H. 1931. Die Coelolepiden und Acanthodier des Obersilurs der Insel Oesel. *Palaeontographica*, **76**: 35-94.

Jeppsson, L. & Laufeld, S. 1986. The late Silurian Öved-Ramsåsa Group in Skåne, south Sweden. *Sveriges Geologiska Undersökning, Ser. Ca,* **58**: 1-45.

Karatajute-Talimaa, V. 1978. *Silurian and Devonian Thelodonts of the USSR and Spitsbergen.* Mokslas Publishers Vilnius, 334 pp. [In Russian.]

Larsson, K. 1979. Silurian tentaculitids from Gotland and Scania. *Fossils & Strata,* **11**: 1-180.

Lehman, J-P. 1937. Les Poissons du Downtonien de la Scanie (Suède). *Mémoire de la Faculté des Sciences de l' Université de Paris. N° d'ordre: 664.* Université de Paris, Rennes: 1-98.

Leonhardt, H. 2000. *Sesam atlas van de anatomie. Deel 2. Inwendige organen*. Sesam/uitgeverij Intro, Baarn: 363 pp.

Märss, T. 1982. *Thelodus admirabilis* n. sp. (Agnatha) from the Upper Silurian of the East Baltic. *Eesti NSV Teaduste Akadeemia Toimetised, 31. Köide Geoloogia*, **3**: 112-116.

Märss, T. 1986a. Squamation of the thelodont agnathan *Phlebolepis*. *Journal of Vertebrate Paleontology*, **6**: 1-11.

Märss, T. 1986b. Silurian Vertebrates of Estonia and west Latvia. *Fossilia Baltica*, **1**: 1-104 [In Russian, with English abstract.]

Märss, T. 1997. Vertebrates of the Pridoli and Silurian-Devonian boundary beds in Europe. *Modern Geology*, **21**: 17-41.

Märss, T. 1999. A new Late Silurian or Early Devonian thelodont from the Boothia Peninsula, Arctic Canada. *Palaeontology*, **42**: 1079-1099.

Märss, T. 2000. Silurian vertebrate studies during 1990-1997. *Courier Forschungsinstitut Senckenberg*, **223**: 81-90.

Märss, T. & Ritchie, A. 1998. Articulated thelodonts (Agnatha) of Scotland. *Transactions of the Royal Society of Edinburgh; Earth Sciences,* **88**: 143-195.

Miller, C.G. & Märss, T. 1999. A conodont, thelodont and acanthodian fauna from the Lower Pridoli (Silurian) of the Much Wenlock Area, Shropshire. *Palaeontology* **42**: 691-714.

Moberg, J.C. 1910. Guide for the principal Silurian districts of Scania (with notes on some localities of Mesozoic beds. *Geologiska Föreningens i Stockholm Förhandlingar*, **32**: 45-194.

Moberg, J.C. & Grönwall, K.A. 1909. Om Fyledalens Gotlandium. *Kungliga Fysiografiska Sällskapets Handlingar. N.F. Bd 20,* **1**: 84 pp.

Otto, M. & Laurin, M. 1999. Osteostracan tesserae from the Baltic Middle Devonian: morphology and microanatomy. *Neues Jahrbuch für Geologie und Paläontologie, Monatshefte*, 464-476.

Pander, C.H. 1856. *Monographie der fossilen Fische des Silurischen Systems der Russisch-Baltischen Gouvernements.* St. Petersburg: 91 pp.

Reif, W.-E. 1985. Squamation and ecology of sharks. *Courier Forschungsinstitut Senckenberg*, **78**: 1-255

Rohon, V. 1893. Die obersilurischen Fische von Oesel. II. Theil. *Mémoires Académie Impériale des Sciences de St. Pétersbourg,* **41** (5): 1-124

Turner, S. 1973. Siluro-Devonian thelodonts from the Welsh Borderland. *Journal of the Geological Society of London*, **129**: 557-584.

Turner, S. 1984. *Studies on Palaeozoic Thelodonti* (Craniata: Agnatha). Unpublished Ph.D. Thesis, University of Newcastle-upon-Tyne.

Turner., S. 1986. Vertebrate fauna of the Silverband Formation, Grampians, Western Victoria. *Proceedings of the Royal Society of Victoria,* **98**: 53-62.

Turner, S. 1991. Monophyly and relationships of the Thelodonti. *In* Chang, M-M., Liu, Y.-H. & G.-R. Zhang, G.-R. (eds), *Early Vertebrates and Related Studies of Evolution:* 87-119. Science Press, Beijng.

Turner, S. 1992. Thelodont lifestyles. *In* Mark-Kurik, E. (ed.), *Fossil Fishes as Living Animals. Academia*, **1**: 21-40. Acad. Sci, Tallinn.

Turner, S. 1995. Devonian thelodont scales (Agnatha, Thelodonti) from Queensland. *Memoirs of the Queensland Museum*, **38**: 677-685.

Turner, S. 1997. Sequence of Devonian thelodont scale assemblages in East Gondwana. *Geological Society of America Special Paper*, **321**: 295-315.

Turner, S. 2000. New Llandovery to early Pridoli microvertebrates including Lower Silurian zone fossil, *Loganellia avonia* nov. sp., from Britain. *Courier Forschungsinstitut Senckenberg*, **223**: 91-127.

Turner, S. *submitted*. Thelodonti. *In* Schultze, H.-P. (ed.), *Handbook of Paleoichthyology*. Gustav Fischer Verlag, Stuttgart.

Turner, S. & Young, G.C. 1992. Thelodont scales from the Middle-Late Devonian Aztec Siltstone, southern Victoria Land, Antarctica. *Antarctic Science*, **4**: 89-105.

Turner, S. & van der Brugghen, W. 1993. The Thelodonti, an important but enigmatic group of Palaeozoic fishes. *Modern Geology*, **18**: 125-140.

Valiukevicius, J. 1992. First articulated *Poracanthodes* from the Lower Devonian of Severnaya Zemlya. *In* Mark- Kurik, E. (ed.), *Fossil Fishes as Living Animals. Academia*, **1**: 193-213. Acad. Sci., Tallinn.

Valiukevicius, J. 1998. Acanthodians and zonal stratigraphy of Lower and Middle Devonian in East Baltic and Byelorussia. *Palaeontographica, A*, **248**: 1-53.

Vergoossen, J.M.J. 1997. Revision of poracanthodid acanthodians. *In* Ivanov, A., Wilson, M.V.H. & Zhuravlev, A. (eds), *Palaeozoic Strata and Fossils of the Eurasian Arctic. Abstracts. Ichthyolith Issues, Special Publication*, **3**: 44-46.

Vergoossen J.M.J. 1999a. Late Silurian fish microfossils in an East Baltic-derived erratic from Oosterhaule, with a description of new acanthodian taxa. *Geologie & Mijnbouw*, **78**: 231-251.

Vergoossen, J.M.J. 1999b. Late Silurian fish microfossils from Helvetesgraven, Skåne (southern Sweden. (1). *Geologie & Mijnbouw*, **78**: 267-280.

Vergoossen, J.M.J. 1999c. Siluro-Devonian microfossils of Acanthodii and Chondrichthyes (Pisces) from the Welsh Borderland/south Wales. *Modern Geology*, **24**: 23-90.

Vergoossen, J.M.J. 2000. Acanthodian and chondrichthyan microremains in the Siluro-Devonian of the Welsh Borderland, Great Britain, and their biostratigraphical potential. *Courier Forschungsinstitut Senckenberg*, **223**: 175-199.

Vergoossen, J.M.J. 2002a. Late Silurian fish microfossils from Ramsåsa, locality H, Scania, south Sweden, with some remarks on the body zonation scheme used in thelodont studies. *Scripta Geologica*, **123**: 41-69.

Vergoossen, J.M.J. 2002b. Late Silurian fish microfossils from Klinta and Rinnebäcks Bro (Scania, south Sweden), with remarks on the morphology of *Nostolepis striata* trunk scales. *Scripta Geologica*, **123**: 71-92.

Vergoossen, J.M.J. 2002c. Late Silurian fish microfossils from Ramsåsa (sites D and 'south of church'), Skåne, south Sweden. *Scripta Geologica*, **123**: 93-158.

Vergoossen, J.M.J. 2003. *Fish fossils from the Upper Silurian Öved Sandstone Formation,Skåne, southern Sweden.* Unpublished Ph.D. Thesis, University of Groningen, The Netherlands. http://www.ub.rug.nl/eldoc/dis/science/ [search with Google].

Vergoossen, J.M.J. *submitted*. Late Silurian fish microfossils from Ramsåsa (site E), Skåne, southern Sweden. *Scripta Geologica.*

Vieth, J. 1980. Thelodontier-, Acanthodier- und Elasmobranchier-Schuppen aus dem Unter-Devon der Kanadischen Arktis (Agnatha, Pisces). *Göttinger Arbeiten zur Geologie und Paläontologie*, **23**: 69 pp.

Wang, R. 1993. Taxonomie, Palökologie und Biostratigraphie der Mikroichthyolithen aus dem Unterdevon Keltiberiens, Spanien. *Courier Forschungsinstitut.Senckenberg*, **161**: 1-205.

Appendix 1

Possible scleritome taxa grouped together between [ ]; species not described or figured in this paper are followed by author's name.

Agnathous fishes from Ramsåsa C

Osteostracans: hemicyclaspid **-** Thelodonts: [*Thelodus parvidens* s.s.[1] - forma *T. pugniformis* Gross, 1967- forma *T. bicostatus* Hoppe, 1931 - forma *T. trilobatus* - forma *T. querceus*] - [*Thelodus traquairi* - forma *T. ramosus* -forma *baltica*, forma nova] -*Thelodus admirabilis* - [*Thelodus sculptilis* - forma *T. radiosus*] - *Loganellia cuneata* Gross, 1967- *Paralogania ludlowiensis*.

Gnathostome assemblage from Ramsåsa C

Acanthodians: [*Nostolepis striata* - forma '*elegans*'] - squamae proniae - nostolepid stellate plates - nostolepid coronate scales and plates - nostolepid squamae umbellatae[2] - nostolepid spines[2] and tooth platelets - *Gomphonchus sandelensis* (Pander, 1856) - *Gomphonchus volborthi* - *Poracanthodes? lehmani* - *Poracanthodes* cf. *P. punctatus* - *Radioporacanthodes biblicus* -indeterminable poracanthodid, forma *bifurcata,* forma nova - ischnacanthid teeth, spines[2] and whorls[2] - acanthodian morph 2 cf. forma *bifurcata* - acanthodian morph 3 - morph 4 **-** morph 5

[1] glabrous scales only
[2] fragments only

Appendix 2

Nostolepis striata, check list of trunk scale characters.

Crown, general features: 1-10 (symmetry 1-2; shape 3; dimensions 4; plane 5-6; dorsal/ventral surfaces 7-8).

1 symmetric - asymmetric **2** asymmetric: surface facing left - or right **3** shape: triangular (trapezoid)- ellipsoid -pyramidal – [TES: inverted v-shaped - approximately tubercular] **4** dimensions: narrow - wide (in relation to width of base)- short -long (in relation to length of base) **5** plane: inclined - horizontal **6** inclination: low -moderate - steep **7** dorsal surface: concave-flat **8** ventral surface: midposterior keel

Crown rims: 9-15

9 starting position: same latitudinal level - one rim begins further posteriorly **10** anteroposterior path in anterior view: straight – convex – sigmoidal- mixed **11** if mixed, how and in which rim: e.g. centrad twist of the right rim in its upper part **12** anteroposterior path in lateral view: one or both crown rims arched -or not **13** if arched, which rim and where: in its lowermost part -halfway -elsewhere (specify) **14** the angles at which the rims meet posteriorly **15** constricting anterior crown by bending inwards - or not

Lateral crown rims: 16-22

16 number: left - right **17** starting position of most anterior lateral crown rims: at the level of the lateral corners of the base - further anterior/posterior **18** anteroposterior path in anterior view: straight - curved (convex - concave) **19** bending inwards

anteriorly - or not **20** converging with posterior crown tip - ending well below tip **21** narrow (ridge-like) - broad (ledge-like) **22** plain - ornamented

Lateral crown surfaces: 23

23 present - absent

Anterior crown margin 24-26

24 straight - irregular - with 'Vorkrönchen' or 'Nebenkrönchen'- lobed **25** TES: lobed - separated lobes (in combination with inverted V-shaped crown, feature 3) **26** TES: with median 'bay' present - absent

Anterior riblets (27-33) *or lobes* (27, 30), *forward projected anteromedian median rib pair* (34-35) *or lobe* (36)

27 present (their number) - absent **28** arched - or ascending from the neck at right angles **29** all sharp-edged - or not (specify) **30** starting position: at same latitudinal level - or not (if not, which is/are positioned further posteriorly than others) **31** length: of same length - of different lengths - laterad longer - otherwise (specify) **32** orientation: towards lateral left - towards lateral right - longitudinal - mixed (specify) **33** orientation: all parallel (to what?) - partly parallel (to what?) **34** forward projected median pair: present - absent **35** forward projected median pair: of parallel - posteriorly diverging - posteriorly converging riblets **36** forward projecting anteromedian lobe: lobe widening posteriad- lobe narrowing posteriad

Median dorsal crown: (37-38)

37 median opening in lower crown half 38 midposterior ridge

Lateral riblets: (39-40)

39 present: between lateral rim and crown rim - between lateral rims - on one lateral surface - on both lateral surfaces - left - right; - absent **40** orientation - length - number

Crown in relation to base: (41-46)

41 crown filling: entire upper basal platform - part of platform **42** unornamented zone of basal platform: anterior - anterolateral - lateral - posterolateral - posterior - all around **43** distance between crown and edge or rim of basal platform; narrow - wide **44** surface between crown and basal edge or rim of basal platform (not the neck); concave - flat - convex- sloping **45** crown protruding over base - or not **46** protrusion of crown: posterior tip- posterior/lateroposterior third - posterior/lateroposterior half

Neck: (47-49)

47 lateral - posterior – lateroposterior **48** low - high - moderately high **49** openings of vascular system: none - tiny - medium - large (size relative to 0.1 mm bar)

Neck ribs: (50-57)

50 developed as: sharp ridges - ribbons (=broader) - sheets (=still broader) **51** straight - curved **52** where: on the left - on the right - posterior - on the left and right - on the left, right and posterior **53** number **54** starting point: near base level - higher in

the neck - near the end point of a more anterior neck rib **55** length: as long as the lateral neck - shorter - mixed (specify further) **56** direction: oblique - vertical - in continuation of a more anterior neck rib - parallel to the crown rim -parallel to the lateral crown rim(s) - parallel to other neck rib **57** converging: with posterior crown point - with posterior part of crown rim - with the median part of the crown rim - with the anterior part of the crown rim -with lateral crown rim (low-halfway-high) - with another neck rib

Neck/base junction: (58-59)

58 with sharp edge - blunted edge **59** anterior basal edge or rim: straight - infolding - rounded - angular

Base: (60-62)

60 shape: rhombic - otherwise (specify) **61** plane: concave - flat - convex (low - deep - moderately deep in relation to total scale height) **62** dimensions: longer than wide - wider than long

All figured specimens are from Ramsåsa C. Scalebars represent 0.1 mm unless stated otherwise. Morphology is shown in Figs. 1-109, histology in Figs. 110-128.

Plate 1 (Figs. 1-8)

Figs. 1-7. Osteostracan fishes.

Figs. 1-5. Variant 1.

Fig. 1. P9030. Hemicyclaspid? (a) External view. (b) Close up of external openings. Bar 0,01 mm. (c) More lateral view than 1a.

Fig. 2. P9031. Hemicyclaspid? (a) Lateral view. (b) Dorsal view.

Fig. 3. P9032. (a) Dorsolateral view. (b) Detail of 3a. (c) Anterior view.

Fig. 4. P9033. Hemicyclaspid scale? (a) Anterior view. (b) Lateral view.

Fig. 5. P9034. (a) Dorsolateral view, anterior to the left. (b) Anterior view.

Figs. 6-7. Variant 2.

Fig. 6. P9035. (a) Lateral view of ridge. (b) Anterior view.

Fig. 7. P9036. Anterolateral view of ridge.

Fig. 8. *Thelodus parvidens* (scleritome) *sensu* Märss, 1986b.

Fig. 8. P9038. Head scale. (a) Anterior view. (b) Lateral view. (c) Dorsal view.

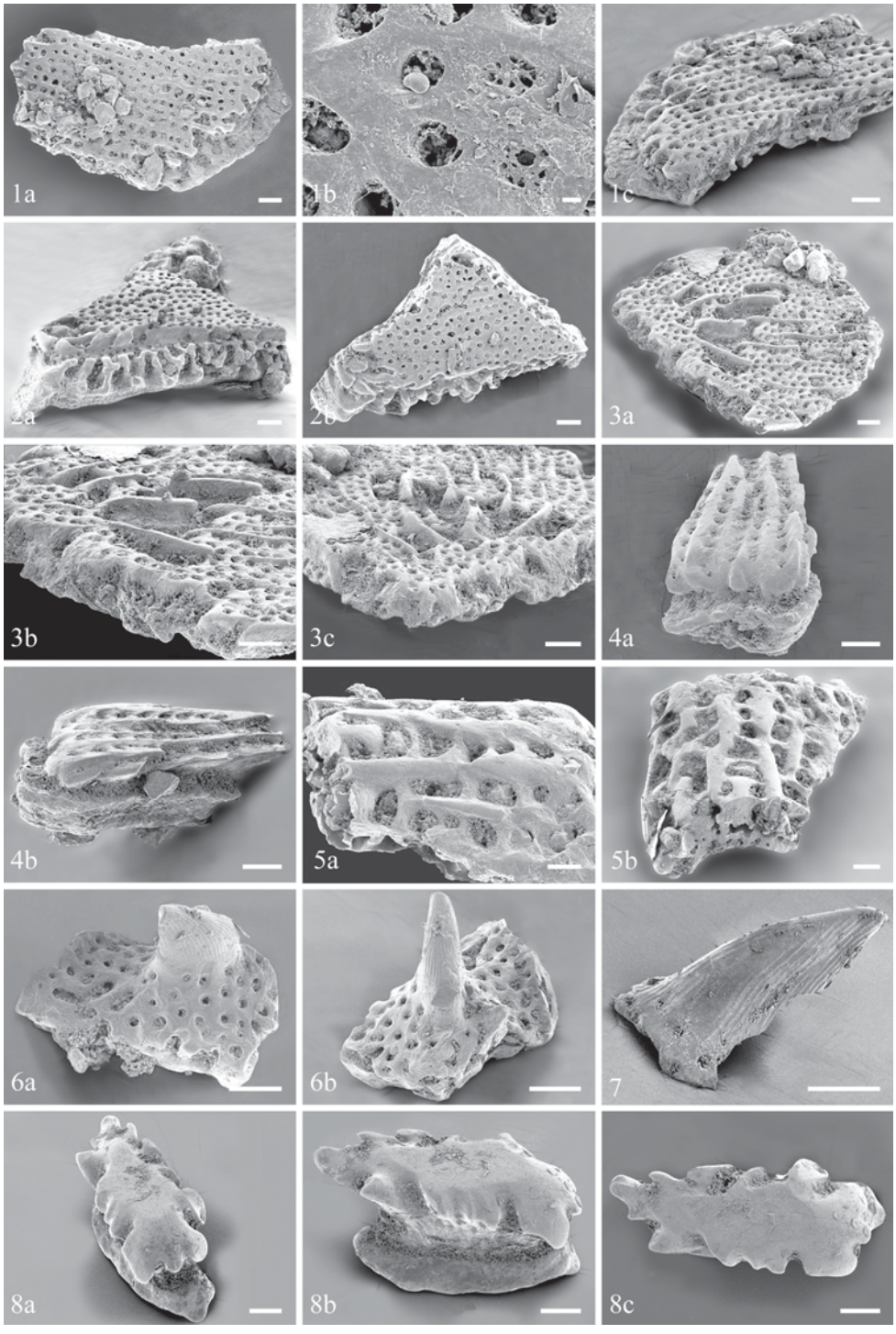
1a
1b
1c
2a
2b
3a
3b
3c
4a
4b
5a
5b
6a
6b
7
8a
8b
8c

Plate 2 (Figs. 9-17b)
Figs. 9-17b. *Thelodus parvidens* (scleritome) *sensu* Märss, 1986b.

Fig. 9. P9039. Glabrous, shallowly latero-incised head scale. (a) Dorsal view. (b) Lateral view.
Fig. 10. P9040. Glabrous, shallowly postero-incised head scale. (a) Anterolateral view. (b) Posterior view.

Figs. 11-17b. Forma *Thelodus trilobatus* Hoppe, 1931 *sensu* Gross, 1967.
Figs. 13-17b. Scales with monocuspid crowns, including forma *Thelodus querceus* Lehman, 1937.
Fig. 11. P9042. Scale transitional between several scale forms of the head. (a) Anterior view. (b) Lateral view.
Fig. 12. P9043. Scale transitional between several scale forms of the head. (a) Crown view. (b) Lateral view.
Fig. 13. P9044. (a) Anterior view. (b) Lateral view.
Fig. 14. P9045. (a) Anterior view. (b). Lateral view.
Fig. 15. P9046. (a) Anterior view. (b) Lateral view.
Fig. 16. P9047. Scale with double spur and monocuspid? crown. (a) Anterior view. (b) Lateral view.
Fig. 17. P9048. (a) Crown view. (b) Lateral view.

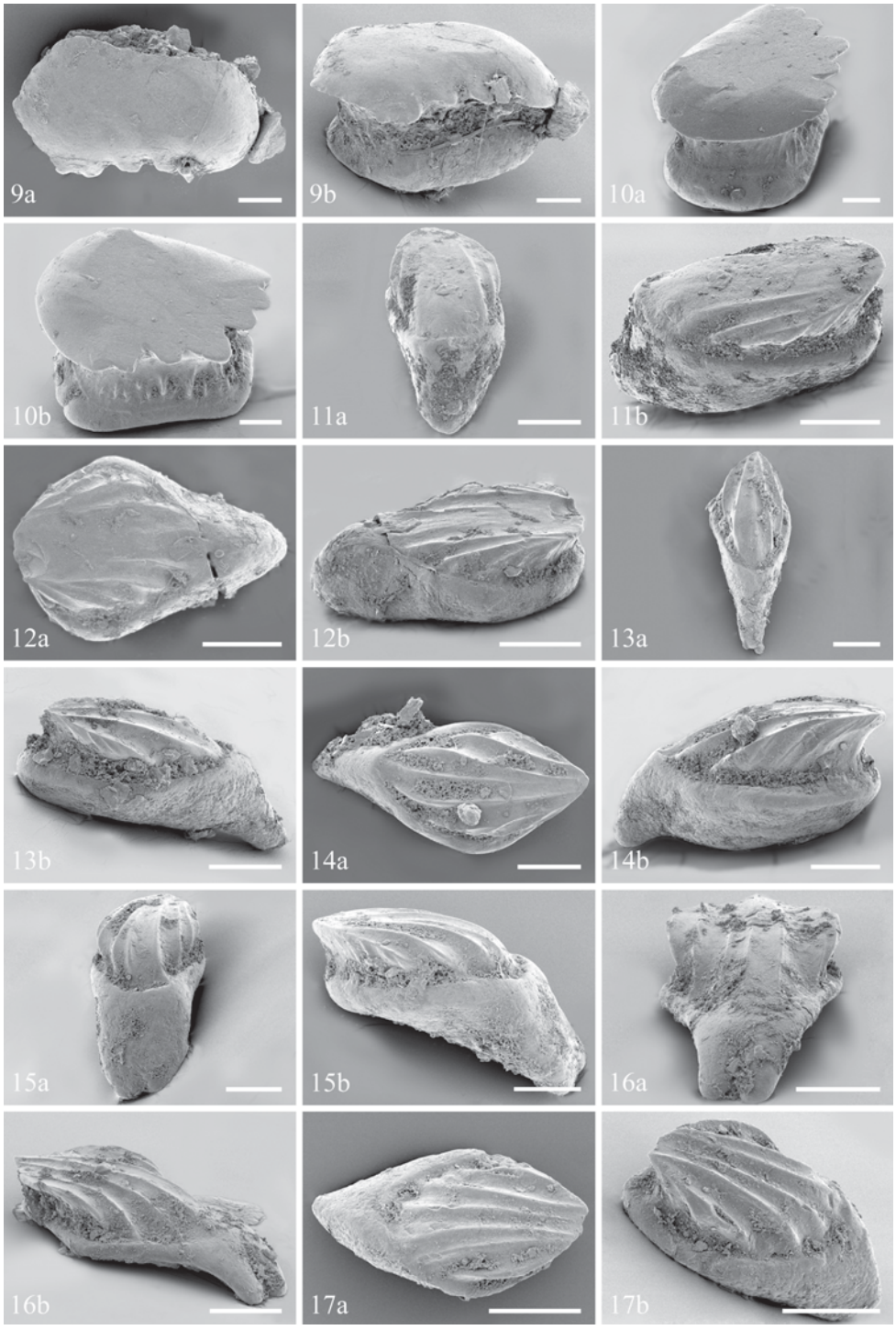
9a
9b
10a
10b
11a
11b
12a
12b
13a
13b
14a
14b
15a
15b
16a
16b
17a
17b

Plate 3 (Figs. 17c-27)
Figs. 17c-23. *Thelodus parvidens* (scleritome) *sensu* Märss, 1986b.

Figs. 17c-18. Forma *Thelodus trilobatus* Hoppe, 1931 *sensu* Gross, 1967. Scales with monocuspid crowns, including forma *Thelodus querceus* Lehman, 1937.
Fig. 17. P9048. (c) Lateral view.
Fig. 18. P9049. (a) Lateral view. (b) Anterolateral view.

Figs. 19-23. Forma *T. trilobatus* Hoppe, 1931 *sensu* Gross, 1967. Scales with polycuspid crowns.
Fig. 19. P9052. Crown view.
Fig. 20. P9053. Scale with double spur and beginning rhizoid formation. (a) Crown view. (b) Anterolateral view.
Fig. 21. P9054. Scale with double spur. (a) Anterior view. (b) Lateral view.
Fig. 22. P9055. Scale with double spur. (a) Anterior view. (b) Lateral view.
Fig. 23. P9056. Scale with beginning rhizoid formation. (a) Lateral view. (b) Anterior view.

Figs. 24-27. *Thelodus sculptilis* Gross, 1967.
Fig. 24. P9060. Lateral view.
Fig. 25. P9061. Crown view.
Fig. 26. P9063. (a) Crown view. (b) Posterior view.
Fig. 27. P9064. (a) Anterior view. (b) Lateral view.

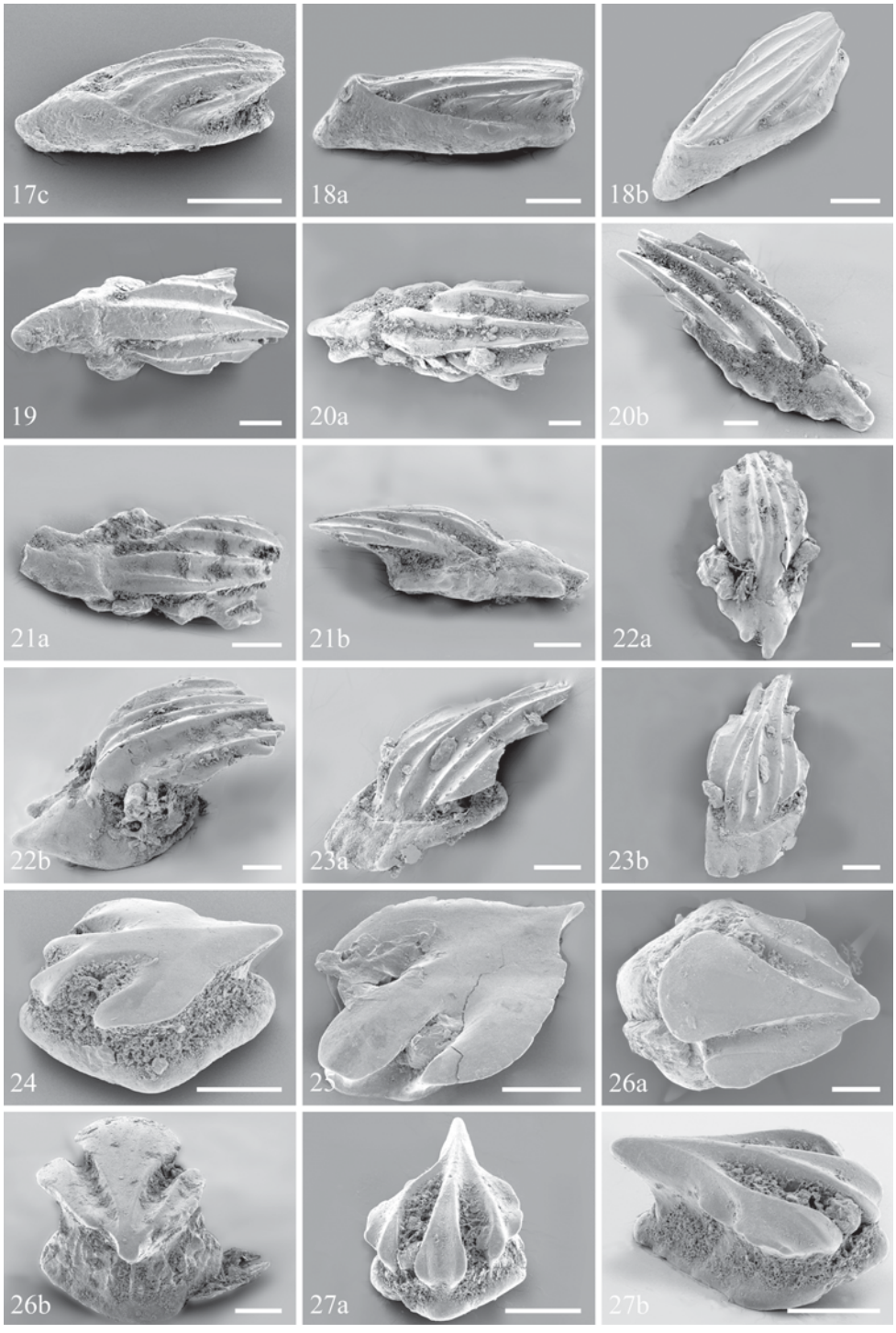
17c
18a
18b
19
20a
20b
21a
21b
22a
22b
23a
23b
24
25
26a
26b
27a
27b

Plate 4 (Figs. 28-36)

Fig. 28. P9065. *Thelodus sculptilis*? Pinnal scale? (a) Anterior view. (b) Lateral view.

Fig. 29. P9066. *T. sculptilis*? or *T. admirabilis*? Oral scale. Lateral views. (a) Posterior right. (b) Anterior right.

Fig. 30. P9067. *T. sculptilis*. Cephalopectoral scale. (a) Lateral view. (b) Anterolateral view.

Fig. 31. P9068. *T. sculptilis*? Cephalopectoral scale. (a) Anterolateral view. Anterior base damaged. (b) Posterolateral view.

Fig. 32. P9069. *T. sculptilis*. Cephalopectoral scale. Anterior view.

Figs. 33-36. Forma *Thelodus radiosus* Lehman, 1937. *T. sculptilis* (scleritome) *sensu* Märss, 1986b?

Fig. 33. P9070. (a) Crown view. (b) Anterior view.(c) Posterior view.

Fig. 34. P9071. (a) Crown view. (b). Lateral view.

Fig. 35. P9072. (a) Posterior view. (b) Anterior view.

Fig. 36. P9073. (a) Lateral view. (b) Anterior view.

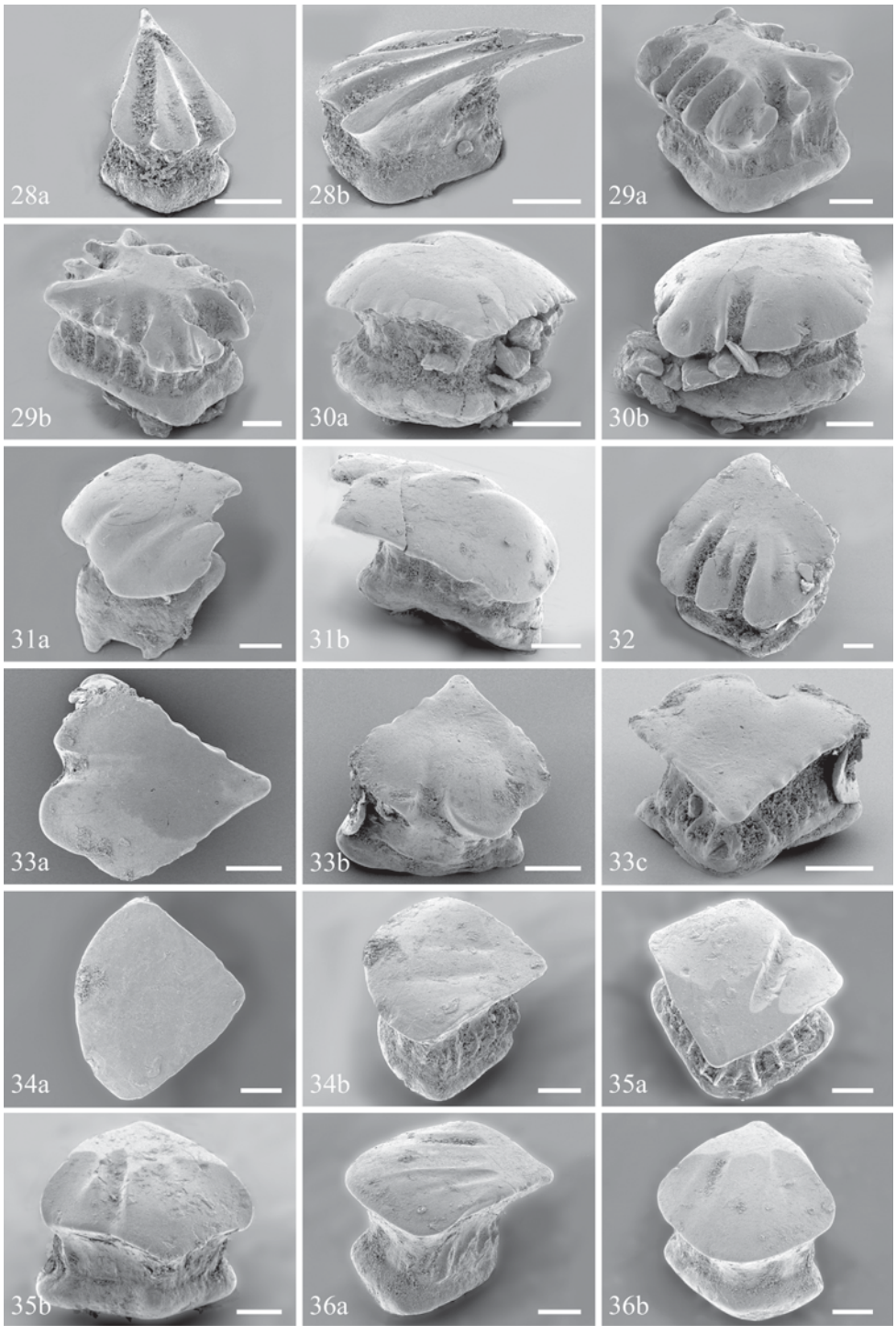
28a
28b
29a
29b
30a
30b
31a
31b
32
33a
33b
33c
34a
34b
35a
35b
36a
36b

Plate 5 (Figs. 37-47b)

Figs. 37-38, 40-41. Forma *Thelodus radiosus* Lehman, 1937. *T. sculptilis* (scleritome) *sensu* Märss, 1986b?
Fig. 37. P9074. Anterior view.
Fig. 38. P9075. Crown view.
Fig. 40. P9077. Dorsolateral view.
Fig. 41. P9078. (a) Anterior view. (b) Lateral view.

Fig. 39. P9076. *Thelodus admirabilis* Märss, 1982. Anterior view.

Fig. 42. P9079. *Thelodus sculptilis*. Postpectoral scale? (a) Anterior view. (b) Lateral view.
Fig. 43. P9080. *T. sculptilis*? cf. Polycuspid forma *T. trilobatus* scales. (a) Anterior view. (b) Lateral view.
Figs. 44-45. *T. sculptilis.*
Fig. 44. P9081. (a) Anterior view. (b) Lateral view.
Fig. 45. P9082. (a) Crown view. (b) Lateral view.

Figs. 46-47b. *Thelodus traquairi* Gross, 1967.
Fig. 46. P9083. Scale transitional to conical. (a) Crown view. (b) Posterior view.
Fig. 47. P9084. Oral scale. (a) Dorsoposterior view. (b) Lateral view.

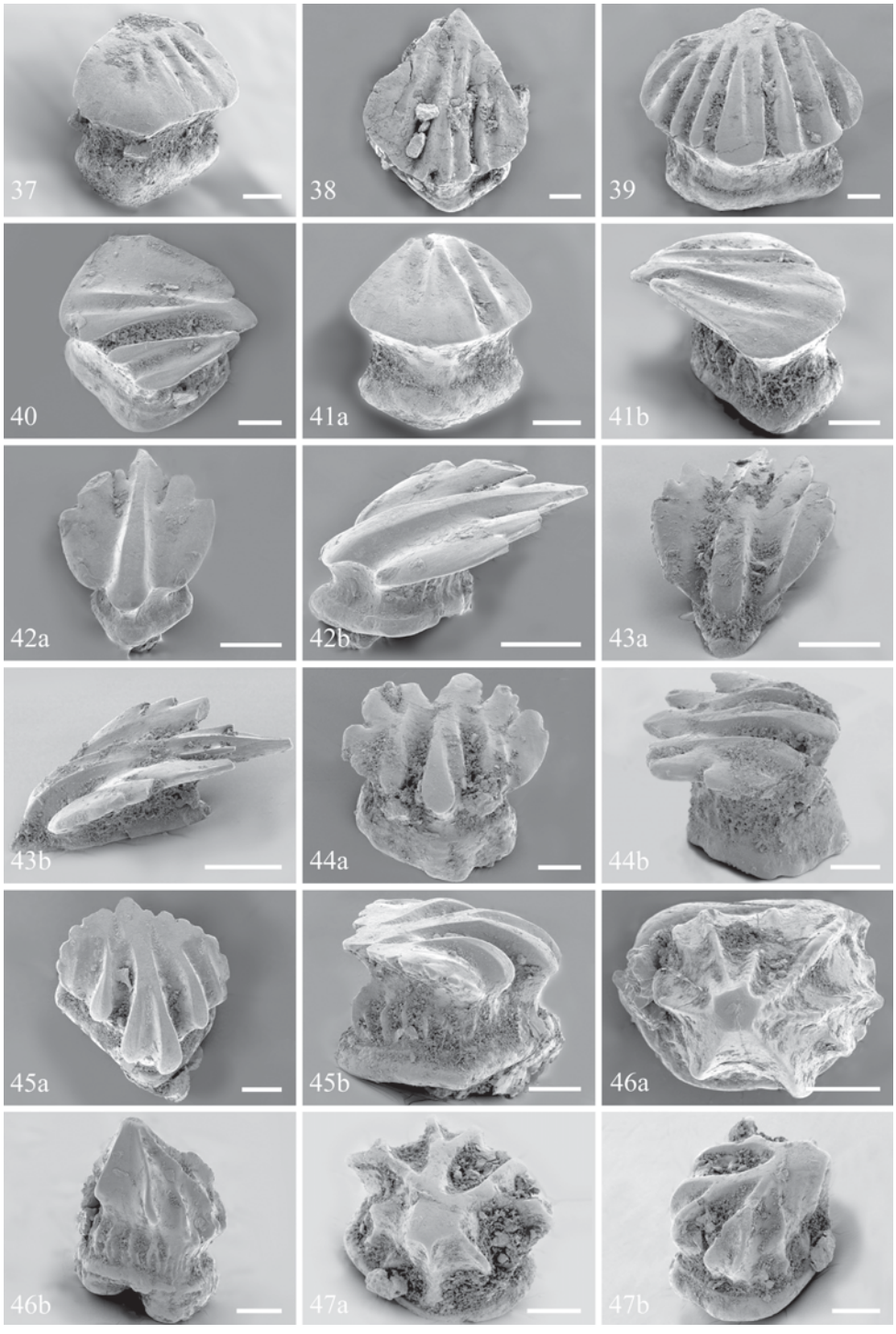
37
38
39
40
41a
41b
42a
42b
43a
43b
44a
44b
45a
45b
46a
46b
47a
47b

Plate 6 (Figs. 47c-55a)
Figs. 47c-55a. *Thelodus traquairi* Gross, 1967.
Fig. 47. P9084. Oral scale. (c) Anterior view.
Fig. 48. P9085. Oral scale. (a) Posterior view. (b) Anterior view.(c) Crown view.

Figs. 49-53. Forma *Thelodus ramosus* Lehman, 1937. Transitional to head scales?
Fig. 49. P9086. Oral scale. (a) Dorsolateral view. (b) Lateral view.
Fig. 50. P9087. Oral scale. (a) Lateral view. (b) Crown view.
Fig. 51. P9088. Oral scale. (a) Crown view. (b) Lateral view.
Fig. 52. P9089. (a) Anterolateral view. (b) Posterolateral view.
Fig. 53. P9090. (a) Lateral view. (b) Crown view.

Fig. 54. P9091. (a) Crown view. (b) Lateral view. (c) Posterolateral view.
Fig. 55. P9092. Postpectoral scale? (a) Anterior view.

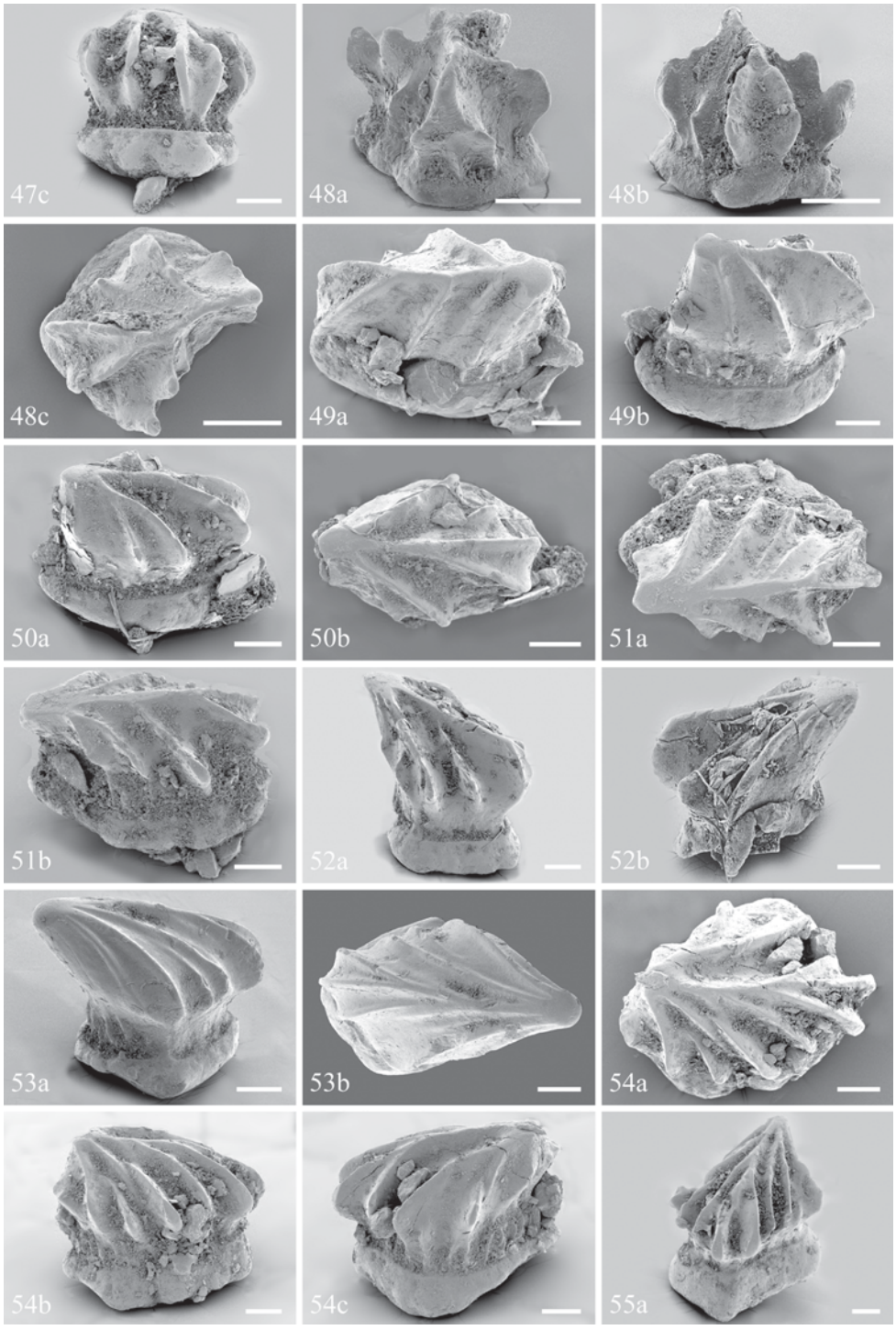
47c
48a
48b
48c
49a
49b
50a
50b
51a
51b
52a
52b
53a
53b
54a
54b
54c
55a

Plate 7 (Figs. 55b-62a)
Figs. 55b-62a. *Thelodus traquairi* Gross, 1967.
Fig. 55. P9092. Postpectoral scale? (b) Lateral view. (c) Posterior view.
Fig. 56. P9093. (a) Anterior view. (b) Lateral view. (c) Posterior view.
Fig. 57. P9094. (a) Anterior view. (b) Lateral view. (c) Posterior view.
Fig. 58. P9095. (a) Anterior view. (b) Posterior view.
Fig. 59. P9096. (a) Anterior view. (b) Posterior view.
Fig. 60. P9097. (a) Anterior view. (b) Posterior view. (c) Lateral view.
Fig. 61. P9098. (a) Anterior view. (b) Top view.
Fig. 62. P9099. (a) Anterior view.

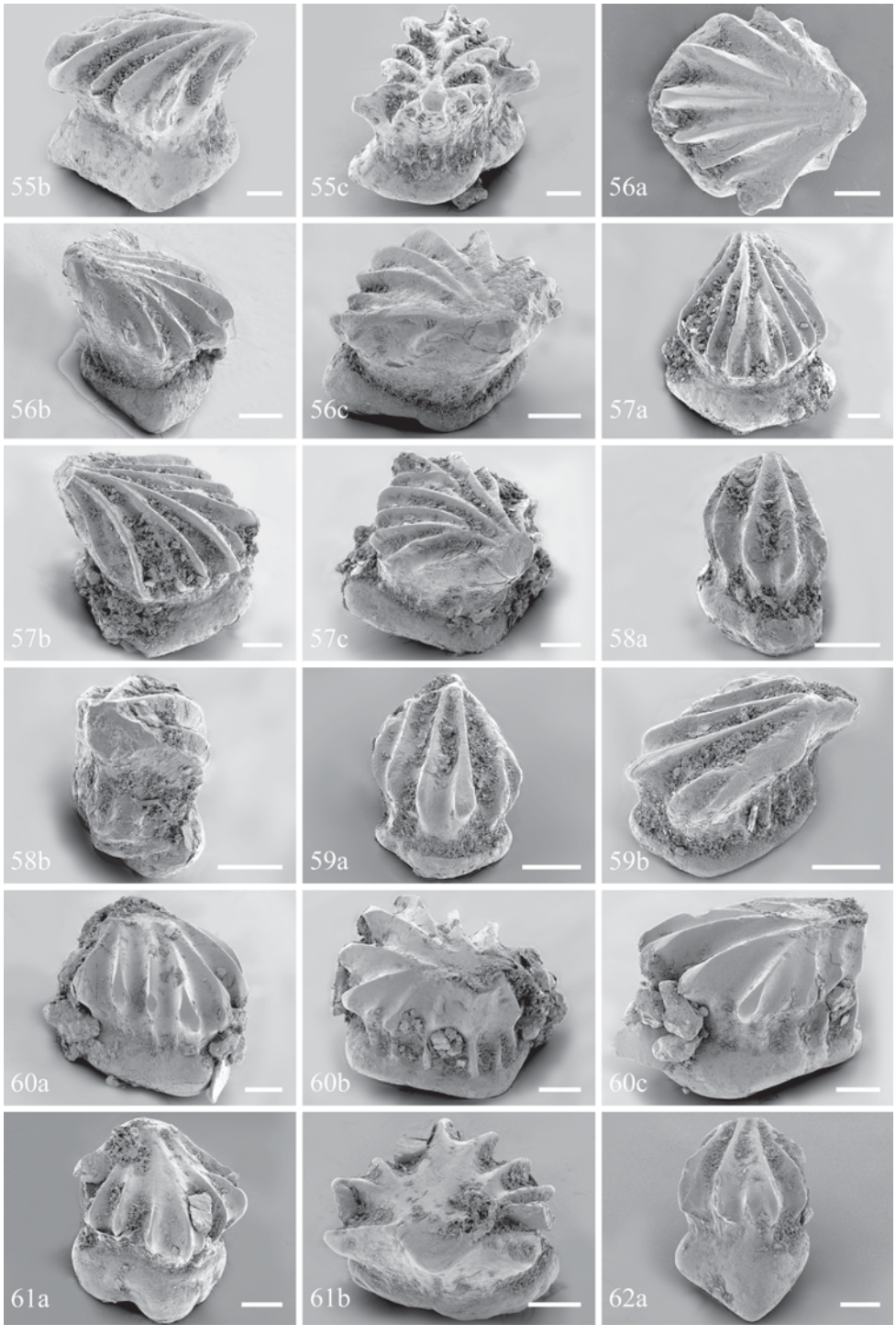
55b
55c
56a
56b
56c
57a
57b
57c
58a
58b
59a
59b
60a
60b
60c
61a
61b
62a

Plate 8 (Figs. 62b-70)
Figs. 62b-65. *Thelodus traquairi* Gross, 1967.
Fig. 62. P9099. (b) Lateral view.

Figs. 63-64. Forma *baltica*, forma nova.
Fig. 63. P9100. (a) Anterior view. (b) Lateral view.
Fig. 64. P9101. (a) Anterior view. (b) Lateroposterior view.

Fig. 65. P9102. (a) Crown view. (b) Lateral view.

Figs. 66-68. *Thelodus* cf. *traquairi.*
Fig. 66. P9103. (a) Anterior view. (b) Lateral view. (c) Posterior view.
Fig. 67. P9104. (a) Anterior view. (b) Lateral view.
Fig. 68. P9105. (a) Anterior view. (b) Lateral view.

Fig. 69. P9107. Indeterminable pinnal thelodont scale (only specimen). (a) Crown view. (b) Lateral view.

Fig. 70. P9108. *Nostolepis striata* Pander, 1856 *sensu* Gross, 1971. Trunk scale. (a) Anterolateral view. (b) Detail of posterior crown point.

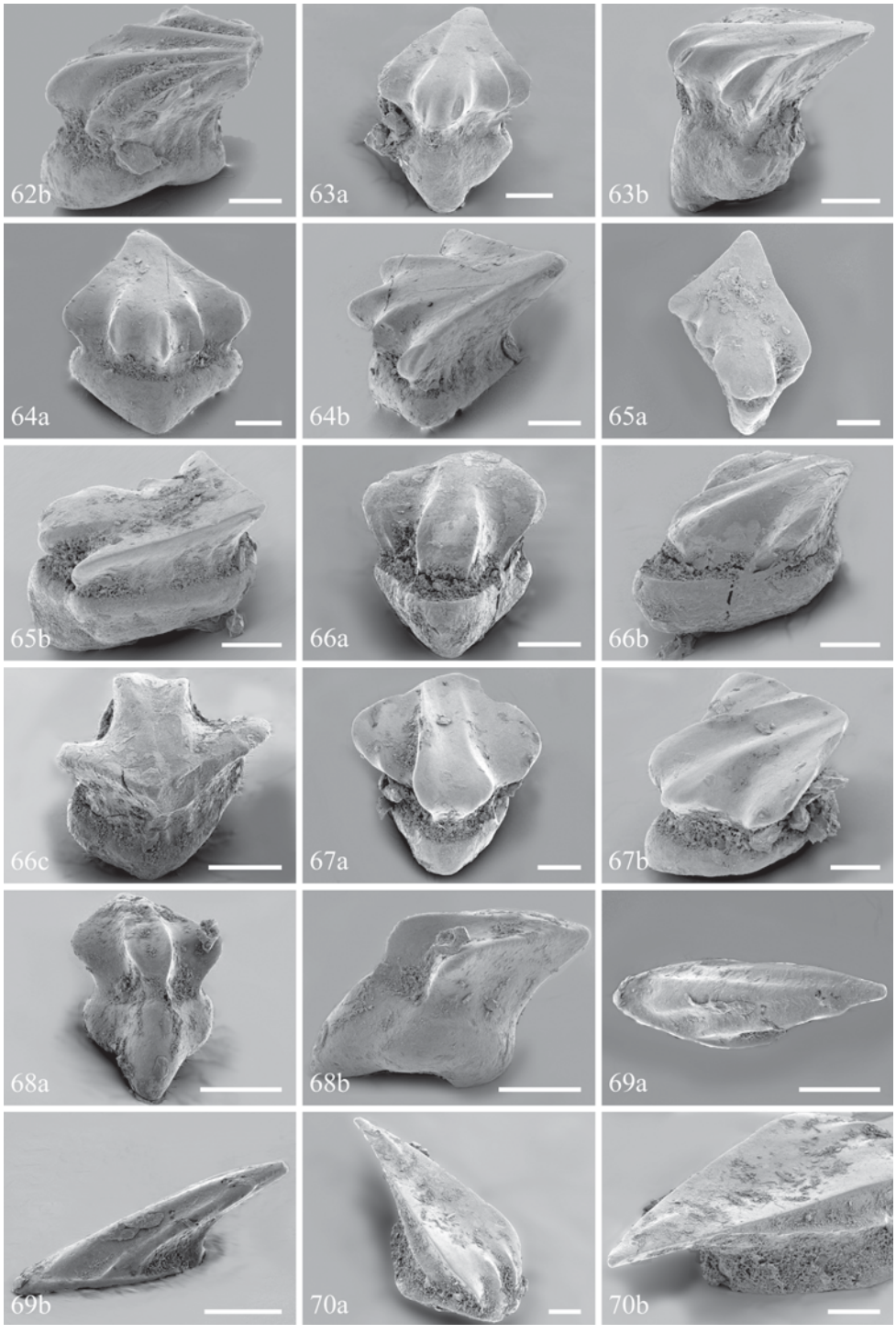
62b
63a
63b
64a
64b
65a
65b
66a
66b
66c
67a
67b
68a
68b
69a
69b
70a
70b

Plate 9 (Figs. 71-80)
Figs. 71-77. *Nostolepis striata* Pander, 1856 *sensu* Gross, 1971.
Figs. 71-76. Trunk scales.
Fig. 71. P9109. (a) Crown view. (b) Lateral view.
Fig. 72. P9111. (a) Anterior view. (b) Lateral view.
Fig. 73. P9112. Anterior view.
Fig. 74. P9113. (a) Anterior view. (b) Lateral view.
Fig. 75. P9114. (a) Anterior view. (b) Lateral view.
Fig. 76. P9115. (a) Anterior view. (b) Dorsolateral view.

Fig. 77. P9116. Anterior view.

Figs. 78-80. Nostolepid platelets and tesserae.
Fig. 78. P9117. Platelet. (a) Crown view. (b) Lateral view.
Fig. 79. P9118. Tritubercular platelet. (a) Crown view. (b) Lateral view.
Fig. 80. P9119. Tritubercular platelet. (a) Crown view. (b) Lateral view.

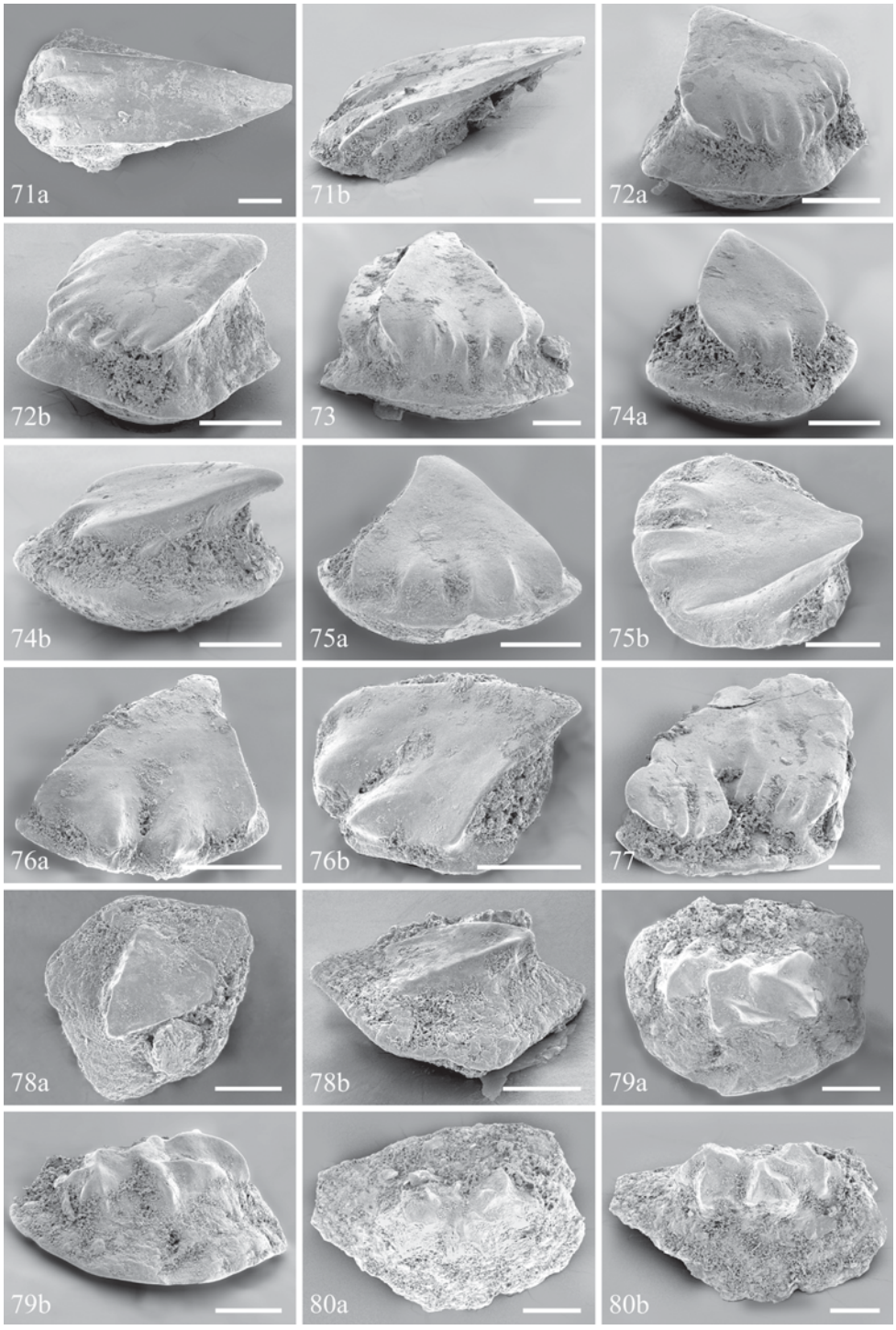
71a
71b
72a
72b
73
74a
74b
75a
75b
76a
76b
77
78a
78b
79a
79b
80a
80b

Plate 10 (Figs. 81-90a)
Figs. 81-83. Nostolepid platelets and tesserae.
Fig. 81. P9120. Tritubercular platelet. (a) Lateral view. (b) Crown view.
Fig. 82. P9121. Stellate tessera. Dorsolateral view.
Fig. 83. P9122. Stellate tessera. (a) Crown view. (b) Lateral view.

Figs. 84-87. Nostolepid tooth platelets?
Fig. 84. P9123. (a) Anterior view. (b) Lateral view.
Fig. 85. RGM 323060. Lateral view. From erratic V 85, Groningen, northern Netherlands.
Fig. 86. P9124. (a) Lateral view. (b) Anterior view.
Fig. 87. RGM 323061. (a) Anterolateral view. (b) Anterior view. From a Pridoli erratic, Groningen.

Figs. 88-90a. *Poracanthodes? lehmani* Vergoossen, 1999a.
Fig. 88. P9126. (a) Anterior view. (b) Detail of crown. (c) Detail of tissue sheet. Bar 0.01 mm in b-c.
Fig. 89. P9127. (a) Lateral view. (b) Detail of crown; bar 0.01 mm
Fig. 90. P9128. (a) Anterodorsal view.

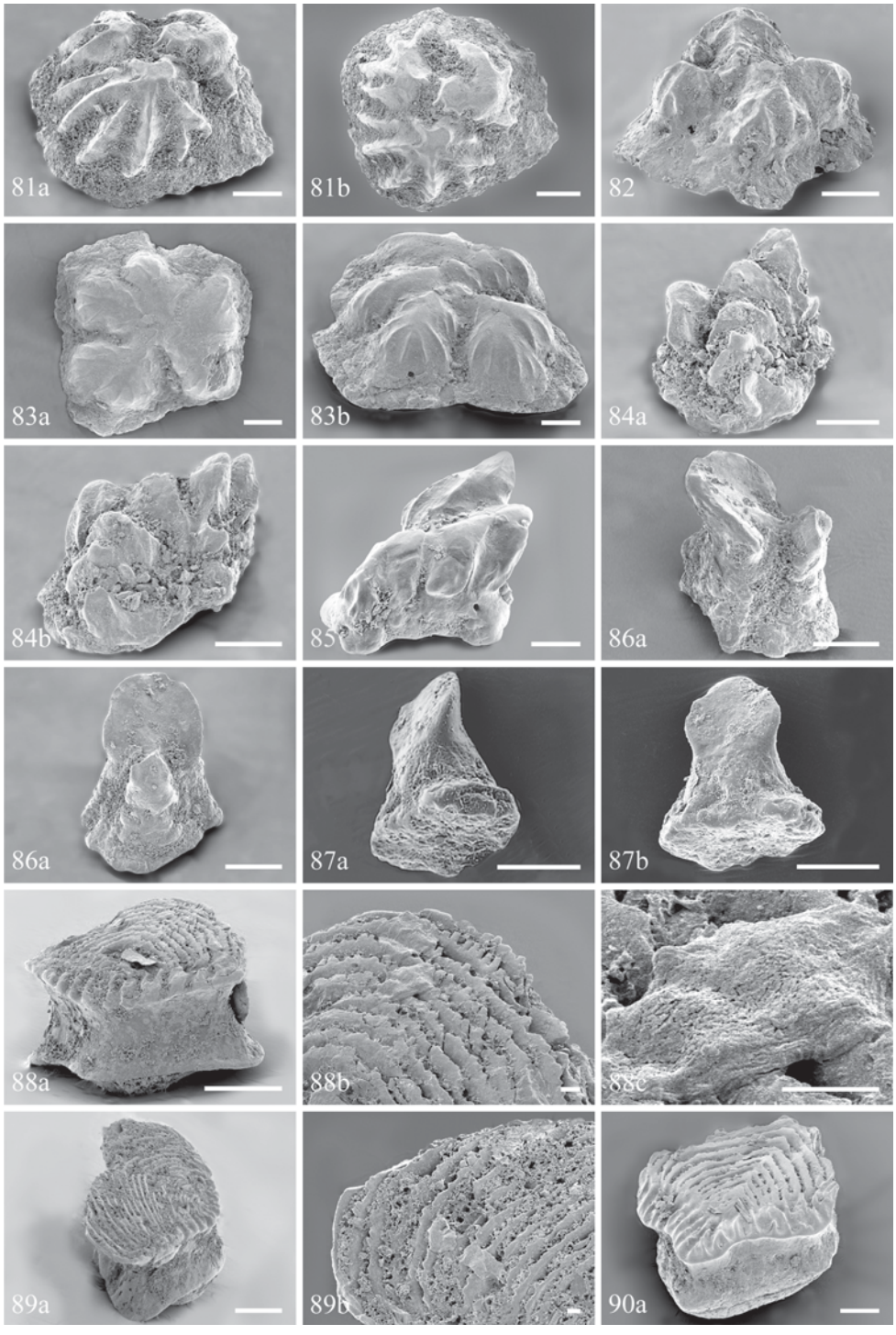
81a
81b
82
83a
83b
84a
84b
85
86a
86a
87a
87b
88a
88b
88c
89a
89b
90a

Plate 11 (Figs. 90b-99b)

Figs. 90b-94. *Poracanthodes? lehmani* Vergoossen, 1999a.
Fig. 90. P9128. (b) Detail of crown. Bar 0. 01 mm.
Fig. 91. P9129. (a) Anterior view. (b) Lateral view.
Fig. 92. P9130. Posterolateral view.
Fig. 93. P9131. Posterior view.
Fig. 94. P9132. (a) Anterodorsal view. (b) Detail of lamellar apposition in posterior crown.

Figs. 95-99b. Indeterminable poracanthodid, forma *bifurcata*, forma nova. Scales in Figs. 96-99 from Tahula 709 drill core, - 7.8 m Estonia.
Fig. 95. P9133. Crown view.
Fig. 96. RGM 323062. (a) Anterior view. (b) Detail of anterior crown. (c) Detail of posterior crown.
Fig. 97. RGM 323063. (a) Anterior view. (b) Lateral view. (c) Posterior view.
Fig. 98. RGM 323064. (a) Anterior view. (b) Posterior view.
Fig. 99. RGM 323065. (a) Anterior view. (b) Detail of crown.

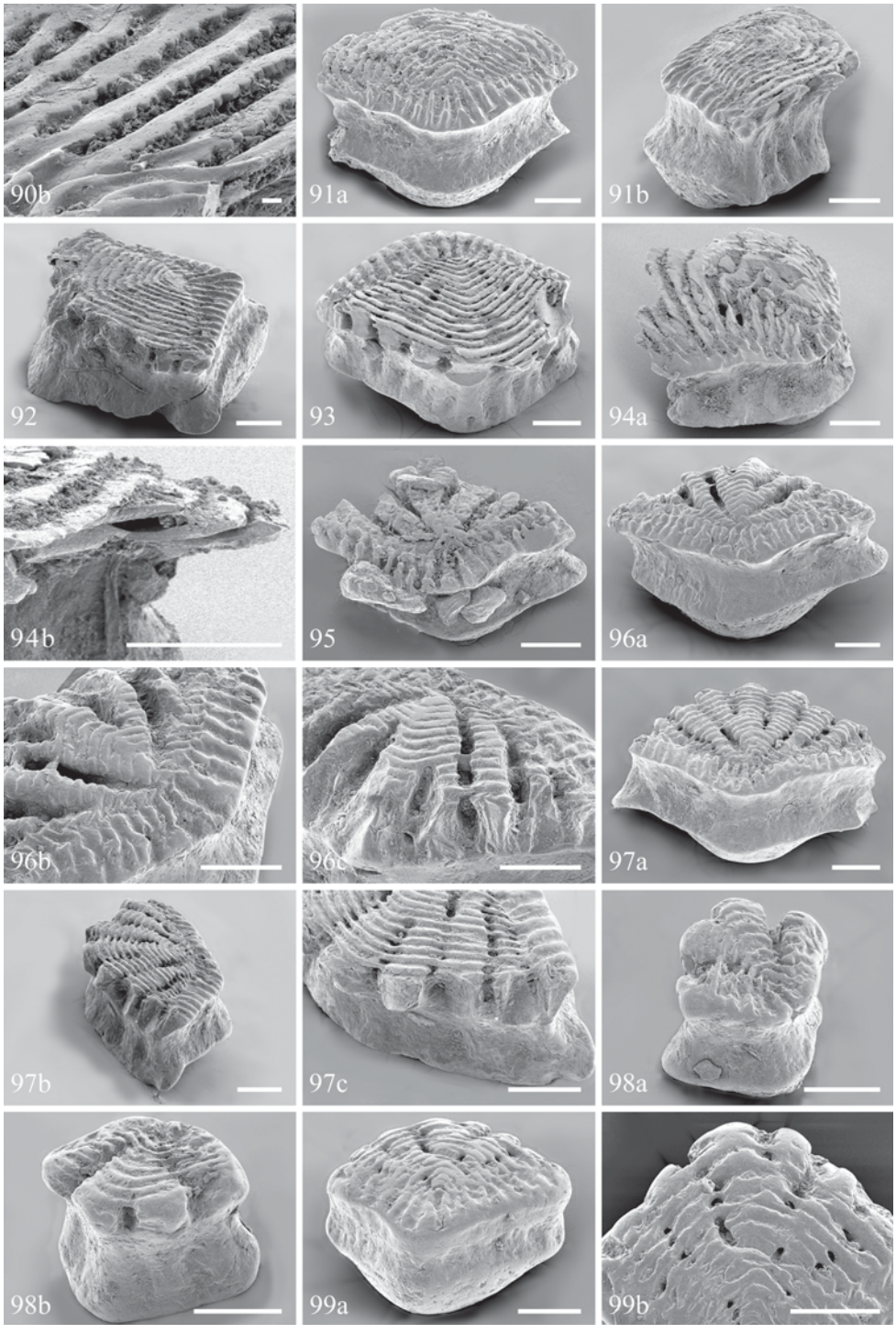
90b
91a
91b
92
93
94a
94b
95
96a
96b
96c
97a
97b
97c
98a
98b
99a
99b

Plate 12 (Figs. 99c-108)
Figs. 99c-102. Indeterminable poracanthodid, forma *bifurcata*, forma nova. Scales in Figs. 99-101 from Tahula 709 drill core, - 7.8 m, Estonia. Scale in Fig. 102 from - 8.4 m.
Fig. 99. RGM 323065. (c) Posterior view.
Fig. 100. RGM 323066. (a) Crown view from anterior. (b) Detail of midposterior scale part.
Fig. 101. RGM 323067. (a) Crown view from anterior. (b) Lateroposterior view.
Fig. 102. RGM 323068. Crown view from anterior.

Fig. 103. P9134. (a) Ischnacanthid spine fragment. (a) Leading edge. (b) Distal end. (c) Proximal end.

Fig. 104. P9135. *Gomphonchus volborthi* (Rohon, 1893). Anterior view.

Figs. 105-108. Indeterminable acanthodian scale variants.
Fig. 105. P9137. cf. Forma *bifurcata*. (a) Crown view. (b) Lateroposterior view.
Figs. 106-108. Morph 5.
Fig. 106. P9138. (a) Lateral view. (b) Anterior view.
Fig. 107. P9139. (a) Anterolateral view. (b) Anterior view.
Fig. 108. P9140. (a) Lateral view. (b) Crown view from anterior.

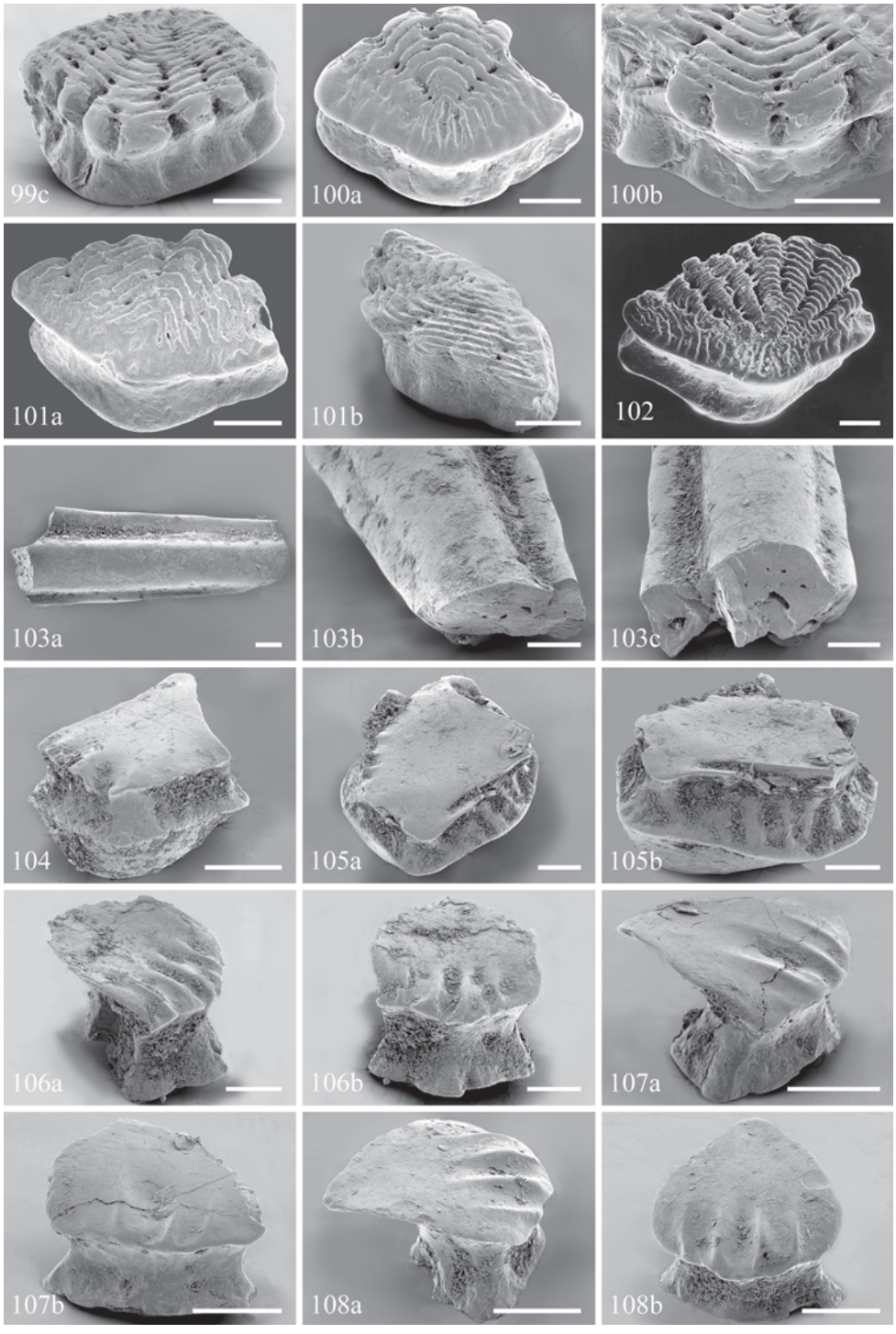
99c
100a
100b
101a
101b
102
103a
103b
103c
104
105a
105b
106a
106b
107a
107b
108a
108b

Plate 13 (Figs. 109-120a)
Fig. 109. P9141. Indeterminable acanthodian scale variant, morph 5. (a) Crown view from lateroposterior. (b) Anterior view.

The following specimens (Plate 13, Fig. 110 - Plate 20, Fig. 128) are from the Varbla 502 drill core (Ludlow, Tahula Beds, Estonia), depth 19.10 m (see Märss, 1986b). Magnification *c.* 400x. Unless stated otherwise. For histological descriptions see text.

Fig. 110a-b. RGM 323075. *Thelodus traquairi* Gross, 1967. Vertical sections through scale.

Figs. 111-112. RGM 323074. *Gomphonchus volborthi* (Rohon, 1893). '9g' Beds, Ringerike, Norway.
Fig. 111a-b. Vertical sections through scale.
Fig. 112. Vertical section through scale.

Figs. 113-115. P8822. *Poracanthodes? lehmani* Vergoossen, 1999b. Helvetesgraven, Skåne, Sweden.
Fig. 113. Horizontal section through crown.
Fig. 114. Horizontal section through crown.
Fig. 115. Horizontal section through crown.

Figs. 116-120a. RGM 323057. *Radioporacanthodes biblicus* Lehman, 1937 *sensu* Vergoossen, 2002a.
Fig. 116. Horizontal section through crown.
Fig. 117. Horizontal section through crown.
Fig. 118. (a-c) Horizontal sections through crown. Magnification b *circa* 100% of a. Magnification c *circa* 200% of a.
Fig. 119. (a-b) Horizontal sections through crown. Magnification b *circa* 250% of a.
Fig. 120. (a) Horizontal section through crown.

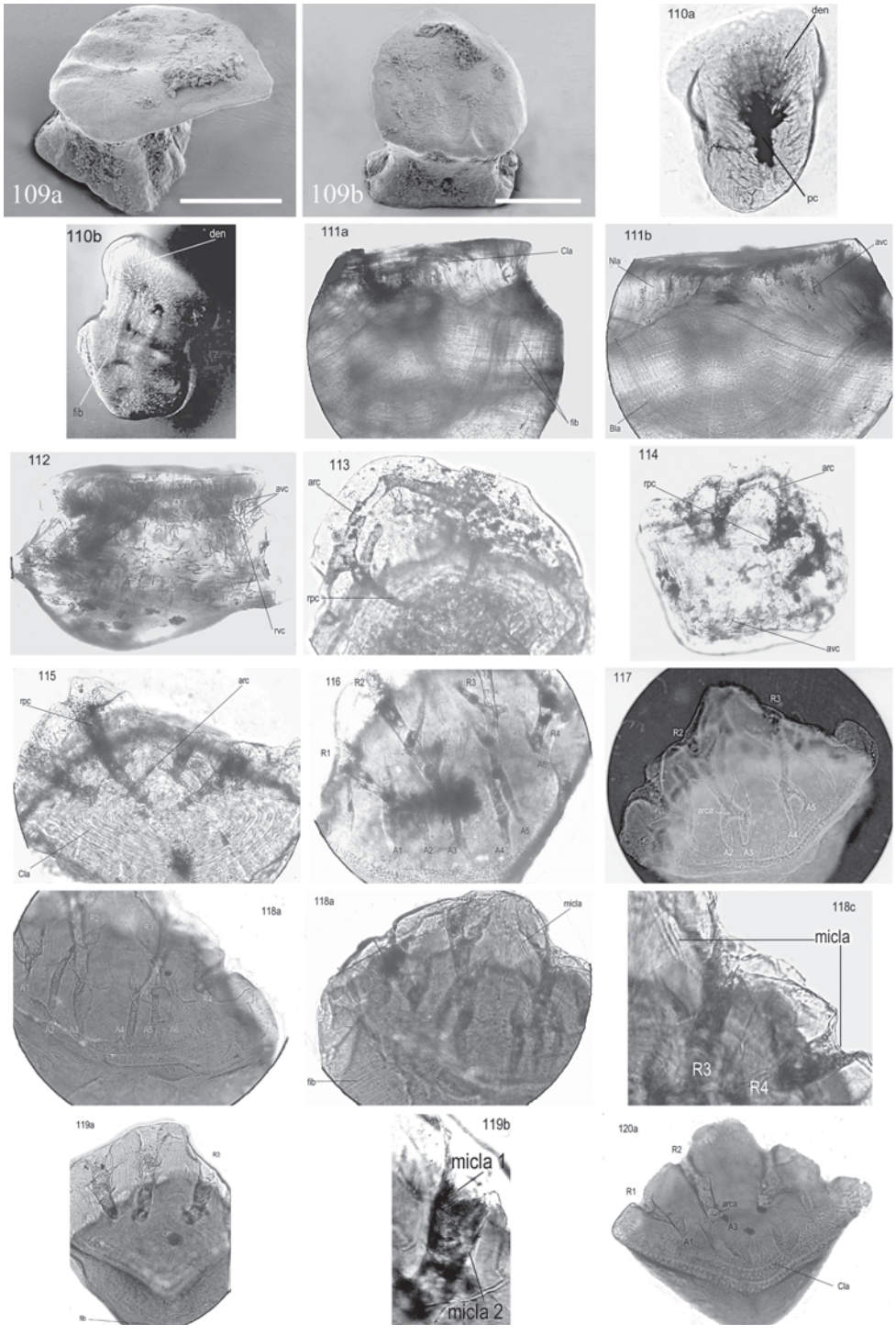
109a
109b
110a
den
pc
110b
den
fib
111a
Cla
fib
111b
avc
Nla
Bla
112
avc
rvc
113
arc
rpc
114
arc
rpc
avc
115
arc
rpc
Cla
116
R2
R3
R1
R4
A5
A1
A2
A3
A4
117
R3
R2
arca
A5
A4
A2
A3
118a
118a
micla
fib
118c
micla
R3
R4
119a
R3
fib
119b
micla 1
micla 2
120a
R2
R1
arca
A3
A1
Cla

Plate 14 (Figs. 120b-127a)

Figs. 120b-122. RGM 323057. *Radioporacanthodes biblicus* Lehman, 1937 *sensu* Vergoossen, 2002a.

Fig. 120. (b) Horizontal section through crown. (c) Vertical section through base.

Fig. 121. Vertical section through neck and base.

Fig. 122. Horizontal section through part of crown.

Figs. 123-127a. RGM 323072. Indeterminable poracanthodid, forma *bifurcata*, forma nova.

Fig. 123. (a-b) Horizontal sections through crown. (c) Horizontal section through part of posterior crown; magnification *circa* 100% of a.

Fig. 124. Horizontal sections. (a) Through crown. (b) Through scale.

Fig. 125. Horizontal section through crown and neck.

Fig. 126. (a) Horizontal section through crown. (b) Detail of primary crown region; magnification *circa* 200% of a. (c) Detail of posterior crown; magnification *circa* 300% of a. (d) Detail of median crown; magnification *circa* 230% of a. (e) Detail of primary crown region; magnification 200% of a. (f) Vertical section through anterior scale part. (g) Vertical section through posterior scale part.

Fig. 127. (a) Vertical section through lateroposterior scale part; ola= older lamella, yla= younger lamella.

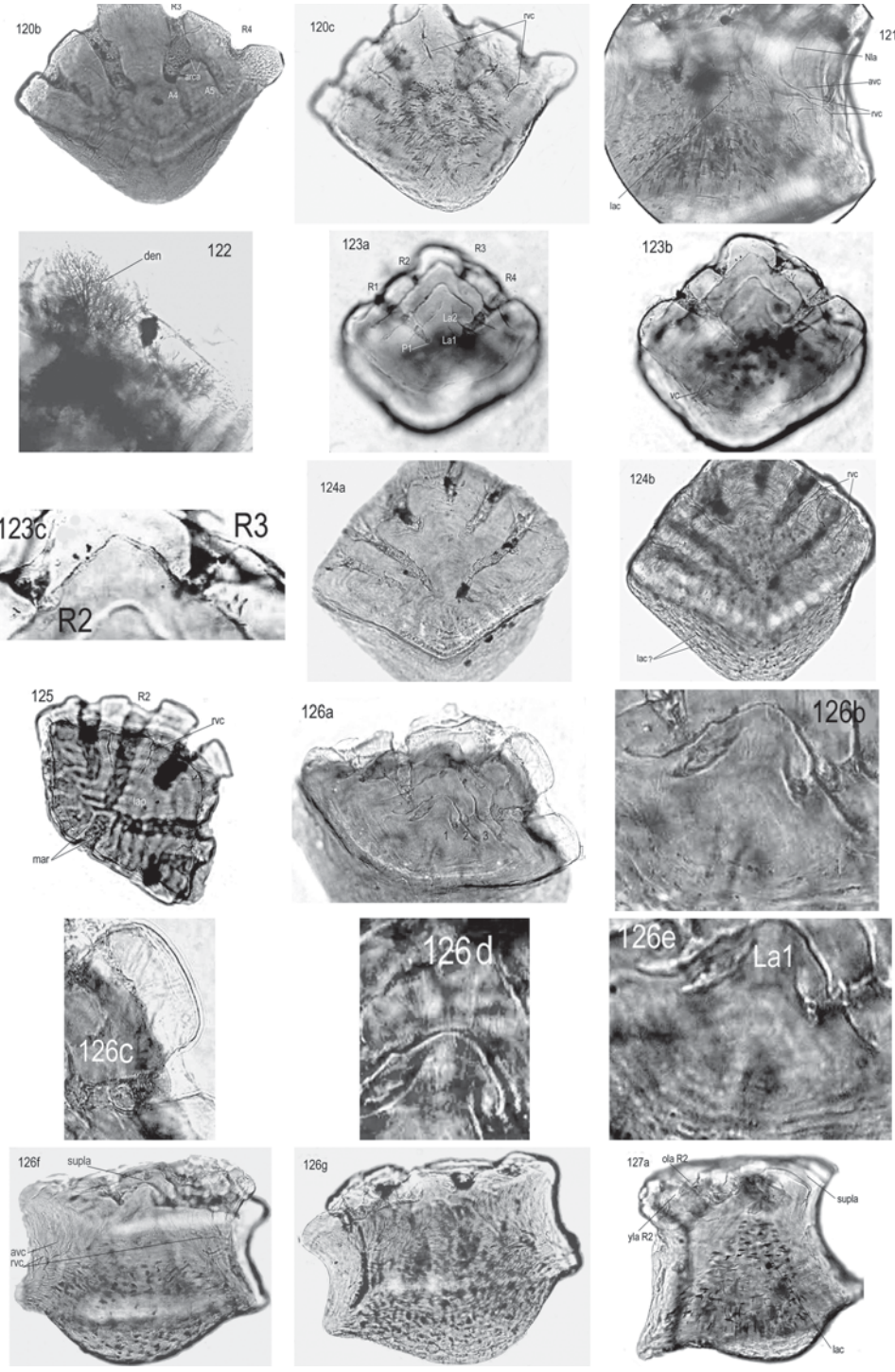
120b
R3
R4
arc
A4
A5
120c
rvc
121
Nla
avc
rvc
lac
122
den
123a
R3
R2
R1
R4
La2
P1
La1
123b
vc
123c
R3
R2
124a
124b
rvc
lac ?
125
R2
rvc
lac
mar
126a
1
2
3
126b
126c
126 d
126e
La1
126f
supla
avc
rvc
126g
127a
ola R2
supla
yla R2
lac

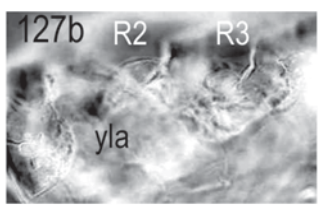

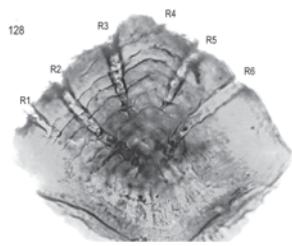

Plate 15 (Figs. 127b-128)
Figs. 127b-128. RGM 323072. Indeterminable poracanthodid, forma *bifurcata*, forma nova.
Fig. 127. (b) Detail of posterior crown. Magnification *circa* 100% of 127a; ola= older lamella, yla= younger lamella.
Fig. 128. Horizontal section through crown.